Stock assessment for oceanic whitetip shark in the Western and Central Pacific Ocean

WCPFC-SC15-2019/SA-WP-06

Laura Tremblay-Boyer[1], Felipe Carvalho[2], Philipp Neubauer[3] and Graham Pilling[4]

Image credit: Dr Lindsay Marshall

[1]Dragonfly Data Science, Wellington, New Zealand
[2]National Oceanic and Atmospheric Administration, Honolulu, United States
[3]Dragonfly Data Science, Wellington, New Zealand
[4]Oceanic Fisheries Programme, Nouméa, New Caledonia, The Pacific Community

Stock assessment for oceanic whitetip shark in the Western and Central Pacific Ocean

Authors:
Laura Tremblay - Boyer
Felipe Carvalho
Philipp Neubauer
Graham Pilling

DRAGONFLY
Data Science

EXECUTIVE SUMMARY

This is the second stock assessment for oceanic whitetip shark in the WCPO following that of Rice and Harley (2012), and the first since CMM2011-04 became active in 2013, enacting a no-retention measure for this species for WCPFC Members, Cooperating Non-Members and Participating Territories (CCMs). This assessment for oceanic whitetip shark was performed in the Stock Synthesis modelling framework (Methot Jr & Wetzel 2013), an integrated age-structured population model previously used to assess the status of sharks in the Pacific Ocean and elsewhere. The population dynamics model was informed by three sources of data: historical catches, time series of catch-per-unit-effort and length frequencies. We maintained the four-fleet structure used in the previous stock assessment, splitting the longline fishery into bycatch and target fleets, and the purse-seine fishery into fleets of associated and unassociated sets.

A new development in this assessment was the inclusion of discard mortality (DM) scenarios in the historical catches. This was a key step to account for the potential impacts of the no-retention measure for oceanic whitetip sharks. Three scenarios were used assuming 25%, 43.75% and 100% mortality on the discards, accounting for mortality at different stages of the discarding process from the catch event and crew handling to post-release mortality. In addition, results from two new WCPO growth studies predicted a much less productive profile for the stock than what had been assumed previously. Because growth was a key uncertainty in this assessment, we use two growth and fecundity assessment 'profiles' to reflect the differences between growth studies, and ensure that conclusions about stock status were robust to the uncertainty about life-history parameters.

We developed a diagnostic case for the assessment based on the model with the best overall diagnostics, an informative likelihood profile, and the most reasonable assumptions about biology and fleet settings based on current knowledge about oceanic whitetip shark and the fisheries that catch this species. Based on the results from the one-off sensitives from the diagnostic case and previous discussions at the Pre-Assessment workshop (Pilling & Brouwer 2019), a set of uncertainty axes for the model was defined outlining alternative values for key uncertainties and influential model or biological parameters. The combination of all levels across axes forms the structural uncertainty grid with a total of 648 individual model runs.

Stock status was obtained by summarizing reference points over all grid runs to account for the assumptions about life-history parameters and impact of fishing underpinning the assessment. We estimate the stock to be overfished and undergoing overfishing based on SB/SB_{MSY} and F/F_{MSY} reference points and assuming equal weightings for grid levels. This overall conclusion is the same as that from the previous assessment, despite a wider range of uncertainties being considered, notably in the growth and fecundity parameters. In terms of the depletion of the spawning biomass, most model runs predict SB/SB_0 to be below 0.05, and all model runs predict SB/SB_0 to be below 0.1. Given the high levels of depletion, we focus on SB/SB_0 as a biomass-based reference point throughout.

We found that F-based reference points improved in the period since CMM2011-04 became active, which covers the last 4 years of the assessment's time-span (2013–2016). Notably, F/F_{MSY} is predicted to have declined by more than half from 6.12 to 2.67 (median) for the last year of the assessment when the impact of CMM2011-04 on survival is accounted for under the 25% and 43.75% discard mortality scenarios. F levels relative to two alternative reference points, $F/F_{lim,\text{AS}}$ and $F/F_{crash,\text{AS}}$, follow similar trends following the adoption of the measure.

All catch scenarios accounting for DM $< 100\%$ showed a very slight increase in spawning biomass since 2013, but final levels of depletion (SB/SB_0) remain very low over all grid runs (median: 0.0367, 95%CI: 0.021–0.061). Given the assessment assumes oceanic whitetip sharks to become mature after 4 or 8 years, stock recovery should be expected to be slow in the period following the conservation measure while the spawning biomass rebuilds. Despite the relative improvements in F-based reference points since 2013, the median value of F/F_{crash} over all 648 grid runs for 2016 remains above 1 (median: 1.41, 95%CI: 0.98–2.15), indicating that the population should go extinct on the long-term under current levels of fishing mortality.

Recommendations

This assessment estimates that CMM2011-04 may have had a positive impact on stock status by decreasing fishing mortality. However, there are two key sources of data informing stock assessments that are compromised by observer practices not having adapted to the post-CMM-2011-04 period:

- Longline observer programs need to ensure there are clear and consistent directives about how unobserved discarded-cut-free (DCF) individuals are to be recorded. Not recording DCF events can seriously compromise the quality of the catch rates time series used both as an index of abundance and to reconstruct historical catches for shark assessments. **We recommend that all DCF events are recorded even if unobserved, and that in the instance where the species could not be identified, that the species be recorded at the highest taxonomical level possible**, even if in the absence of information that level is 'shark' or 'unidentified'.

- **We recommend that approximate length measurements should be recorded even if individuals are not brought on-deck, with an estimate of precision**. This would ensure that the time series of length measurements is not compromised even if the precision of length estimates is lower.

- **We recommend that alternative analytical methods incorporating coarser bin lengths for part of the time series be investigated.**

We make the following recommendations about additional research into the biology of oceanic whitetip shark and of data inputs that impact its assessment:

- Given predictions of recent and latest stock status were sensitive to assumptions made

about discard and post-release mortality, **we recommend that ongoing and new studies on this topic for this species be prioritized and projections of current stock status be updated with estimates of PRM specific to oceanic whitetip shark in the WCPO. We recommend that observers record the length of the trailing branchline when individuals are cut-free, in order to improve modelled estimates of PRM rates**.

- **We recommend that spatial trends in shark length for the longline dataset be analysed in a dedicated study in order to determine the likely cause for a north-south positive gradient in the mean length observed, and that approaches to standardize the length dataset be investigated accordingly.**

- **We recommend that additional length-length conversions be obtained, and, more specifically, a length-length conversion from total length (TL) to fork length measurements starting from the lower jaw (LFL).**

- **We recommend that a direct collaboration with countries having participated in the shark target fleet be undertaken to either produce an historical time series of targeted catch, or reliable anchor points that can be used to scale catches reconstructed from observer longline datasets.**

- While CMM-2011-04 allows for scientific sampling, traditional destructive sampling might not be optimal given the current state of the population. **We recommend that SC investigates non-lethal approaches to collect growth and maturity samples for sharks and oceanic whitetip shark in particular.**

- **We invite SC to note the alternative reference points $F/F_{lim,\text{AS}}$ and $F/F_{crash,\text{AS}}$ included in this assessment.**

CONTENTS

1. INTRODUCTION

1.1 Background

This paper presents the stock assessment for oceanic whitetip shark (*Carcharhinus longimanus*) for the Western and Central Pacific Ocean (WCPO) covering the period from 1995 to 2016. Oceanic whitetip shark is a large species, found in tropical and warm-temperate waters across all oceans, with a marked preference for oceanic waters distant from the continental shelf (Bonfil et al. 2008). The species was previously considered one of the most common sharks in offshore tropical waters, and it was reportedly frequently caught in tuna-target fisheries, but its population size is considered to have declined in recent decades.

Worldwide, there has only been a single stock assessment for this species to date, which was focused on the Western and Central Pacific Ocean region and included the period between 1995 and 2009 (Rice & Harley 2012). This assessment started in 1995 as there was little collection of catch statistics for sharks in the WCPO before that year. Rice and Harley (2012) concluded that the stock was overfished: spawning biomass had declined by 86% from 1995 levels, and current fishing mortality was 6.5 times the mortality estimate predicted to achieve maximum sustainable yield (MSY). In addition, a recent review surveyed additional abundance metrics of this species across all main oceans, and concluded that oceanic whitetip shark had experienced considerable historical declines throughout its range (Young et al. 2018).

In an effort to slow the rate of population decline of this species, the Western and Central Pacific Fisheries Commission (WCPFC) introduced a Conservation and Management Measure (CMM2011-04) that included a non-retention policy for oceanic whitetip shark across the WCPFC Convention Area. Under this measure, vessels belonging to all member countries are prohibited from retaining or landing oceanic whitetip shark. Implementation of CMM2011-04 should reduce fishing mortality of oceanic whitetip sharks if individuals caught by longliners or purse seiners are released back to the water alive; however, rates of discard and post-release mortality (PRM) are still poorly known. Under WCPFC Circular 2016/51, a research project was designed to assess longline post-release mortality of sharks once hooked, but oceanic whitetip sharks were not included in the study (although research for this species is on-going, Common Oceans (ABNJ) Tuna Project 2019). Furthermore, while CMM2011-04 officially came into effect in 2013, a recent review documented that it was unevenly applied across WCPFC Members, Cooperating Non-Members and Participating Territories (CCMs), and some oceanic whitetip shark individuals were still observed as being retained (Rice 2018).

The current assessment provides an update of the previous stock assessment by Rice and Harley (2012), including seven years of additional data and a revised assessment model within the same modelling framework (Stock Synthesis, Methot Jr & Wetzel 2013). In addition, the current assessment model includes new methodology to predict historical catches and updates key biological parameters of this species. In parallel to the current study, a separate risk assessment was undertaken as part of Western and Central Pacific Fisheries Commission Project 92 (Neubauer et al. 2019). The risk assessment evaluated different methods for data-

poor situations as alternative assessment methods for this species.

1.2   Distribution and biology

Oceanic whitetip sharks are primarily found in shallow depths at latitudes between 10°S and 10°N, although their habitat can extend to 30°S and 30°N. The distribution of this species is primarily tropical, but they can occasionally be found in waters at relatively low temperatures of 15°C (Bonfil et al. 2008).

Observer data from longline fisheries in the Western and Central Pacific Ocean (analysed in the current assessment) included temperature records, and the lowest sea surface temperature (SST) associated with the capture of an oceanic whitetip shark individual was 16.4°C; the highest latitude was 43°N, but less than 1% of individuals were observed outside of the 30°S to 30°N band.

In spite of the species' preference for warm waters, a recent study found that individuals tended to avoid high sea surface temperatures (i.e., above 28.5°C), and engaged in thermoregulatory behaviour *via* swim cycles to cooler depths in the water column (Andrzejaczek et al. 2018). In addition, recent tracking studies with pop-up satellite archival tags documented that individuals of this species are able to dive below 1000 metres depth, but that they spent most of their time in shallow waters (typically less than 200 m depth) (Filmalter et al. 2012, Howey-Jordan et al. 2013, Tolotti et al. 2015). These temperature and depth preferences affect the overall and seasonal exposure of oceanic whitetip shark to fisheries, and their vulnerability to specific fishing strategies (e.g., shallow longline sets).

There is limited information about the population structure of oceanic whitetip sharks in the Western and Central Pacific Ocean. The most recent population study identified Atlantic Ocean and Indo-Pacific Ocean stocks but no within-ocean differentiation, indicating that large-scale movements are common for individuals or that the genetic markers used were sensitive to small amounts of gene flow (Ruck 2016). There is currently no evidence that there is more than one population within the Western and Central Pacific Ocean; however, the limited extent of horizontal movement inferred from satellite tagged individuals highlights a potential for regional residency in the Pacific Ocean (Musyl et al. 2011) and other ocean basins (Howey-Jordan et al. 2013, Tolotti et al. 2015).

The oceanic whitetip shark is typically considered a slow-growing species, although there has been some contention about this classification (Clarke et al. 2015). Three relatively recent studies (within the last 20 years) documented different growth rates of oceanic whitetip shark across different areas of the Pacific Ocean (Figure 1). The slowest growth rate was based on 103 individuals from the Bismarck Sea around Papua New Guinea (D'Alberto et al. 2017), with a slightly higher rate documented from 188 individuals sampled from the Taiwanese fishing fleet in the Western North Pacific Ocean between latitudes 23°and 28°N (Joung et al. 2016). The highest growth rate was based on 225 individuals sampled from Japanese longline vessels fishing in the North Pacific Ocean to 30°N (Seki et al. 1998), and growth data from this study

were the basis of the previous stock assessment of this species. None of the studies detected significant differences in growth rates between males and females.

Differences across the studies also included estimates of fecundity and maturity (Table 1); estimates reported here are from the study with the largest sample size (Seki et al. 1998). The oceanic whitetip shark is viviparous, and litter sizes vary with an average of six pups (ranging from one to 14 pups), which is comparable to other species for this type of shark (Clarke et al. 2015). Pups measure between 55 and 77 cm total length (TL) at birth. Males of this species reach sexual maturity at 167 to 195 cm TL, compared with 175 to 189 cm TL for females; the mid-point of these estimates corresponds with an age of 4.5 years (based on the Seki et al. (1998) growth curve). There is some uncertainty about the longevity of this species, and the oldest individual recorded was 17 years old (D'Alberto et al. 2017). Model-based extrapolation based on growth curves from Seki et al. (1998) led to an implausibly high value of 36 years, and the Western and Central Pacific Fisheries Commission expert panel on shark life-history agreed that 17 years was a more realistic value (Clarke et al. 2015).

In general, the parameters from the study by Seki et al. (1998) predicted faster growth and more productive fecundity parameters (i.e., younger age-at-maturity) than estimates from the other two studies by Joung et al. (2016) and D'Alberto et al. (2017). It is possible that the differences across studies reflect regional patterns in growth, but the studies also differed in time, covering different periods of exploitation of this species (early 1990s for Seki et al. (1998), 2002 to 2006 for Joung et al. (2016), and 2014 for D'Alberto et al. (2017)).

1.3 Fisheries

Longline and purse-seine fisheries in the WCPO catch oceanic whitetip shark, primarily as bycatch; however, there was a longline fishery targeting shark in the Bismarck Sea from the 1990s to the mid-2010s (White et al. 2018). Annual and spatial trends in the distribution of effort for these fleets is shown in Figure 2.

Longline fisheries in the Western and Central Pacific Ocean primarily target albacore, bigeye, yellowfin and bluefin tuna, or swordfish. These fisheries are active at all latitudes and longline effort has increased two-fold since 1995. Oceanic whitetip shark are caught as bycatch by longline sets in warmer waters, especially shallow sets due to the species' preference for surface waters. The size of individuals caught ranges between 75 and 240 cm (mean $\sim$ 160 cm, total length). There have also been larger individuals in the catch, although it is likely that large-sized individuals are able to bite-off the hook without getting caught if the lead line is made of monofilament, the material typically used for longline sets in the Pacific Ocean (Burgess et al. 2005). Conversely, the lack of small-sized oceanic whitetip shark in longline catches has led to the suggestion that newly-born individuals have little overlap with the offshore fishing grounds of longliners (Joung et al. 2016).

Most of the oceanic whitetip sharks caught in the Western and Central Pacific Ocean are bycatch in the longline fleets, so the adoption of CMM2011-04 should have reduced the impact

of this fishery on the population. In addition, CMM2014-05 banned the simultaneous use of shark lines and wire traces from July 2015 onwards. While this should lower the number of sharks that get caught in the first instance, a simulation study found that much higher reductions in fishing mortality would be achieved by banning both practices (Harley et al. 2015).

There is evidence of a longline fishery targeting sharks in the Bismarck Sea area (Papua New Guinea) during the 1990s and part of the 2000s which used gear modifications to increase the catch rates of sharks (Kumoru 2003). These modifications included shallow sets (e.g. hooks between floats (HBF) = 4) and wire traces. Although this fishery is no longer active due to the retention ban on silky sharks (the main catch), an artisanal coastal shark fishery has remained active to some extent. Nevertheless, a recent examination of DNA of shark fins from this fishery found no evidence of oceanic whitetip shark in the catch (Appleyard et al. 2018), but this might be related to the coastal extent of the fishing grounds surveyed. Statistics of oceanic whitetip catch for the earlier target shark fishery are uncertain, as observer coverage was sparse and logsheet records of effort targeting shark are incomplete. In addition, logbook-reporting of key shark catches, including oceanic whitetip shark, only became mandatory in 2012 with the enaction of CMM2010-07.

Purse seine fleets are mostly active in waters between 10°N and 10°S. These fleets target skipjack tuna and encounter oceanic whitetip shark as bycatch, but at a markedly lower rate than longliners. Effort can be classified as associated (e.g., using fishing aggregating devices, FADs, or floating objects) or unassociated (e.g., free schools). There is some evidence from observer coverage of these fleets that catch rates of oceanic whitetip shark are higher on drifting FADs and lower on free school sets (Tremblay-Boyer & Neubauer 2019).

2. METHODS

2.1 Overview

This assessment was performed in the Stock Synthesis modelling framework (Methot Jr & Wetzel 2013), an integrated age-structured population model. The population dynamics model was informed by three sources of data: historical catches, time series of catch-per-unit-effort and length frequencies. Included below are descriptions of the processing of the input datasets used to inform the assessment, the population dynamics model and the grid approach to characterise uncertainty (details of the methodology for the data inputs are available in the companion report by Tremblay-Boyer & Neubauer 2019). The boundaries for the assessment region are shown in Figure 3.

2.2   Inputs to the stock assessment

2.2.1   Description of datasets

Datasets from the database of the Pacific Community (SPC) included catch, effort and observer data.

- **L_BEST:** SPC's best estimates of longline catch and effort (in hooks) for fleets in the WCPFC Convention Area (WCPFC-CA), available at the $5° \times$ month $\times$ year $\times$ flag $\times$ fleet resolution for key species of tuna and billfish, and sharks in some years. A version of this database (**L_BEST.HBF**) was available with an additional strata for hooks-between-floats (HBF), but effort coverage is uneven over fleets and years (see Figure 2 for the distribution of total effort for this fleet over time and space in the assessment region).

- **S_BEST:** SPC's best estimates of purse-seine catch and effort (sets and days) for fleets in the WCPFC-CA, available at the $1° \times$ set type $\times$ month $\times$ year $\times$ flag $\times$ fleet resolution for key species of tuna and billfish, and sharks in some years (see Figure 2 for the distribution of total effort for this fleet over time and space in the assessment region).

- **Observer programmes for longline and purse-seine fleets:** The full observer dataset for longline and purse-seine fleets available to SPC was used for the analysis, including data from the SPC's Regional Observer Programme and national observer programmes. Records collected by longline observers that are relevant to this assessment are key gear and attributes (including date and time, location, HBF) and, for each observed hook with a positive catch event, the species, the fate of the catch (e.g., discarded or retained), the condition, the length and the sex of the individual. The quality and coverage for most variables changes over time and between programmes. For observed purse-seine sets, observers estimate the number of sharks caught of a given species from the brail net and, when possible, measure their length.

Data preparation

Extracts from SPC's databases were obtained in April 2019. All datasets were filtered to retain records within the Western and Central Pacific Ocean area only (Figure 3), over the period of the stock assessment from 1995 to 2016. For the longline observer datasets, number of hooks observed, when missing, was estimated from the product of hooks-between-floats and the number of baskets observed. Sets were classified as shallow when the number of HBFs was lower or equal to 10, following Peatman et al. (2018). Oceanography covariates (sea surface temperature, chlorophyll-*a*, bathymetry and distance from the coast) were extracted at the lowest resolution possible and aggregated to match the resolution of each dataset. Longline sets occurring in sea surface temperatues below $16°$C were removed as they were considered to be outside of oceanic whitetip shark habitat. When relevant, extreme values of oceanography covariates were bounded or filtered out ($> 99.5^{th}$ quantile). Records from implausible locations (e.g., on land) were omitted. Longline records without HBF information and purse-seine records without set-association information were also omitted.

2.2.2 Catch reconstruction

Historical catches for sharks in the Western and Central Pacific Ocean were poorly recorded until 2010, when CMM2010-07 became active (replacing CMM2009-04), mandating the reporting of catches of key shark species, including oceanic whitetip shark. Nevertheless, reported shark catch was likely underestimated even after CMM2010-07 came into effect. As logbook-reported catches of oceanic whitetip shark were considered unreliable for the present assessment period, we applied two strategies to reconstruct catches. In the first instance, we created a prediction-model from observer catch rates to apply this model to known longline and purse-seine effort across the Western and Central Pacific Ocean. In the second instance, we applied the trade-based approach from Clarke (2018) to predict global catches of oceanic whitetip shark based on fin trade statistics. The latter were apportioned to the Western and Central Pacific Ocean using a set of alternative scaling methods. All catch predictions were made in number of individuals.

Prediction of catch rates from observed sets

Previous approaches to reconstruct catches for this species have also been based on observer catch data (see Lawson 2011, Rice 2012a, Peatman et al. 2018). The basis for these methods is similar: a model of catch-per-unit-effort is built based on observed sets and relevant covariates, and the model is then used to predict catches based on a reliable measure of total effort by fleet across the assessment region. The previous approaches differ in the modelling framework used to build the catch rate model, the covariates considered and the treatment of uncertainty. Lawson (2011) and Rice (2012a) both used Generalised Linear Models (GLMs), assuming delta-log-normal error distributions (i.e., two-stage or hurdle model), but Rice (2012a) filtered the data more extensively (e.g., only sets at SST $\geq 25°$C were retained) and permitted extra variability around the year effects. Uncertainty around model predictions of catches was not explicitly considered. Peatman et al. (2018) used Generalised Estimating Equations (GEEs) to model catch rates, also with a delta-log-normal model structure. The GEE framework allows for the correlation between observed sets in the same observer trips to be accounted for. Catch predictions and uncertainty were estimated with a Monte Carlo simulation approach drawing samples from modelled catch distributions.

Here, we used Markov chain Monte Carlo (MCMC) methods to model catch rates in number of individuals for the observer longline and purse-seine datasets, assuming a negative binomial error distribution. Negative binomial error distributions are well suited at representing catch rates, as they can naturally account for high proportions of zero in the response variable without the requirement of a parallel model (such as required when assuming delta-log-normal error distribution). Negative binomial error distributions can also predict infrequent but high catch events. An advantage of the MCMC approach to fitting GLMs is that the uncertainty for any estimated parameter or derived quantity can be easily estimated by drawing from the posterior samples of the converged MCMC chains. Because of this, the scale of alternative catch scenarios can be informed by model-derived uncertainty instead of user-defined multipliers.

We used the R package "brms" (Bürkner 2017) to implement our approach. This package provides an efficient interface for fitting GLMs in the Stan language for Bayesian statistics (Carpenter et al. 2015). In addition, the brms package allows the user to customise probability distributions to improve their suitability for representing some features of the response variables and, therefore, improve the quality of the fit. Although the GLMs were fitted within a Bayesian framework, we did not use informative priors for any of the models. Finally, all models included a random effect for the vessel flag (Table 2), allowing the prediction of a distribution for flag effects, which can then be used to predict catches for countries without any observer coverage.

There was a high degree of overdispersion in the response variable, with most fishing sets reporting no captures ($\geq$ 90% and $\geq$ 99% zero sets in the longline and purse-seine datasets, respectively). The impact of varying effort by fishing record on the probability of a positive capture event was accounted for by parameterising the negative binomial distribution by the number of "trials", defined by the number of fishing hooks or sets used in the fishing set group. In addition, a new parameter ν was added to the parameterisation of the negative binomial distribution to allow more flexibility in how the overdispersion behaves as mean catch rates increase.

In the model, catches, c_i, in a longline or purse-seine set group, i, were thus modelled as samples from a negative-binomial distribution:

$$c_i \sim \mathsf{NegativeBinomial}(\mathrm{mean} = \mu_i n_i, \ \mathrm{shape} = \theta n_i), \qquad (1)$$

where n_i is the number of hooks or sets. The shape parameter, θ, allows for extra dispersion in the number of captures relative to a Poisson distribution. The negative binomial distribution has the property that the mean of n samples from a negative binomial distribution ($\mathsf{NegativeBinomial}(\mu, \theta)$) is itself negative binomially distributed, with mean μn and shape θn. For this reason, while c_i is the number of catches per group, μ_i needs to be interpreted as the mean catch rate per longline hook or purse-seine set. The custom distribution facility of brms was used to code the negative binomial distribution for aggregated data. The mean capture rate within each group was then estimated as the exponential of the linear predictor, which was the sum of fixed and random effects.

A novel configuration of the negative binomial distribution was trialled in model fitting. Under the usual approach to fit a negative binomial GLM, overdispersion compared to mean catch rates μ is determined by the estimate of a single parameter θ assumed for all observations:

$$\psi = \mu + \frac{\mu^2}{\theta}. \qquad (2)$$

This aspect can be challenging when combinations of covariate levels have considerably higher catch rates than others, as high μ combined with low θ can result in error distributions

predicting implausibly high values (i.e., very long tails) at times. Although estimating covariate effects on θ as part of the model is possible, the results can be difficult to interpret as μ and θ are often correlated. For this reason, any covariate effect attributed to θ might otherwise be confounded with a covariate effect on μ. We modified instead the definition of θ, so that it includes a new parameter, ν, scaling the extent of overdispersion as a function of μ:

$$\theta \to \mu^\nu \theta, \tag{3}$$

so that overdispersion to the negative binomial distribution becomes:

$$\psi = \mu + \frac{\mu^2}{\mu^\nu \theta}. \tag{4}$$

This configuration allows for the overdispersion parameter to change as a function of μ: as ν approaches 2, it cancels out μ^2 in the numerator, so that the negative binomial distribution effectively becomes a Poisson distribution; as ν approaches 0, the additional μ^n term goes to 1 and the distribution behaves in the usual way. Therefore, adding this new term in the model allowed for additional flexibility in the realised error distribution between observations with the estimation of a single additional parameter.

Prior to fitting, all observed sets were first aggregated to a spatial resolution of 5°to match the resolution of the L_BEST datasets (S_BEST has a 1°-resolution, but a 5°-resolution was chosen for both datasets for consistency in predictions), and observer programme, flag, year, month and set depth (for longline, shallow or deep) or set type (for purse seine). Because of the low observer coverage for some fleets, year and locations, and the aggregation at the 5°-scale, a minimum number of records were removed for the catch reconstruction component of the analysis. For the longline fleet, aggregated records with less than 50 hooks observed in total were removed. Each of the remaining aggregated records was considered a "fishing set group" and catch rates of oceanic whitetip shark were calculated over all sets in the event to use as the response variable in the GLM. The number of hundred hooks of the sets of the fishing event was treated as the number of "trials" in the negative binomial distribution.

Candidate model covariates were selected to retain operational features of sets likely to impact catch rates and environmental variables that might be representative of oceanic whitetip shark habitat and, therefore, local abundance (Table 2). We were limited in the choice of covariates by their availability in the L_BEST and S_BEST datasets, as model predictions from these datasets require all model covariates to be available. All models were also trialled with and without the addition of ν to the negative binomial distribution.

Models were fitted with four separate chains and 2000 iterations, including a 1000 iterations burn-in period that was discarded from posterior samples. Best model selection was performed on the basis of model diagnostics (including chain convergence) and leave-one-out cross-validation (LOO; Vehtari et al. 2016). The LOO Information Criterion (LOOIC) is a

Bayesian equivalent to the Aikake Information Criterion (AIC) metric that balances additional complexity in model structure against the improvement in model performance. Models using the same dataset and nested model structures can be directly compared, with lower LOOIC values indicating models that maximize fit and minimize complexity.

Three independent catch rate models were optimised for the catch reconstruction based on the fleet.

Longline bycatch fleet

The bycatch model for the longline bycatch fleet was fitted separately from the target model based on different assumptions underlying the response variable. Records belonging to vessel with flags from Papua New Guinea and Solomon Islands were removed from the analysis. In previous research by Rice (2012a), sets with evidence of shark targeting were also removed from the analysis (e.g., the use of wire traces, shark lines or the specification by the observer that the set was targeting shark). Owing to the poor coverage and reliability of these covariates over fleet and years, we were more conservative in retaining data, and did not filter sets based on these variables.

The best model for the longline bycatch fleet was:
OCS.obs | trial(sets) = Year + s(SST, k=3) + HBF.cat + cluster + (1Flag) + (1yy:Flag),
including the ν coefficient to scale overdispersion as a function of average catch rates.

Alternative models included observer programme instead of flag, different configurations for the oceanography covariates and the flag-year interaction, and also the modelling of the overdispersion (key diagnostics for the best model are shown in Appendix A of Tremblay-Boyer & Neubauer 2019).

Longline target fleet

Little is known about the longline target fleet, so that it was not included in recent catch reconstructions (e.g., Peatman et al. 2018). An estimation of oceanic whitetip captures assumed that 5% of effort in the L_BEST database was targeting sharks, but apart from this aspect, predictions of catches for the targeting fleet were from the same model as that used for the bycatch longline fleet by Rice (2012a).

In the current assessment, we created a model of catch rates for the target longline fishery. Given the scarcity of observer records for the countries with this fishery, a subset of representative flags from Pacific Island countries and territories was retained, in addition to Papua New Guinea and Solomon Islands sets (American Samoa, Kiribati, Cook Islands, Fiji, Federated States of Micronesia, Marshall Islands, Samoa and Tuvalu). Recent records from Papua New Guinea and Solomon Islands with observer programmes from distant-water nations were removed, as they were considered to be unlikely to be representative of domestic fisheries (but noting that there is some evidence of shark targeting by distant-water nations too). Observer records from Papua New Guinea for 1996, 2000 and 2003 were removed as the total catches of oceanic whitetip shark in these years were very low, indicating that observed

catches might not have been recorded. There is evidence that the shark target fisheries in the Bismarck Sea region have stopped (White et al. 2018); however, based on the uncertainty of the timespan of target fisheries, we assumed that target fisheries were ongoing for the catch reconstruction.

The best model for the longline target fleet was:

OCS.obs | trial(sets) = yy + s(SST, k=3) + hbf.cat + cluster + (1:Flag),
including the ν coefficient to scale overdispersion as a function of average catch rates.

This model did not include a flag-year interaction by design, so that the overall temporal trend in catches would be informed by the catch observed in other Pacific country fleets, but the scale determined by the vessel flag. This approach was used to compensate for the lack of reliable records for the target fisheries for some years. Key diagnostics for this model are shown in Appendix A of Tremblay-Boyer & Neubauer 2019.

Purse-seine fleet

A single model of observed catch rates was built for the purse-seine fleet, including associated and unassociated sets, but with set type as a covariate to allow for reconstructed catches to be predicted for each fleet separately.

The best model for the purse-seine fleet was:
OCS.obs | trials(sets)   yy + s(dist2coast, k=3) + (1|Flag) + (1|yy:Flag) + SetType.

This model had a random effect for flag and a random-effect interaction for year and flag, and fixed effect for set type and the distance of sets to the nearest coast. The model including ν did not result in a considerable improvement to the fit according to the LOOIC metric, presumably because there was less variation between flags fishing the same area in purse-seine than for longline catch rates.

Alternative models considered observer programme instead of flag, different configurations for the oceanography covariates and the flag-year interaction, and also the modelling of the overdispersion. Key diagnostics for this model are shown in Appendix A of Tremblay-Boyer & Neubauer 2019.

Extrapolation of observed catch rates to WCPO-wide effort

Catch rates predicted from the observer models were projected at the scale of the Western and Central Pacific Ocean based on estimates of effort from the L_BEST and S_BEST datasets.

For L_BEST, species-targeting clusters were predicted from species proportion for each record (as described in Table 2). Hooks-between-float information was missing for numerous records in L_BEST, especially in earlier years. HBFs are a proxy for the depth of the longline set, and a key factor for predicting and extrapolating catches of oceanic whitetip shark, as this species

primarily occupies surface waters.

CCMs recently started reporting longline catch and effort statistics disaggregated by HBF; however, coverage for many countries remains lacking over most or part of the time period of this assessment.

In the previous catch reconstruction by Peatman et al. (2018), ratio estimators were used to classify L_BEST records that were missing HBF information. Here, we used a Random Forest model instead (Liaw & Wiener 2002), as it allows the inclusion of covariates to predict the likely depth of sets (instead of assuming that unclassified sets for a country are directly representative of classified sets). The Random Forest model also provides outputs for the probability of a record having a given classification, which can be used to propagate uncertainty about this step into catch estimates as needed.

We used the dataset of HBF-disaggregated L_BEST to train a Random Forest model to predict whether a record should be assigned to a shallow- (<10 HBF) or deep-effort category (≥10 HBF), assuming a binomial error distribution:

- We used the Random Forest algorithm provided in the R package "randomForest" (Liaw & Wiener 2002).

- Covariates used to build the tree were: year, month, targeting cluster, 5°-longitude cell, 5°-latitude cell, and catches for albacore, yellowfin, bigeye and bluefin tuna, swordfish and other billfish (in numbers). We did not use shark catches, even though these data are available in L_BEST and likely provide information about set depth since sets that target sharks tend to be shallow. These data were not included as low shark catches in the early part of the time series are misrepresented owing to the lack of reporting.

- The L_BEST.HBF dataset was split evenly between a training and a testing dataset. The training dataset was used to fit the Random Forest model and model performance was assessed by predicting HBF classification for the testing dataset.

- The Random Forest model was tuned by first running the model with a high number of trees (500), and verifying the Area-Under-the Curve score to asses the number of trees required to reach a plateau. Five covariates were randomly considered at each node for splitting. The optimal tree depth was assessed to be 200.

The Random Forest model with optimised parameters was used to assign shallow- or deep-effort depth to L_BEST records lacking HBF information, based on the probabilities estimated by the binomial error model. Where partial HBF information for a stratum was available, predictions were only made for the effort lacking HBF classification. An uncertainty distribution of the final predictions of HBF classification for L_BEST by member countries was estimated by drawing 1000 draws from a Bernoulli distribution for each L_BEST record, assuming the probability of success is the probability estimated by the Random Forest model of the record being classified as deep. Predictions of the proportion of deep sets over time by

fleet is shown in Figure 4, including the fit to the training dataset and 95% credible intervals based on sampling of the error distributions.

Once all effort in L_BEST was assigned to a shallow- or deep-set category, we were able to make predictions of L_BEST-wide catch for the assessment region, based on the catch models developed for the longline bycatch and target fleets (Figures 5 and 6). Predictions for the target longline fleet were derived on effort assigned to Papua New Guinea and Solomon Islands only.

The S_BEST dataset already contained all the required covariates (historical catch predictions for the associated and unassociated purse-seine fleets are shown in Figure 7). Predictions of catches over time by fleet and year were aggregated for each model over each posterior draw, and summary statistics extracted. The median prediction was used as a baseline catch scenario, and the 90th quantile of the predictions as a high catch scenario. Discard and post-release mortality scenarios were then applied to these overall catch predictions by fleet as described in Section 2.2.4.

2.2.3 Trade-based historical catch estimates

Reconstructing catches from observer data over 1995–2016 can be difficult because of the low coverage rates for longline observer programmes throughout the time series, operational challenges for purse-seine observers to estimate accurate shark catches over the full set given the process of brailing and sorting, and sparse and unreliable reporting of shark catches for both purse-seine and longline programmes before 2003. An alternative approach was developed by Clarke et al. (2006b) and more recently applied to reconstruct historical silky shark catches (Clarke 2018). This approach relies on an estimate of the number of individuals (or biomass) of the species of interest used in the fin trade for a reference year in a sampled fin market (the "anchor point"), an estimate of the share of the global fin market transiting through the sampled market over time, and a scaling method to assign global catch to a specific region.

Here, we provide a brief summary of the approach by Clarke (2018) applied to oceanic whitetip shark:

- Clarke et al. (2006b) estimated traded fin weights by species and fin size by sampling the Hong Kong market between 2000 and 2002. They estimated the corresponding number and biomass of sharks by species, with conversion factors also accounting for fin type (dorsal, pectoral and caudal). This number was projected to the global scale based on an estimation of Hong Kong's share of the global fin trade during the sampling period. The resulting estimate of global catch for oceanic whitetip shark (in thousand individuals) was 600 (95%CI: 220–1210).

- An estimate of shark fins imported by Hong Kong for each year was calculated from corrected government records. Hong Kong's share of the global fin market for each decade since the 1980s, and its relative change compared to the anchor year of 2000, was estimated from expert judgement. This comparison reflected a declining share,

owing to an increasing proportion of the fin trade occurring through mainland China and southeast Asia.

- The global catch in numbers for oceanic whitetip shark was predicted in a Monte Carlo framework by drawing randomly from the distributions defined for each quantity: a triangle distribution for the catch of oceanic whitetip shark in the Hong Kong trade in 2000, with catch $\sim$ triangle(600, 220, 1210); a constant for Hong Kong market imports relative to 2000; a uniform distibution for the relative change (ratio) in the share of Hong Kong's market to the global market compared to 2000, with the lower and upper bounds informed by expert opinion. The predicted catches is the product of these three quantities.

- Global catch estimates were then assigned to the Western and Central Pacific Ocean by dividing the global shark trade with three alternative methods: area of the global oceans made up by the Western and Central Pacific Ocean, proportion of the global fishing effort occurring in the Western and Central Pacific Ocean, proportion of the global tuna catch occurring in the Western and Central Pacific Ocean (see details in Clarke 2018).

Predictions of oceanic whitetip shark catches for the Western and Central Pacific Ocean under the trade-based method revealed that total catches were predicted to increase over time, based on the increased size of the Hong Kong fin trade in conjunction with a decreasing global market share (Figure 8). The predictions were also based on the assumption that the proportion of oceanic whitetip shark to all shark fins traded in the Hong Kong market stayed constant over time. The estimates were greater when assigning catch to the Western and Central Pacific Ocean based on the proportion of total tuna catch. The estimates based on an area-breakdown and an effort-breakdown were similar in 2000 (the anchor year).

The 2000 estimate of Hong Kong catch quantity used to anchor the reconstruction was considered accurate, as fins of oceanic whitetip shark are easily identifiable, minimising erroneous fin category classification by traders in the statistics (Clarke et al. 2006a). In the DNA-analysis of species composition by market fin trade category, 100% of samples of the market fin category called *Liu qiu* belonged to oceanic whitetip shark. This species was the only species that had a perfect match to a fin market category (Clarke et al. 2006a). For this reason, estimates of traded fins for oceanic whitetip shark from Hong Kong market records should be more precise than for other species.

The assumption of constant species composition in the Hong Kong fin trade since 2000 is a limitation in the application of the trade-based method to oceanic whitetip shark in the Western and Central Pacific Ocean. Clarke et al. (2006a) estimated that the proportion of oceanic whitetip shark in the Hong Kong fin trade market was 1.8% (95%CI: 1.6–2.1%). This estimate is unlikely to still be current if the abundance of the Western and Central Pacific Ocean stock has declined to the levels predicted by Rice and Harley (2012), as the depletion of oceanic whitetip shark is predicted to be more severe than for most species of sharks, noting also the presence of a non-retention policy for the latter part of the time series. At the scale of the Pacific Ocean,

oceanic whitetip shark fins may reach the Hong Kong market from the eastern Pacific Ocean, as there are shark fisheries in Central and South American countries (e.g., Mexico, Cardeñosa et al. 2018). Nevertheless, these fisheries should not be accounted in the catch estimates for the current stock assessment given they occur outside of the assessment region.

A recent study resampled the Hong Kong market to estimate species composition from traded fins, and found 1% of samples were from oceanic whitetip shark (Fields et al. 2018). Although this number cannot be directly compared with previous values by Clarke et al. (2006a), it is useful as a reference. In contrast, official trade statistics from the Convention on International Trade in Endangered Species of Wild Fauna and Flora (CITES) database reported 5.6% of total fin weight assigned to oceanic whitetip shark; however, when trimmings were genetically analysed, less than 2% of samples were predicted to belong to this species (Cardeñosa et al. 2018).

Without further sampling, there appears to be no robust method to ascertain the proportion of oceanic whitetip shark fins from the Western and Central Pacific Ocean in the Hong Kong market in the recent period. Based on the likely decline in the proportion of fins of this species due to the population decline, the reliability of the trade-based historical catch reconstruction was considered highest in 2000 for this species, and lower thereafter.

The predictions of historical catch for oceanic whitetip shark using the trade-based approach are shown in Figure 8. We were initially going to include a separate catch scenario based on these estimates. Given the concordance between this approach and the alternative based on observer data for the year 2000, as well as the problematic assumption of a constant WCPO oceanic whitetip shark proportion in the global fin trade, we decided to only retain catch scenarios from the observer-based catch reconstruction approach.

2.2.4 Post-release mortality

WCPFC non-retention measures like CMM2011-04, country-specific legislations like shark sanctuaries[1], declining market demand for shark products, gear logistics and/or concerns over crew safety can lead to part or all of the catch for some species of sharks to be discarded. If discarded individuals are alive when released, an unknown proportion might survive the catch-and-release event. Under WCPFC Circular 2016/51, the WCPFC and funding partners commissioned a study aimed at estimating post-release mortality (PRM) of sharks from discarded bycatch in longline fisheries. No oceanic whitetip shark were included in the study but findings for shortfin mako and silky shark predicted higher rates of PRM for smaller sharks as well as sharks released with long trailing leaders relative to their size. Additional datasets highlighted that silky sharks that were injured when released alive had lower chances of survival. Overall, it was predicted that the proportion of sharks that survive the combination

---

[1] In the Western and Central Pacific Ocean, shark sanctuaries or shark-fishing prohibitions have been implemented over part or all of the Economic Exclusive Zones of Cook Islands, Federated States of Micronesia, French Polynesia, Guam, New Caledonia, Marshall Islands, Palau and Tokelau. Most of these measures were implemented between 2012 and 2015.

of haulback, crew handling and post-release mortality was 0.44 and 0.56 for shortfin mako and silky sharks, respectively.

Nomenclature for mortality at different stages of the fishery interaction from hooking to hauling and crew handling, and following release if alive, differs between authors. In this report we used the term 'discard mortality' (DM) to refer to the total mortality resulting from the fishery interaction across all stages, and 'post-release mortality' (PRM) to refer only to the mortality rate for the stage following individuals being released to the water alive.

Catch reconstructions that do not account for discard mortality implicitly assume a discard mortality rate of 100%. This assumption was considered accurate for purse-seine sets as most sharks are brought on-board and go through the process of catch brailing and sorting; it was also considered accurate for longline fisheries targeting sharks (by definition). Nevertheless, a proportion of sharks caught as bycatch and released from tuna and swordfish longline sets are likely to survive. Common Oceans (ABNJ) Tuna Project (2019) included an analysis by SPC of recent longline observer data (2017–2018) that assessed the proportion of oceanic whitetip shark individuals released alive. They found that 75% of individuals were released alive in "good" condition (assessed by the observer). In addition, no oceanic whitetip shark individuals were marked as retained, indicating that CMM2011-04 was fully operational for those years (for comparison many fleets still retained individuals over the post-CMM-2012-04 period of 2013 to 2016 covered in this analysis). Data from the two most recent years were considered better suited to estimate the proportion of individuals released alive, owing to the improved observer coverage and higher reliability of the "condition" covariate required to assess the state of individuals at release.

We used 25% mortality (75% survival) as an optimistic lower bound for the mortality rate for longline discards, and 100% as a pessimistic upper bound (0% survival). We also added an intermediate scenario of PRM for individuals released alive, informed by the findings of Common Oceans (ABNJ) Tuna Project (2019). Under this intermediate scenario 25% of individuals released alive suffer mortality following the release event, in addition to the 25% mortality rate applied to individuals before they are discarded under the optimistic survival scenario. This amounts to a total discard mortality of 43.75% covering all stages of fishery interactions, which is similar to the value estimated by Common Oceans (ABNJ) Tuna Project (2019) for silky shark (44%) and lower than that estimated for shortfin mako (56%).

A 100% discard mortality rate was the value implicitly used by Rice and Harley (2012) in the reference case and sensitivity runs, as hooking, crew handling and post-release mortality were not accounted for in catch estimates (noting also that CMM2011-04 was not yet active over the timespan of the earlier 2012 assessment). White et al. (2018) surveyed observed trips in the shark-targeting fisheries of Papua New Guinea before their closure, and reported that 36% of sharks were dead or dying when brought onboard, and 70% of sharks were dead when discarded. Our three scenarios bound this latter value and also the estimates for shortfin mako and silky sharks in Common Oceans (ABNJ) Tuna Project (2019). Table 3 summarizes the catch scenarios used in the stock assessment.

Given that discard rates have changed over time and between fleets, and that the adoption of CMM2011-04 was not immediate across fleets, we predicted the probability of an individual oceanic whitetip shark being discarded by fleet over year based on the observer data. We used Markov chain Monte Carlo (MCMC) methods with the R package "brms" (Bürkner 2017) to model the probability of an individual being discarded. The observer longline dataset was filtered to retain only sets where at least one oceanic whitetip shark individual had been caught. We aggregated data by flag, year, month and 5°-cell, and calculated the numbers of oceanic whitetip shark individuals discarded and retained from reported fate codes ('DXX' vs. 'RXX'). Individuals discarded with the fate code "DFR" (discarded-fins-retained) were considered as retained. We used a binomial error distribution where the number of successes was the number of discarded individuals, and the number of trials the total number of oceanic whitetip shark individuals caught over the aggregated report. The model was fitted with a categorical effect for year and a random effect for flag. The random effect for flag allowed the prediction of discard rates for flags without observed fishing sets. The model was run with four chains over 2000 iterations, discarding the first 1000 as part of the burn-in period. Summary statistics and predictions by fleet were obtained by drawing from the posterior samples and extracting the median and relevant quantiles.

The year effects estimated for the proportion of individuals discarded by year, independent of flag, show a slow increase in discard rates over time from 1995, and a distinct increase after 2012 (Figure 9). Discard effects estimated for each flag are shown in Figure 10. These are combined into a final model fit in Figure 11 showing both observed and predicted discard rates by key longline observed flags over time.

DM-adjusted catch for the longline bycatch fleet are shown in Figure 12 under the three different scenarios described above applied to the median (baseline) and high catch scenarios. We assumed 100% discard mortality for all catches from the target longline fishery, as well as the two purse seine fleets.

2.2.5 CPUE standardisation

Although the coverage rates of observed longline effort were considerably lower than for purse seine, the reliability of catch numbers estimated by longline sets is considered much higher as observers report every hook with a positive catch event. The previous assessment for this species (Rice 2012b) included standardised indices for other fleets, but these indices were not used in the reference model or the uncertainty grid. At the SPC 2019 Pre-Assessment Workshop (PAW) (Pilling & Brouwer 2019) it was agreed to focus on developing standardised CPUE indices for the longline bycatch fleet, as the underlying data were deemed the most reliable of those available, and also covered the greatest extent within the assessment region.

A similar approach to fitting the CPUE models was used to that for the catch reconstruction model, including the use of a negative binomial error distribution with an additional ν parameter (Section 2.2.2). In practice, the year effects estimated from the catch reconstruction models can be considered to be standardised CPUE rates. Nevertheless, a constraint to

this approach of fitting the catch reconstruction models was that total catch rates would be predicted from the L_BEST and S_BEST datasets, which meant that (1) sets had to be aggregated at a lower spatial resolution of 5 degrees (for the longline dataset), and (2) only covariates available in L_BEST and S_BEST could be considered. In addition, as we were predicting catches across all flags fishing in the Western and Central Pacific Ocean, we had to retain as many flags as possible in the analysis to inform the value of the flag effect in the random effect distribution. Otherwise, the flag effect for a country fishing in the Western and Central Pacific Ocean but excluded from the model fit would be randomly drawn from that distribution. For this reason, we retained as many different flags as possible in the model dataset. These constraints were not present for the CPUE analysis as the key result was the estimated year effects, independent from flags.

As a result, we filtered the observer dataset to retain only observer programmes that had consistent observer coverage over time across the spatial distribution of oceanic whitetip shark. These observer programmes were: American Samoa, Fiji, Federated States of Micronesia, Hawaii, Kiribati, Marshall Islands, New Caledonia and French Polynesia. Sets were filtered to retain only those occurring in SST $\geq 16°$C; sets with catch rates higher than the 99.5[th] quantile of positive catch rates were excluded as they were considered to be active shark targeting. The remaining sets were aggregated over flag, programme code, HBF category (shallow or deep), year, month, and 1°cell.

A range of model structures and combinations of covariates were trialled with the objective of improving model diagnostics and minimising the LOOIC metric. Covariates are described in Table 2.

The best model was:
OCS.obs | trial(sets) = Year + s(SST, k=3) + (1|Program) + s(HBF, k=4) + cluster + (1|Year:Program), including the ν coefficient to scale overdispersion as a function of average catch rates.

This model was similar to the catch reconstruction model for this fleet, but included hooks-between-floats as a continuous instead of categorical variable, and an effect on observer programme instead of flag. These changes were based on comparisons between alternative models using the LOOIC metric.

The first year of the CPUE time series (1995) was the model's intercept. Standardised year-effects for 1996 to 2016 were scaled according to the intercept. The MCMC draws were mean-standardised and back-transformed from the log-link, and summary statistics for each year (median, 2.5[th] and 97.5[th]) extracted to form the standardised index of abundance. The mean-standardised CPUE index resulting from the best model is shown in Figure 13, with diagnostics in Appendix A of (Tremblay-Boyer & Neubauer 2019).

2.2.6   Length-composition data

Length information for captured oceanic whitetip shark individuals exists for most observed longline catch events. Purse seine samples are considerably sparser given length

measurements by purse seine observers are opportunistic.

We extracted length measurements from SPC's longline and purse seine observer databases, filtered to only retain locations within the assessment region (Western and Central Pacific Ocean bounded by 30°N and 30°S) from 1995 to 2016. There was a total of 17457 and 1340 individuals measured in longline and purse seine catch, respectively. Of the total for longline fisheries, data for 6340 individuals were discarded of no length measure was specified, or if no length-length conversion was available for oceanic whitetip shark for the length measure used. Lengths for remaining individuals measured in fork length (FL, tip of the snout to split in the fork) were converted to total length (TL) by adapting the TL-to-FL relationship reported in Joung et al. (2016):

$$TL = 1.22 \times FL + 2.29.$$

To our knowledge, this conversion is the only FL-to-TL conversion available for this shark species in the Pacific Ocean. The most common length-length relationship otherwise used by authors in Pacific Ocean studies of oceanic whitetip shark is:

$$TL = 1.397 \times PCL,$$
where PCL is the pre-caudal length, but this relationship is from a 1976 study of South African oceanic whitetip shark (Bass 1976).

Records with total lengths less than 55 cm were discarded based on the lower bound reported for length-at-births at this value (Seki et al. (1998); Table 1). For the longline fleets, we also removed two individuals with TL exceeding 350 cm, as their sizes exceeded the measure of maximum length reported for this species of 340 cm (Clarke et al. 2015).

Lengths measurements were split between the four model fleets: longline bycatch, all flags but Papua New Guinea and Solomon Islands ($n = 7867$), longline target fisheries, including Papua New Guinea and Solomon Islands ($n = 3048$), purse seine associated sets ($n = 1037$) and unassociated sets ($n = 209$). All measured individuals from Papua New Guinea and Solomon Islands were assumed to come from the target longline fleet as there was no reliable covariate to separate shark targeting sets. The resulting overall distributions are shown in Figure 14.

When disaggregated over time, no clear trend in length composition was apparent, except for the last few years of the assessment period, when there was a decline in the average lengths measured for the longline by-catch fleet (Figure 15). In general, this aspect could be interpreted as a sign of increasing fishing mortality on the population. Nevertheless, the onset of this trend coincided with the adoption of CMM2011-04 and a series of shark protection measures across the Western and Central Pacific Ocean. In addition, larger sharks are more difficult to handle, and might preferably be discarded by cutting the lead before they are brought onboard so that these large-sized individuals may not be measured.

There were also a clear latitudinal spatial trends in measured lengths in the longline bycatch fleet across the Western and Central Pacific Ocean (Figure 16), which was evident across observer programmes active within the same area (Figure 17). Alternatively, this finding might also be due to the distribution of shallow versus deep longline sets, as larger individuals could be more frequently caught in deeper sets. We attempted to reweight the data to ensure that the representation of latitudes stayed constant over time, but the high number of empty or low frequency length bins when disaggregated between latitudes and year created unrealistic features in the resulting re-weighted distributions. Once data were prepared as described above, the length observations were thus aggregated by fleet, year and 5 cm bins, before using them as catch-at-length inputs to the stock assessment without further processing.

2.3   Stock assessment model

The assessment was conducted with Stock Synthesis version 3.30 (Methot Jr & Wetzel 2013). Stock Synthesis is an integrated statistical length-based, age-structured population model that can use a range of data inputs to calibrate the underlying population dynamics model. It has been used in a number of previous shark assessments in the Pacific, including oceanic whitetip shark (Rice & Harley 2012), shortfin mako (ISC Shark Working Group 2018), and silky shark (Clarke et al. 2018). For the current assessment we used three data inputs to inform the model: historical catches, catch-per-unit-effort, and length-frequency data. We maintained the four-fleet structure used in the previous stock assessment, splitting the longline fishery into bycatch and target fleets, and the purse seine fishery into fleets of associated and unassociated sets. We describe below the model structure and parameters. Additional technical details on the Stock Synthesis modelling framework can be found in Methot Jr and Wetzel (2013).

A shark life-history expert panel was convened in 2015 to review existing information for all biological parameters for WCPFC sharks, including oceanic whitetip (Clarke et al. 2015). The biological parameters used for this assessment were informed from this review but also accounted for two more recent papers (published after the expert workshop) that estimated growth and maturity for oceanic whitetip sharks sampled in the WCPO (Joung et al. 2016 and D'Alberto et al. 2017). Biological parameters used in the assessment are described below, see also Table 1 for a comparison between studies.

2.3.1   Population dynamics

Spatial and temporal span: The model covers the WCPFC convention area bounded by the parallels of 30°N and 30°S, and assumes a single well-mixed stock within this region (Figure 3). The assessment covers the period 1995 to 2016. The first year matches the start of observer programs in the WCPO, and thus the collection of shark catch statistics. The end year of 2016 was chosen to maximize the number of observer records as a significant number of entries for 2017 were still missing at the time of extraction from SPC's databases.

Sex-structure: Population dynamics are sex-structured but in practice this only scales the

estimates of spawning biomass since the only sex-differentiated input is that for the weight-length relationships. The sex-differentiated weight-length relationships from Seki et al. (1998) were translated from pre-caudal length (PCL) to total length (TL) using the conversion from Bass (1976), yielding:

$1.1810^{-5} \times TL^{2.86}$ for males;
$2.0210^{-5} \times TL^{2.76}$ for females.

There was otherwise no consistent sex-specific length signals from growth studies, or evidence of a sex ratio differing from 1:1 (Joung et al. 2016). Recruitment was thus evenly split between males and females at birth. Length-frequencies inputs were pooled across males and females (noting also that only some of the measured individuals were assigned a sex by observers). Growth (see below) was also assumed to be the same for males and females.

Recruitment: The model has an annual time-step with recruitment following a Beverton-Holt relationship and a function of spawning biomass at the start of the year. Steepness, representing the proportion of recruits of R_0 when the stock is at 20% of unfished spawning biomass, was fixed at 0.409 following Rice and Harley (2012). In the absence of other information, they defined a range of low steepness values reasonable for sharks, of which 0.409 was the mid-point. Deviates from the stock-recruit relationship (SRR) were estimated but minimal deviation from the relationship was specified ($\sigma_R = 0.1$) as recruitment variability in sharks is unlikely to be high. Further, there was no modal structure in the length-frequency data that could have informed the model on the presence of weak or strong cohorts between years.

Age and growth:

The growth for the diagnostic case was parameterised using a recently published sex-combined Von Bertalanffy growth function for oceanic whitetip sharks in the North-West Pacific (Joung et al. 2016, see also Section 2.4). This relationship was chosen as it ressembled that estimated from another recent WCPO study (D'Alberto et al. 2017) but also included larger sample sizes for fecundity and maturity estimates. A comparison of the different growth curves available for this species in the Pacific is shown in Figure 1, including the Seki et al. (1998) curve that was used in the previous assessment.

The population was divided into 25 age classes including a 'plus-group' for individuals older than 25 years. This differs from the maximum age of 36 used by Rice and Harley (2012). The shark life-history expert panel instead suggested a longevity of 17 years based on observed values (Clarke et al. 2015). D'Alberto et al. (2017) in Papua New Guinea estimated that females mature at 15.8 years of age (albeit from a sample size of two) so 17 years seems unrealistically low. We used a value of 25 as a compromise between these two bounds, and also based on the growth parameter k (see below) and the approach from Mollet et al. (2002) developed for other elasmobranchs.

Lengths were apportioned to 5 cm bins, with a minimum bin size of 55 cm and a maximum bin size of 325 cm. The variation in length-at-age was set to a constant CV of 8.5% of the mean

length-at-age. This value was set to mirror that used in Rice and Harley (2012), noting that the same value was used for the recent silky shark assessment (Clarke et al. 2018), and a similar value of 10% was used in the 2016 North Pacific mako shark assessment (ISC Shark Working Group 2018).

We did not attempt to estimate growth due to the lack of growth-related information in the input datasets.

Natural mortality: Natural mortality was fixed and assumed to be constant across all age classes. For the diagnostic case it was fixed at 0.18, similar to the previous stock assessment for this species. This value was calculated according to the relationship of Pauly (1980).

Maturity and fecundity: Maturity follows a logistic relationship as a function of length. 50% of individuals are assumed to be mature at 194cm, following Joung et al. (2016) who found almost no difference for this value between males and females. This corresponds to an age of about 9 which is much lower than what was found by D'Alberto et al. (2017), but their sample sizes for mature females were very small. The first mature age is set at 8; this differs from Rice and Harley (2012) who used 6. Fecundity is related to female biomass and set to 6 pups per female, independent from length or weight (Seki et al. 1998).

Initial population size and structure: There is little to no information about initial age structure, pre-1995 exploitation rates or catches for oceanic whitetip sharks prior to the first year of the assessment (1995). It is reasonable to assume that the population had already been in an exploited state given its vulnerability to longline fishing gear and the history of this fleet in the WCPO (e.g. Bonfil et al. 2008).

In the absence of an initial age-structure, there are two approaches to parameterize the initial population state in Stock Synthesis. The first approach fits an initial equilibrium F without fitting to uncertain initial equilibrium catches. This gives the model the flexibility to set the initial F in a way that improves fit during the main assessment period when catches are better known. The alternative is to provide an estimate of initial equilibrium catches pre-1995, and fix the equilibrium initial Fs.

We tried both approaches but given the sensitivity of early depletion estimates to initial F values, we used this value as an axis in the structural uncertainty grid (see Table 4) and fixed it to a cumulative value of 0.15 across fisheries for the diagnostic case. Given the lack of information on pre-1995 catches, we set equilibrium catches for each fishery to the average of the catch for the first five years (i.e. 1995-1999). We also included a one-off sensitivity run where initial F was estimated (see Section 2.4).

2.3.2 Fishery dynamics

Fishing mortality:

Fishing mortality in Stock Synthesis is directly estimated to match the observed catch. Fishing

mortality is modelled using a hybrid method that first calculates the initial harvest rate from Pope's approximation, then iteratively adjusts a continuous F so that it matches corresponding catches for each fishery at each time step (Methot Jr & Wetzel 2013). Annual catches were specified in numbers and taken halfway through the year from each fishery. In the diagnostic case, catches for each fleet are assumed to be known with very little error (CV=0.05). Uncertainty about catch levels is instead accounted for as part of the structural uncertainty grid (see Table 4).

Selectivity:

Selectivity defines the proportion of the population that is vulnerable to each fleet for each length- or age-class. We defined selectivity as length-based and time-invariant for each fishery. Selectivities were estimated in the exploration phase but fixed for the diagnostic case and the structural uncertainty grid. This was done to prevent unrealistic selectivity fits for grid runs using extreme combinations of axis levels. We used a double-normal selectivity for each fleet. Double-normal selectivities allow a range of selectivity shapes relevant to oceanic whitetip shark, from dome-shaped with different spread for the right-hand and left-hand limb, to an asymptotic shape with full selectivity for the larger length classes. Based on model diagnostics we assumed an asymptotic shape for the bycatch longline fishery and a dome-shaped selectivity for the remaining fleets (i.e. with selectivity declining back to zero for the larger length classes). A dome-shaped selectivity would make more sense for longline fisheries where larger sharks should be able to bite-off the hook if the lead is monofilament, but diagnostics for an asymptotic shape were better for the bycatch longline fishery. Conversely, an asymptotic shape could also make sense for purse seine fisheries. In practice however, very few large individuals were observed in purse seine length samples, such that diagnostics for dome-shaped selectivities for those fleets were much better. We accounted for these uncertainties by adding one-off sensitivities including dome-shaped selectivity for the longline bycatch fleet and asymptotic selectivities for the purse seine fleets.

Catchability: Catchability is estimated as a scaling constant between the expected value for the fitted CPUE index and corresponding population numbers. It is assumed to be constant over time for the standardized fleets (i.e. the bycatch longline fleet).

2.3.3 Statistical fit to observations

Stock Synthesis estimates population and fishing parameters by minimizing the negative log-likelihood of an objective function from the provided input datasets or assumptions.

Index of abundance (CPUE): A single CPUE index was included in the stock assessment model, for the longline bycatch fleet (Section 2.2.5). The standard error for each year was set to 0.15 on the log-scale in the diagnostic case (i.e. CV=0.15) but this assumption was also tested with one-off sensitivities (Section 2.4).

Length-composition: Length compositions for all fleets were included (see Section 2.2.6) with the variance determined by the observed sample size and frequencies. The variance adjustment

scales the effective sample size for each fleet compared to the actual sample size and was set to 0.01.

Stock-recruit relationship: The stock-recruit relationship (SRR) was assumed to follow a Beverton-Holt spawner-recruitment relationship with a steepness of 0.409 and normal deviates assuming $\sigma_R = 1$ standard deviation for the log-recruitment.

For the oceanic whitetip shark the objective function for the model was thus composed of three main components: the fit to the bycatch longline CPUE index (assuming a lognormal error structure), the fit to the length-composition data (assuming a multinomial error structure), and the fit to the assumed stock-recruitment relationship (assuming a lognormal error structure).

An additional component for the likelihood could be the deviation from specified prior distributions, but no priors were used for the parameters in this model.

See appendix A in Methot Jr and Wetzel (2013) for more details on the formulation of each of the components.

2.4 Assessment strategy

During the model development phase we first focused on improving the fits to the observed data (CPUE and length) and obtaining a stable likelihood profile with an informative minimum. A key part of the early exploration involved assessing which parameters could be informed from the input data and which needed to be fixed. In parallel, different approaches were trialled to handle conflicts between the main sources of input data, as CPUE indicates a steep decline in abundance but there was no clear disappearance of large individuals in the length-composition samples for the same time-period.

The **diagnostic case** was chosen as the version of the model with the best fit to the data while also making reasonable assumptions about model parameterization. From this diagnosic case a set of **one-off sensitivities** was chosen to test the impact on model results of choices about fishery or biological parameters for which there are otherwise no clear justification. These sensitivies are outlined here.

Steepness: Steepness is a challenging parameter to estimate from observations or within a stock assessment model, but it tends to be very influential on assessment predictions given it mediates the relationship between spawners and recruits. We examined the impact of values of steepness of 0.34 and 0.49 in comparison to that of 0.409 used in the diagnostic case.

Natural mortality: Natural mortality is another parameter that is hard to estimate and is influential in most assessments. We tested alternative values of 0.1 and 0.26 in addition to the value of 0.18 used in the diagnostic case.

Alternative growth profile: Growth was a key uncertainty in this assessment given the differences between the two more recent growth studies for oceanic whitetip shark. Changing the parameters for the growth curve can not be made in isolation of other fecundity parameters

that also differed between the biological studies, like the length at 50% maturity, as well as adjustments to the shape of the selectivity curves. We created an alternative growth and fecundity assessment 'profile' based on (Seki et al. 1998) to reflect those differences. A comparison between the variables that differ between the Joung and Seki growth profile is shown in Figure 18. Note that for the Seki profile we also used 30 age-classes instead of the 25 used in the diagnostic case, and lowered the first age at maturity to 4 instead of the value of 6 that was used in the previous assessment. This adjustment was done because the L_{50} from the maturity curve estimated by Seki et al. (1998) corresponded to an age of 4.5 on the growth curve from that same study, and so was not consistent with an age at first maturity of 6.

Catch scenarios: Historical catch estimates form a high source of uncertainty in sharks assessments in general, and this one in particular. The diagnostic case scenario used the median prediction from the catch reconstruction model assuming a 25% mortality on discards and 0% post-release mortality on individuals released alive. Figure 19 shows a summary of historical catches under this catch scenario for all fleets. Two alternative discard mortality scenarios were included, one where 25% of individuals released alive suffered additional mortality and one where the overall discard mortality was 100% (see Section 2.2.4). In addition, a high catch scenario setting annual catches to the 90th quantile of predictions from the catch reconstruction models was used in combination with the 3 discard mortality scenarios described above. This lead to a total of 6 catch scenarios, described in Table 3.

Initial fishing mortality: Initial fishing mortality was fixed in this assessment which means that it can scale the productivity on the stock based on the combination of initial fishing mortality and equilibrium catch (e.g. a higher initial F for the same amount of catch implies a less productive stock than one with a lower initial F). We used scenarios of cumulative initial Fs across fleets of 0.1 and 0.2 in addition to the value of 0.15 used in the diagnostic case. We also included a scenario where we let Stock Synthesis estimate initial F for each fleet based on fit to the observed catch time series, without specifying initial equilibrium catches.

Standard deviation in recruitment: In the diagnostic case very little deviation around the SRR (σ_R) was allowed under the assumption that such deviations should be minimal for a species of shark. We tested the impact of this assumption by setting σ_R=0.2, thus allowing a greater amount of deviation.

Dome-shaped selectivity on longline bycatch fleet: The diagnostic case assumed asymptotic selectivity for the bycatch fleet, i.e. full selectivity for larger individuals. We tested this assumption by forcing the right-hand limb of the selectivity curve for the longline bycatch curve back to zero, resulting in a dome-shaped selectivity for this fleet. Under this sensitivity, there are thus no asymptotic selectivities for any fleet.

Asymptotic selectivities on purse seine fleets: The diagnostic case assumed dome-shaped selectivity for both purse seine fleets, implying that large individuals are not caught by this fleet. We tested this assumption by setting selectivity to be asymptotic for these fleets instead.

Estimating all selectivities: Selectivities in the diagnostic case were fixed based on previous

model explorations. Under this sensitivity run we allowed all six parameters for the double-normal selectivities of the four fleets to be fitted by the assessment model.

Fixed CPUE standard error: The standard error estimated from the CPUE standardization model were quite large especially in the earlier part of the time series. This implied that the assessment model was less constrained by the CPUE index, and resulted in poor fits to the CPUE. We forced the model to a closer fit to the CPUE in the diagnostic case by setting the CPUE CV to 0.15 but also tested the sensitivity of predictions to the chosen value with alternatives of 0.10 and 0.20.

CPUE standard error from model: As above but using the standard error estimated from the CPUE standardization model directly.

Decreasing recruitment lambda: Stock Synthesis allows the contribution of each component to the total likelihood to be independently modified. In the diagnostic case the total likelihood is strongly driven by assumptions about recruitment. With this sensitivity run we decreased by half the importance of recruitment in the total likelihood calculation.

Finally, based on the results from the one-off sensitivies and previous discussions at the Pre-Assessment workshop (Pilling & Brouwer 2019), a set of uncertainty axes for the model was defined outlining alternative values for key uncertain and influential model or biological parameters. The combination of all levels across axes forming the *structural uncertainy grid* is described in Table 4 and results in a total of 648 model runs.

2.5 Reference points

Final indicators of stock status are determined from summary statistics of the model runs included in the structural uncertainty grid. Higher weights can be given to levels within specific axes that are deemed more plausible. We calculated reference points over the full grid with equal weights to all levels but included suggested weights for each axis level in Table 4.

We use the following reference points as indicators of stock status, noting that the WCPFC has yet to adopt reference points for sharks. These metrics can be calculated over a single year (e.g. the last assessed year, 2016) or a recent time-period (e.g. the last 3 or 4 years of the assessment, excluding the last year). In this assessment the *latest* time-period was 2016 and the *recent* time-period was 2013 to 2016. This definition was used for both F-based and SB-based reference points. The 'recent' range was chose to represent the post-CMM2011-04 period (i.e. after January 1$^{\text{th}}$ 2013 when the measure became active). See Table 5 for a summary of all catch measures and reference points used.

- SB/SB_0: The unfished spawning biomass (SB_0) can be calculated from the estimated recruitments *via* the Beverton-Holt SRR. This allows the comparison of the exploited population for an index year or time-period to the population subject to natural mortality only. This definition does not account for environmental impacts on recruitment, so SB_0 is always equal to $SB_{F=0}$. At the PAW (Pilling & Brouwer 2019) it was agreed to present

SB/SB_0 as a useful metric of stock status that is also used for other stocks managed by the WCPFC. Under this metric, an increase in depletion is linked to a lower value for SB/SB_0 and a worsening in stock status. Conversely a decrease in depletion is linked to a higher value for SB/SB_0 and an improvement in stock status.

- SB/SB_{MSY} is the ratio of the spawning biomass for an index year or time-period to the spawning biomass predicted to result in Maximum Sustainable Yield (MSY).

- F/F_{MSY} is the fishing mortality over the assessed stock for an index year or time-period across all fleets divided by the fishing mortality predicted to result in Maximum Sustainable Yield (MSY). A value of F/F_{MSY} in excess of 1 means that the stock is fished at a rate beyond that expected to maximize stock productivity.

- $F/F_{lim,\text{AS}}$ and $F/F_{crash,\text{AS}}$: The PAW requested the presentation of alternative reference points, if possible, and Zhou et al. (2018) evaluated candidates reference points for elasmobranchs for consideration by SC in 2018. We are thus including here a version of two of the F-based reference points they considered, F/F_{lim} and F/F_{crash}, and note that another reference point they presented, F/F_{msm}, can be considered equivalent to F/F_{MSY} in the context of an age-structured model. F/F_{lim} is the fishing mortality that leads to a biomass decline to 0.5 of B_{MSY}; F/F_{crash} is the minimum unsustainable instantaneous fishing mortality rate that could lead to population extinction in the long-term (Zhou et al. 2011). A value of F/F_{crash} in excess of one implies that the population will go extinct should that rate be maintained on the long-term. F_{lim} and F_{crash} can be derived directly from R_{max}, the maximum theoretical net productivity rate for a stock at a small size. R_{max} can be estimated from life-history parameters, including von Bertalanffy growth rates, age-at-maturity, maximum age, sex ratio, litter size and breeding interval. Alternatively, in an age-structured stock assessment model, F_{lim} and F_{crash} can be obtained from yield simulations, in which case F_{lim} is the value of F leading to biomass declining to $0.5SB_{\text{MSY}}$, and F_{crash} is the value of F at which yield becomes 0 (for values of F greater than F_{MSY})[2]. This is the approach we took here. We also used spawning biomass and not total biomass to determine F_{lim}, to match with other spawning biomass-based reference points used by the SC. Because we are calculating these reference points from an age-structured model instead of the surplus production framework where they were initially defined, we refer to them as $F_{lim,\text{AS}}$ and $F_{crash,\text{AS}}$.

3. RESULTS

3.1 Developments from the last assessment

The following changes were made from the Rice and Harley (2012) assessment:

- The Stock Synthesis executable was updated from 3.21 to the latest version (full version

---

[2]Note that in this case there could technically still be individuals remaining in the population if there were length where individuals were not selected by any fleet. In this assessment that is not the case for any length bins.

number: 3.30.08.03);

- The age at first maturity was shifted down from 6 to 4 based on length at M_{50}=175cm specified in the reference case model, corresponding to an age of 4.5 in the Seki growth curve used;

- The historical catch data were updated with the new reconstructions, extending the model from 2009 to 2016;

- The CPUE time series for the longline bycatch fleet was updated;

- The length-composition data for all fleets were updated, including a revision of the range of length bins from 55 cm to 325 cm and an increase of bin width to 5 cm;

- Optimal selectivity shapes were re-defined and fixed at new values;

- The likelihood weight of the purse seine unassociated fleet was reduced to 0.1 compared to default of 1 to reflect the sparsity of length records for this fleet;

- Equilibrium catches were set to the average for 1995-1999 for each fleet, and initial F was redistributed to match the distribution of equilibrium catches between fleets;

- The standard error on the CPUE was constrained to a constant value of 0.15 across years;

- A new growth and fecundity profile was assigned to the population, including updated growth curve parameters, a minimum maturity age of 8, an increase in the length at 50% maturity, and a decrease in the number of age-classes from 36 to 25.

The stepwise impact of these changes on spawning biomass and spawning biomass depletion trajectories are shown in Figure 20. We were able to exactly reproduce the 2012 depletion trajectory with the new executable. Lowering the age at first maturity reduced the initial depletion in spawning biomass, and increased the scaling of the initial spawning biomass. Updating the historical catch time series had an important impact on the depletion trajectory, increasing SB/SB_0 over the full time series (except for the first year when it is constrained by other assumptions), as well as scaling up the spawning biomass by more than half. This resulted from the combination of the same level of initial F with higher equilibrium catches from the new catch reconstruction. The new CPUE time series for the longline bycatch fleet also improved the history of stock status, with stock status predicted to improve slightly from a 2013 low and final depletion levels at ~5% of SB_0 and concurrent higher levels of final spawning biomass. Updating the composition data did not impact the spawning biomass or the depletion trajectory but did increase the initial depletion by a small amount.

The subsequent steps of changing the shape for the selectivities, reducing the likelihood weight of the poorly-sampled unassociated purse seine fleet and re-distributing the initial F and equilibrium catches had minimal effects on spawning biomass or spawning biomass depletion over time. Constraining the fit to the CPUE by fixing the standard error to 0.15 increased both initial and final levels of depletion by a small amount, with a final value predicted to

be at $\sim$4.5% of SB_0. Finally, the new growth and fecundity profile introduced a number of simultaneous changes which shifted the productivity profile of the population from that used by Rice and Harley (2012) towards a less productive one. Under this new growth and fecundity profile, the spawning biomass was scaled down by more than half. The initial depletion was more pronounced ($\sim$0.3 from 0.43 in the previous step), and the spawning biomass tended to be more depleted throughout the assessment span. This new productivity profile in conjunction with the previous changes described here formed our diagnostic case, with predicted final depletion levels to be at 3.1% of SB_0 for the spawning biomass.

3.2 Diagnostic case

The diagnostic case for the assessment is the model with the best overall diagnostics and an informative likelihood profile, that also made the most reasonable assumptions about biology and fleet settings based on current knowledge about oceanic whitetip shark and the fisheries that catch this species. We used growth and fecundity parameters from the Joung et al. (2016) study as they resulted in the best fit to the length data, sampled individuals during the time span of the assessment, and its predictions also overlapped with that of another recent growth study by D'Alberto et al. (2017), also in the WCPO (Figure 1). Other key parameters are shown in Table 4.

The CV for the CPUE was constrained to a value of 0.15 over the whole time-period. This resulted in a moderately good fit to the observed CPUE (Figure 21), with the earlier, more variable period being fit well on average but the more recent increase in CPUE from 2012 onwards being fit at the lower end of the error bounds. The tight constraint on the SRR curve implies that there is relatively little flexibility in the model to adjust recruitments to fit year-to-year variations in CPUE.

An asymptotic selectivity was used for the bycatch longline fleet, with 50% selectivity reached at about 150 cm and maximum selectivity at 200 cm. For the target longline fleet, a dome-shaped selectivity was used with maximum selectivity around 190 cm, declining to $>$ 0.10 selectivity past 250 cm and to zero for the largest length. For the associated purse seine fleet, we used a dome-shaped selectivity peaking at about 140 cm, with $\sim$ 0.1 selectivity for the smaller lengths. Finally, for the unassociated purse seine fleet we also used a dome-shape selectivity but with a flatter dome with full selectivity between lengths 160 cm and 240 cm, starting at $\sim$ 0.1 for the smaller lengths and declining to $>$ 0.10 selectivity past 250 cm. These are shown in Figure 18 along with the selectivities used under the alternative growth and fecundity profile.

The fit to the catch-at-length data was very good for all fleets when observations were aggregated over time (Figure 22) but less consistent for year-to-year predictions (Figure 23). This was expected given the inter-annual variability in the average value for the length observations, paired with time-invariant selectivity which assumes constant selectivity for all fleets over time.

The likelihood profile over the unfished recruitment (R_0) shows that the model fit is largely

driven by assumptions about recruitment, and that there is a clear minimum matching that estimated under the diagnostic case (Figure 24). This comes from the tight constraint on the stock-recruitment relationship implied by setting σ_R to a low value and the fixed steepness. Despite its much lower influence, the likelihood profile for the CPUE also has a minimum matching that of the recruitment component. However the left-hand limb of the profile does not show much contrast, indicating that the CPUE is more useful on its own in setting an upper bound for unfished recruitment, but is relatively uninformative in terms of the lower bound. The individual fleet signals for the catch-at-length components show a conflict between the longline by-catch *vs.* the longline target and the purse seine associated fleets. Fit to the longline by-catch data improves with a lower unfished recruitment, while fit for the longline target and the purse seine associated fleets is better with a higher unfished recruitment. There is a slight decline in mean length over recent years in the longline by-catch fleet, which could explain the relative value in likelihood for this component. The likehood profiles for the target longline and purse seine associated fleets are consistent with the lack of clear signal in length over the duration of the assessment. None of the minima for these individual fleet profiles match those of the combined components. Finally, the purse seine unassociated fleet catch-at-length data was downweighted and it did not influence the total likelihood values.

The predicted SRR curve is shown in Figure 25 with minimal deviations from predicted recruitments given the low value of σ_R assumed for the diagnostic case.

The predictions of total biomass, recruitment and spawning biomass resulting from the diagnostic case are shown in Figure 26, including also the predictions under the alternative growth and fecundity profile based on Seki et al. 1998. There is an overall decline in all three quantities over the time span of the assessment, after a slight increase at the beginning driven by the increase in CPUE between 1995 to 2000. The estimates in total and spawning biomass are scaled up under the Seki alternative growth profile. However, the number of recruits is predicted to be slightly higher under the Joung growth profile used for the diagnostic case. This results from the different predicted distributions of n-at-age between the two curves.

Fishing mortality is highest for the longline by-catch fleet (Figure 27) over the time series. It increases from 1995 levels to about 0.25 over 2000-2010, with high annual variations. It peaks sharply in 2012 and declines thereafter given the diagnostic case catch scenario accounts for discard mortality (scenario 'MedianDM25'). Fishing mortality for all other fleets is predicted to be negligible in comparison to that by the longline by-catch fleet.

Maximum Sustainable Yield (MSY) is predicted to be $\sim$3000mt for the diagnostic case and $\sim$4900mt under the alternative growth and fecundity profile, with F_{MSY} relatively similar and very low for both, at $F = 0.054$ and $F = 0.067$, respectively Figure 28. This very low F_{MSY} reflects the low value of steepness assumed for this stock.

3.3 One-off sensitivities

Figure 29 shows the depletion trajectories for key one-off sensitivities from the diagnostic case. We looked at assumptions under 4 broad categories: biological factors, impact of fishing, fleet selectivities and weights on input data.

Under biological assumptions (Figure 29 top left), the alternative growth profile and the assumed natural mortality had the most impact on spawning biomass trajectories. Under the Seki growth profile the initial depletion was not as important and levels of final depletion are also slightly lower than for the diagnostic case. Increasing and lowering natural mortality respectively lowered and increased the inital depletion, but had minimal effect on final levels.

The most influential assumption for the impact of fishing (Figure 29 top right) was the value for the initial fishing mortality. With a higher initial F the stock was considered to be more depleted at the start of the time series, and conversely with a lower initial F the stock was considered to be less depleted. Alternative catch scenarios had minimal impact on overall spawning biomass trajectories but catch scenarios accounting for discard mortality showed a small increase in SB/SB_0 from 2013 onwards whereas spawning biomass trajectories continued downwards from 2013 levels for the other catch scenarios.

The assumed shape for the fleet selectivities (Figure 29 bottom left) had a small impact on initial levels of depletion, with the sensitivities for model-estimated selectivities and dome-shaped selectivity for the longline by-catch fleet both showing lower levels of initial depletion. The sensitivity including asymptotic selectivity for the purse seine fleets resulted in a small increase in depletion at the start of the time series only.

Finally, changing the influence of different model components on the likelihood (Figure 29 bottom right) had minimal effect on SB/SB_0, except when the influence of recruitment assumptions was diminished by 4-fold (to 0.25) and the constraint on fitting CPUE increased with a standard error of 0.1. In that instance the depletion levels were not as pronounced from 2000 to 2008 but the difference was never more than 0.05. Final depletion levels were unchanged. Also, using the standard error for the CPUE estimated by the CPUE statistical model instead of constraining the standard error to improve the fit to the index resulted in a small increase in final SB/SB_0, by about 1%.

3.4 Structural uncertainty grid

The median 2016 depletion (SB/SB_0) over all runs of the structural uncertainty grid was 3.7% (95%CI: 2.1–6.1%), from an initial median depletion in 1995 of 33.5% (95%CI: 14.7–59.2%). The trajectory is shown in Figure 30, and Figure 31 and Figure 32 show individual runs for each axes highlighting the effect of levels within the axes, and median and inter-quartile bounds by level, respectively. Summary distributions of SB/SB_0 and F-based reference points, and Kobe plots for the final year of the assessment are shown in Figure 33 to Figure 37. Additional panel plots show the distribution of SB/SB_0 against all three F-based reference points Figure 38 to Figure 40. Note that there was a small number of runs (6) with unlikely combinations

of levels (e.g. low steepness, high M, high catches) that did not converge or converged on implausible estimates. These runs were excluded from graphics and from summary statistics for the minimum and maximum values.

All axes of uncertainty had a greater effect on initial levels of depletion than on the final estimates. The three most influential axes were the initial fishing mortality, the natural mortality and the growth profile. Under higher levels of initial fishing mortality the stock was assumed to start at higher levels of depletion provided catch levels were the same. Similarly, lower levels of natural mortality implied a stock that is less productive, and so the initial SB/SB_0 is lower. That trend is maintained over the assessment's time span. Finally, the more productive growth profile using the Seki et al. 1998 implied higher SB/SB_0 throughout the time series compared to the less productive growth profile using the Joung et al. 2016 parameters, but there is more overlap in individual runs based on the value of other parameters. The catch scenarios did not change the overall depletion trajectory but did impact post-2013 rates of change: under the scenarios accounting for discard mortality there is a slight recovery in spawning biomass starting in 2013 due to a decline in catches in the latter part of the time series.

The relative impact of axes of uncertainty on reference points for the final year of the assessment (2016) is especially visible when looking at F-based reference points (Figure 34 and 36). Under F/F_{MSY} (Figure 34), the median and inter-quartile bounds predict the stock to be overfished ($F > F_{MSY}$) under all axes. Unlike for the depletion trajectory, the most influential uncertainty axis was the catch scenario and, more specifically, whether survival rates in the discards is accounted for (i.e. DM < 100%). In that instance F/F_{MSY}, while still being above 1, was reduced from a median value of 5.87 to a median value of 3.08 and 2.14 for the Median catch DM scenarios assuming 43.75% and 25% total discard mortality. Steepness and natural mortility were also influential axes but to a much lesser degree, with F/F_{MSY} being higher and more variable for lower steepness and lower natural mortality. Other axes which were influential on overall population trajectories and especially the initial status of the population had very little effect on the final value for F/F_{MSY}.

The impact of the catch scenario axis was also visible when looking at the $F/F_{lim,AS}$ and $F/F_{crash,AS}$ alternative reference points (Figure 35 and 36). In that case, all runs with catch scenarios not including for discard survivals ('MedianDM100' and 'HighDM100') predict that $F/F_{lim,AS}$ and $F/F_{crash,AS}$ exceed 1, with a median value for $F/F_{lim,AS}$ of 3.86 and 3.96, and for $F/F_{crash,AS}$ of 2.48 and 2.63, for the Median and High catch scenarios respectively. For the catch scenarios accounting for an intermediate amount of discard mortality (43.75% total), all runs exceeded $F/F_{lim,AS}$ = 1 and 77.8% and 84.0% of runs exceeded $F/F_{crash,AS}$ = 1 for the Median and High catch scenarios. Median values for the Median and High catch scenarios were $F/F_{lim,AS}$ = 2.02 and 2.15, and $F/F_{crash,AS}$ = 1.32 and 1.41 respectively. Finally, 83.3% and 84.2% of runs with the optimistic catch scenarios assuming a total discard mortality of 25% exceeded $F/F_{lim,AS}$ = 1, and 33.3% and 45.4% of runs exceeded $F/F_{crash,AS}$ = 1 under the median and high catch scenarios.

The other influential axis was that of the growth profile. Under the more productive Seki growth profile 89.1% of runs exceeded $F/F_{lim,\text{AS}} = 1$ and 58.7% of runs exceeded $F/F_{crash,\text{AS}} = 1$ with median values of 1.83 and 1.18 for these two metrics. Under the less productive Joung growth profile 100% of runs exceeded $F/F_{lim,\text{AS}} = 1$ and 87.9% of runs exceeded $F/F_{crash,\text{AS}} = 1$ with median values of 2.55 and 1.75.

Finally, the Kobe plots highlighting SB/SB_{MSY} vs. F/F_{MSY} in the final year of the assessment for each axis of the structural uncertainty grid (Figure 37) show that all of the grid runs were located in the upper-left quadrat of the plot, indicating a stock that is overfished and undergoing underfishing. Panel plots that compare SB/SB_0 to the three F-based reference points are also included in Figure 38 to 40. These show how interactions between levels across axes can impact the stock status, notably, model runs under the more productive Seki growth profile combined with more optimistic catch scenarios result in lower levels of F and higher levels of spawning biomass compared to SB_0 in the final year of the assessment. Conversely, model runs with the less productive growth profile combined with more pessimistic catch scenarios result in higher levels of F and lower levels of spawning biomass compared to SB_0.

4. DISCUSSION

This is the second stock assessment for oceanic whitetip shark in the WCPO following that of Rice and Harley (2012), and the first since CMM2011-04 enacting a no-retention measure for this species for WCPFC member countries became active in 2013. For the previous assessment and that of sharks in general, biological parameters and catch histories are highly uncertain. Strong assumptions had to be made about the values for a number of key assessment parameters, notably, the spawning-recruit relationship which was assumed to be strongly linked to the number of spawners, with little variability permitted. In addition, there was conflict between the key input datasets of CPUE and catch-at-length compositions: the CPUE showed a steep decline over the assessment's duration but the catch-at-length showed no concurrent decline in mean length that would have been indicative of a degradation of the age structure due to overfishing. Nonetheless, a broad range of assumptions were tested under a structural uncertainty grid and while the 1995 stock status was very sensitive to these assumptions, more than 80% of the 648 uncertainty runs converged to a final depletion status for the spawning biomass below 5% (100% $SB/SB_0 < 0.10$). Even the run with the most optimistic combination of parameters (fast growth, low catches, low initial F, high natural mortality, high steepness, and high recruitment deviation) predicted the stock to be overfished and undergoing overfishing ($SB/SB_0 = 0.059$, $F/F_{MSY} = 1.09$). Therefore, while strong assumptions are made in the stock assessment model, we are confident that the final conclusions about stock status are robust to these.

There were two key differences between the data and life-history inputs in this assessment compared to the previous one. First, the historical catch reconstructions were updated with a new methodology. This updated approach still relied on extrapolation from observed catch rates in the longline and purse-seine fleets, but resulted in historical catches predicted to

be slightly lower in the first part of the time series than for the previous analysis. We also undertook a separate catch reconstruction based on a completely different approach (global fin trade statistics), and there was good concordance between the catches we predicted for the year where the catch predictions for this second approach are the most reliable for oceanic whitetip sharks (2000). This gave us confidence in our catch reconstruction model. Observed rates between 1995 and the early 2000s are unreliable and very variable, and with a very low effort coverage it is expected that catch extrapolations for this method would be highly sensitive to the underlying statistical model.

Uncertainty about historical catches was accounted for by creating scenarios of alternative catches directly based on the distribution of possible catches predicted by the statistical model. For the baseline catch scenario we used the median value of catches predicted and for the high catch scenario we used the 90th quantile of catches predicted. This differs from the 2012 approach where a multiplier of two was applied to the catch history, but accounts for the fact that we have higher certainty in the predictions of catches in the latter part of the time series due to the improved observer coverage.

Our predictions of catches for the target longline fleet were lower than for the previous assessment. They were directly modelled from observer catch rates and effort for the participating countries instead of making an assumption about the amount of shark-targeting effort. Both observed catch rates and overall effort for this fleet are highly uncertain, and we have low confidence in the quality of our catch reconstruction for this fleet based on these data. However, we still felt it was important to attempt to directly model them as a first step. While the assessment's conclusions are robust to assumptions made for this fleet's catch, it should be possible to improve the quality of the data informing the historical reconstruction for this fleet with greater collaboration with the participating countries. This fleet is thought to have halted its activity in 2014 but still forms an important part of the catch history of oceanic whitetip shark.

The second key difference with Rice and Harley (2012) is the assumptions made for the life-history parameters. Two WCPO studies were recently published (Joung et al. 2016 and D'Alberto et al. 2017) which showed different growth and fecundity profiles than what was used for the 2012 assessment based on a study by Seki et al. (1998). Both of these new studies predict slower growth and higher maturity-at-age for this species, implying a less productive stock that could be more sensitive to the impacts of fishing. The new studies were based on smaller areas than the Seki et al. (1998) study which covered a broad area across the North Pacific, but they also sampled individuals during the core of the assessment's time period in contrast to Seki et al. (1998) which sampled individuals from the early 1990s. We accounted for this uncertainty in life-history parameters by defining two growth and fecundity profiles for the assessment and accounting for them as part of the structural uncertainty grid. While the stock status predictions made under the more productive growth profile were predictably more optimistic, the resulting categorization of stock status as overfished and undergoing overfishing remained unchanged.

This assessment accounted for post-release mortality in the predictions of historical catches for longline fleets. To our knowledge, this is the first Pacific shark assessment to directly do so. This additional step was essential in order to properly account for the potential impact of CMM2011-04 on stock status. We used three scenarios of discard mortality, one of which forms a best estimate that accounts for changing discarding rates by fleets over time and recent PRM research. This more-likely scenario assumes a total discard mortality of 43.75% and is bounded by a more optimistic scenario of lower discard mortality (25%) and one assuming 100% mortality on all catches, which is the *de facto* assumption made for historical catch reconstructions that do not account for discard mortality. Our best estimate for PRM when individuals are released alive was informed by PRM tagging studies for shortfin mako and silky shark. While some experimental data has been collected as part of an oceanic whitetip shark PRM study (Common Oceans (ABNJ) Tuna Project 2019), the results are yet to be finalized. Common Oceans (ABNJ) Tuna Project (2019) highlighted considerable uncertainty in the mapping of PRMs from tagging studies to unobserved fishing vessels due to the treatment of captured sharks from the time the line is hauled to when they are released. The bounds in survival rate used for our catch scenarios thus reflect true uncertainty in the value of this variable for oceanic whitetip sharks, but are still deemed to be a reasonable representation of the current state of knowledge on this topic.

Standardized catch-per-unit-effort (CPUE) from the longline bycatch fleet was a key input to the assessment. The standardized index pointed to a general decline in abundance over time from 1999, with highly variable and imprecise estimates for the earlier part of the time series and a slight increase in abundance from 2013 onwards. CPUE indices in both the earlier and the latter period of the assessment are less reliable than for other years. For the early period the observer coverage for the longline fleet was extremely low and very variable among years. This resulted in wide uncertainty bounds estimated for the CPUE during that period, and high year-to-year variations. We ended up constraining the standard error for this time period but also showed that assessment conclusions were robust to the assumed uncertainty for this data input. CPUE as an index of abundance is also less reliable in the later period following CMM2011-04 and CMM-2014-05. In the case of CMM2011-04, the no-retention measure means that many sharks are being cut-off from the line without being brought on-board. There have been anecdotal reports that these cut-off events are not always recorded by observers, and that the way unobserved cut-off events are recorded is not consistent between observer programs or in the years since CMM2011-04 started. This implies that a higher number of sharks might be caught than recorded, which means that any increase in abundance resulting from declining fishing mortality post-CMM2011-04 might not be captured accurately by the CPUE index. In parallel, CMM2014-05 banning the simultaneous use of shark lines and wire traces should reduce catch rates for sharks, including oceanic whitetip shark. However, it is hard to account for this in the CPUE standardization model given these gear variables were recorded unevenly between observer programs and across time.

Catch-at-length data are another key input to the stock assessment as trends in the caught lengths could be indicative of fishing mortality on the overall stock, as well as growth patterns

over time. For this assessment most of the length records came from the longline fleets. There was no clear signal in mean length across time, except in the case of the longline bycatch fleet that showed some decline in mean length from 2012 onwards. This might be linked to CMM2011-04 as length is only recorded for individuals brought on-board for most observer programs (except for the US observer programs), and large individuals are more likely to be cut-free directly from the line instead of being brought on-board. It is possible to approximate length from individuals while they are in the water but the precision is much lower, and such low-precision measurements are typically excluded from WCPFC stock assessments. However, the number of length measurements has markedly declined over the recent period of the assessment due to individuals not being brought on-board. Because of this we are loosing a potentially important index of stock status to inform stock assessments. This is a serious concern as there are already relatively few length measurements for oceanic whitetip sharks over the time-span of the assessment, which challenges the inclusion of this dataset as an informative input to the population dynamics model. There are other features of the length composition data which complicated its interpretation. Notably, there was uneven sampling between fleets over the region covered by the assessment, which means that it may not be truly representative of the catch-at-length for all fleets over time. In addition, there was a distinct north-south increase in mean length that we were unable to standardize for. This spatial trend in length could be due to biology or to sampling, and might confound the identification of a clear time signal from the catch-at-length data. Consequently the catch-at-length data were downweighted in the assessment but this data input could potentially become more informative with further analyses, at least for the longline fleets that hold the most records. Also, a high proportion of longline records had to be discarded as no length-length conversion existed for the measure recorded (lower jaw to fork in tail).

Finally, following the recommendations from PAW (Pilling & Brouwer 2019), we included two alternative reference points in our summaries of stock status, $F/F_{lim,\text{AS}}$ and $F/F_{crash,\text{AS}}$. These were presented by Zhou et al. (2018) in their review of candidate reference points for WCPFC sharks last year and can be related to R_{max} or F_{MSY}. They were initially developed in a surplus production framework but we applied them here to an age-structured model by defining $F/F_{lim,\text{AS}}$ as a function of spawning biomass and $F/F_{crash,\text{AS}}$ from yield simulations.

4.1   Main stock assessment conclusions

Stock status was obtained by summarizing reference points over 648 model runs accounting for assumptions about life-history parameters and impact of fishing underpinning the assessment. We found the stock to be overfished and undergoing overfishing based on SB/SB_{MSY} and F/F_{MSY} reference points and assuming equal weightings for grid levels. This overall conclusion is the same as that from the previous assessment, despite a wider range of uncertainties being considered, notably in the growth and fecundity parameters.

We found that fishing-based reference points were improved in the period since CMM2011-04 became active, which covers the last 4 years of the assessment's time-span (2013–2016).

Notably, F/F_{MSY} is predicted to have declined by more than half from 6.12 to 2.67 (median) for the last year of the assessment when the impact of the conservation measure on survival is accounted for under 25% and 43.75% discard mortality scenarios. This is based on the assumption that observed discarding rates and the range of discard mortality parameters measured on observed trips are representative of those occuring on unobserved vessels. Two alternative reference points, $F/F_{lim,\text{AS}}$ and $F/F_{crash,\text{AS}}$, follow similar relative trends to that for F/F_{MSY} following the adoption of the measure. However, $F/F_{crash,\text{AS}}$ still remains above 1 (median: 1.1, 95%CI: 0.52-2.48), even when accounting only for scenarios that assume discard mortality < 100%.

All catch scenarios accounting for DM < 100% showed a very slight increase in spawning biomass since 2013, but final levels of depletion remain very low over all grid runs (median: 0.0367, 95%CI: 0.021 to 0.061). Given the assessment assumes oceanic whitetip sharks to become mature after 4 or 8 years, it would be expected for stock recovery to be slow in the period following CMM2011-04 while the spawning biomass rebuilds. Despite the relative improvements in F-based reference points since 2013, the median value of $F/F_{crash,\text{AS}}$ over all grid runs for 2016 remains above 1 (1.41), indicating that the population should go extinct in the long-term under this level of fishing mortality.

4.2 Recommendations

This assessment estimates that CMM2011-04 may have had a positive impact on stock status by decreasing fishing mortality. However, there are two key sources of data informing stock assessments that are compromised by observer practices not having adapted to the post-CMM2011-04 period:

- Longline observer programs need to ensure there are clear and consistent directives about how unobserved discarded-cut-free (DCF) individuals are to be recorded. Not recording DCF events can seriously compromise the quality of the catch rates time series used both as an index of abundance and to reconstruct historical catches for shark assessments. **We recommend that all DCF events are recorded even if unobserved, and that in the instance where the species could not be identified, that the species be recorded at the highest taxonomical level possible**, even if in the absence of information that level is 'shark' or 'unidentified'.

- **We recommend that approximate length measurements should be recorded even if individuals are not brought on-deck, with an estimate of precision**. This is already done by some observer programs operating in the WCPO, and would ensure that the time series of length measurements is not compromised even if the precision of length estimates is lower.

- **We recommend that alternative analytical methods incorporating coarser bin lengths for part of the time series be investigated.**

In addition, we make the following recommendations about additional research into the biology of oceanic whitetip shark and of data inputs that impact its assessment:

- The predictions of recent and latest stock status were highly sensitive to assumptions made about discard and post-release mortality for oceanic whitetip shark. In particular, the final status in relation to F-based reference points was more sensitive to assumptions about discard mortality than the scaling of the overall catch. **We recommend that ongoing and new studies on this topic for this species be prioritized and projections of current stock status be updated with estimates of PRM specific to oceanic whitetip shark in the WCPO.**

- **We recommend that observers record the length of the trailing branchline when individuals are cut-free, as current evidence indicates this variable might be influential in PRM rates.**

- **We recommend that spatial trends in shark length for the longline dataset be analysed in a dedicated study in order to determine the likely cause for a north-south increase in the mean length observed, and that approaches to standardize the length dataset be investigated accordingly**. This might enable the detection of a temporal signal in lengths which could inform the assessment model.

- There is a single fork length to total length conversion for the oceanic whitetip shark in the WCPO, based on a fork length measurement starting from the upper jaw (UFL). Comprehensive length-length conversions would facilitate the inclusion of data collected elsewhere in a different length format. **We recommend that additional length-length conversions be obtained, and, more specifically, a length-length conversion from total length (TL) to fork length measurements starting from the lower jaw (LFL)**. A TL-to-LFL conversion would enable the addition of more observed lengths from SPC-held records.

- Historical catches for the target fleet were poorly estimated in the current assessment and previous iterations reconstructing catches for oceanic whitetip sharks. It is unlikely that the data present in SPC's observer records is adequate on its own to provide informative estimates. **We recommend that a direct collaboration with countries having participated in the shark target fleet be undertaken to either produce an historical time series of targeted catch, or reliable anchor points that can be used to scale catches reconstructed from observer longline datasets.**

- Growth studies in the last 20 years have highlighted considerable uncertainty in the growth and fecundity parameters for oceanic whitetip sharks. It is unclear if the variability in estimated parameters is linked to methodology, or the region or time period sampled. Traditional growth and fecundity studies usually imply destructive sampling as vertebrae and gonads are required for aging and to assess maturity. While CMM2011-04 allows for scientific sampling, traditional destructive sampling might not be optimal given the current state of the population. However, clasper condition can be assessed

visually for males, and new non-lethal methods are being developed to assess maturity in females by looking for reproductive hormones in blood samples. **We recommend that SC investigates non-lethal approaches to collect growth and maturity samples for sharks and oceanic whitetip shark in particular.** This would allow to improve knowledge about uncertain life-history parameters used to inform stock assessments even when no-retention measures are in place.

- This assessment included the alternative reference points $F/F_{lim,\text{AS}}$ and $F/F_{crash,\text{AS}}$, which are related to F/F_{MSY}, and can be derived from a stock assessment or a risk assessment. **We invite SC to note the alternative reference points $F/F_{lim,\text{AS}}$ and $F/F_{crash,\text{AS}}$ included in this assessment.**

ACKNOWLEDGEMENTS

5. REFERENCES

Andrzejaczek, S.; Gleiss, A. C.; Jordan, L. K.; Pattiaratchi, C. B.; Howey, L. A.; Brooks, E. J., & Meekan, M. G. (2018). Temperature and the vertical movements of oceanic whitetip sharks, *Carcharhinus longimanus*. *Scientific reports*, *8*(1), 8351.

Appleyard, S.; White, W.; Vieira, S., & Sabub, B. (2018). Artisanal shark fishing in Milne Bay Province, Papua New Guinea: biomass estimation from genetically identified shark and ray fins. *Scientific reports*, *8*(1), 6693.

Bass, A. (1976). Shark of the east coast of South Africa VI. The families Oxynotidae Squalidae Dalatiidae and Echinorhinidae. *Investigational Report Oceanographic Research Institute*, *45*, 1–103.

Bonfil, R.; Clarke, S. C., & Nakano, H. (2008). The biology and ecology of the oceanic whitetip shark, *Carcharhinus longimanus*. In *Sharks of the open ocean: Biology, fisheries and conservation* (pp. 128–139). Oxford: Blackwell Science.

Burgess, G. H.; Beerkircher, L. R.; Cailliet, G. M.; Carlson, J. K.; Cortés, E.; Goldman, K. J.; Grubbs, R. D.; Musick, J. A.; Musyl, M. K., & Simpfendorfer, C. A. (2005). Is the collapse of shark populations in the Northwest Atlantic Ocean and Gulf of Mexico real? *Fisheries*, *30*(10), 19–26.

Bürkner, P.-C. (2017). brms: An R package for Bayesian multilevel models using Stan. *Journal of Statistical Software*, *80*, 1–28. doi:10.18637/jss.v080.i01

Cadigan, N. G. & Farrell, P. J. (2005). Local influence diagnostics for the retrospective problem in sequential population analysis. *ICES Journal of Marine Science: Journal du Conseil*, *62*(2), 256–265.

Cadrin, S. & Vaughan, D. (1997). Retrospective analysis of virtual population estimates for atlantic menhaden stock assessment. *Fishery Bulletin*, *95*(3), 256–265.

Cardeñosa, D.; Fields, A. T.; Babcock, E. A.; Zhang, H.; Feldheim, K.; Shea, S. K.; Fischer, G. A., & Chapman, D. D. (2018). CITES-listed sharks remain among the top species in the contemporary fin trade. *Conservation Letters*, *11*(4), e12457.

Carpenter, B.; Gelman, A.; Hoffman, M.; Lee, D.; Goodrich, B.; Betancourt, M.; Brubaker, M. A.; Guo, J.; Li, P., & Riddell, A. (2015). Stan: A probabilistic programming language. *Journal of Statistical Software*. Retrieved May 18, 2016, from http://www.demonish.com/cracker/1431548798_9226234ebe/stan-resubmit-jss1293.pdf

Clarke, S.; Langley, A.; Lennert-Cody, C.; Aires-da-Silva, A., & Maunder, M. (2018). *Pacific-wide Silky shark* Carcharhinus falciformis *Stock Status Assessment*. WCPFC-SC14-2018/SA-WP-08. Report to the Western and Central Pacific Fisheries Commission Scientific Committee. Fourteenth Regular Session, 8–16 August 2018, Busan, Korea.

Clarke, S. (2018). *Historical Catch Estimate Reconstruction for the Pacific Ocean based on Shark Fin Trade Data (1980-2016)*. WCPFC-SC14-2018/SA-IP-09. Report to the Western and Central Pacific Fisheries Commission Scientific Committee. Fourteenth Regular Session, 8–16 August 2018, Busan, Korea.

Clarke, S.; Coelho, R.; Francis, M.; Kai, M.; Kohin, S.; Liu, K.; Simpendorfer, C.; Tovar-Availa, J.; Rigby, C., & Smart, J. (2015). *Report of the Pacific Shark Life History Expert Panel Workshop*. WCPFC-SC11-2015/EB-IP-13. Report to the Western and Central Pacific Fisheries Commission Scientific Committee. Eleventh Regular Session, 5–13 August 2015, Pohnpei, Federated States of Micronesia.

Clarke, S. C.; Magnussen, J. E.; Abercrombie, D. L.; McAllister, M. K., & Shivji, M. S. (2006a). Identification of shark species composition and proportion in the Hong Kong shark fin market based on molecular genetics and trade records. *Conservation Biology*, *20*(1), 201–211.

Clarke, S. C.; McAllister, M. K.; Milner-Gulland, E. J.; Kirkwood, G.; Michielsens, C. G.; Agnew, D. J.; Pikitch, E. K.; Nakano, H., & Shivji, M. S. (2006b). Global estimates of shark catches using trade records from commercial markets. *Ecology letters*, *9*(10), 1115–1126.

Common Oceans (ABNJ) Tuna Project (2019). Joint analysis of shark post-release mortality tag results. *Western and Central Pacific Fisheries Commission*.

D'Alberto, B. M.; Chin, A.; Smart, J. J.; Baje, L.; White, W. T., & Simpfendorfer, C. A. (2017). Age, growth and maturity of oceanic whitetip shark (*Carcharhinus longimanus*) from Papua New Guinea. *Marine and Freshwater Research*, *68*(6), 1118–1129.

Fields, A. T.; Fischer, G. A.; Shea, S. K.; Zhang, H.; Abercrombie, D. L.; Feldheim, K. A.; Babcock, E. A., & Chapman, D. D. (2018). Species composition of the international shark fin trade assessed through a retail-market survey in Hong Kong. *Conservation biology*, *32*(2), 376–389.

Filmalter, J.; Forget, F.; Poisson, F.; Vernet, A.; Bach, P., & Dagorn, L. (2012). *Vertical and horizontal behaviour of silky, oceanic white tip and blue sharks in the western Indian Ocean*. IOTC–2012–WPEB08–23. Indian Ocean Tuna Commission. 8th Session of the IOTC Working Party on Ecosystems and Bycatch, September 17–19 2012, Cape Town, South Africa.

Harley, S.; Caneco, B.; Donovan, C.; Tremblay-Boyer, L., & Brouwer, S. (2015). *Monte Carlo simulation modelling of possible measures to reduce impacts of longlining on oceanic whitetip and silky sharks*. WCPFC-SC11-2015/EB-WP-02 (Rev 2). Report to the Western and Central Pacific Fisheries Commission Scientific Committee. Eleventh Regular Session, 5–13 August 2015, Pohnpei, Federated States of Micronesia.

Howey-Jordan, L. A.; Brooks, E. J.; Abercrombie, D. L.; Jordan, L. K.; Brooks, A.; Williams, S.; Gospodarczyk, E., & Chapman, D. D. (2013). Complex movements, philopatry and expanded depth range of a severely threatened pelagic shark, the oceanic whitetip (*Carcharhinus longimanus*) in the western North Atlantic. *PloS one*, *8*(2), e56588.

ISC Shark Working Group (2018). *Stock assessment of Shortfin Mako Shark in the North Pacific through 2016*. WCPFC-SC14-2018/SA-WP-11. Report to the Western and Central Pacific Fisheries Commission Scientific Committee. Fourteenth Regular Session, 8–16 August, Busan, Korea.

Joung, S.-J.; Chen, N.-F.; Hsu, H.-H., & Liu, K.-M. (2016). Estimates of life history parameters of the oceanic whitetip shark, *Carcharhinus longimanus*, in the western North Pacific Ocean. *Marine Biology Research*, *12*(7), 758–768.

Kumoru, L. (2003). The shark longline fishery in Papua New Guinea. In *Proceedings of the billfish and by-catch research group, 176th Meeting of the Standing Committee on tuna and billfish* (pp. 9–16). Secretariat of the South Pacific, Noumea, New Caledonia.

Lawson, T. (2011). *Estimation of catch rates and catches of key shark species in tuna fisheries of the western and central pacific ocean using observer data*. WCPFC-SC12-2011/EB-IP-02. Report to the Western and Central Pacific Fisheries Commission Scientific Committee. Seventh Regular Session, 9–17 August, Busan, Korea.

Liaw, A. & Wiener, M. (2002). Classification and regression by randomForest. *R News*, *2/3*, 18–22.

Methot Jr, R. & Wetzel, C. R. (2013). Stock synthesis: A biological and statistical framework for fish stock assessment and fishery management. *Fisheries Research*, *142*, 86–99.

Mollet, H.; Ezcurra, J., & O'sullivan, J. (2002). Captive biology of the pelagic stingray, dasyatis violacea (bonaparte, 1832). *Marine and Freshwater Research*, *53*(2), 531–541.

Musyl, M. K.; Brill, R. W.; Curran, D. S.; Fragoso, N. M.; McNaughton, L. M.; Nielsen, A.; Kikkawa, B. S., & Moyes, C. D. (2011). Postrelease survival, vertical and horizontal movements, and thermal habitats of five species of pelagic sharks in the central pacific ocean. *Fishery Bulletin*, *109*(4), 341–368.

Neubauer, P.; Richard, Y., & Tremblay-Boyer, L. (2019). *Alternative assessment methods for oceanic whitetip shark in the Western and Central Pacific Ocean*. WCPFC-SC15/SA-WP-13. Report to the Western and Central Pacific Fisheries Commission Scientific Committee. Fifteenth Regular Session, 12–20 August, Pohnpei, Federated States of Micronesia.

Pauly, D. (1980). On the interrelationships between natural mortality, growth parameters, and mean environmental temperature in 175 fish stocks. *ICES journal of Marine Science*, *39*(2), 175–192.

Peatman, T.; Bell, L.; Allain, V.; Caillot, S.; Williams, P.; Tuiloma, I.; Panizza, A.; Tremblay-Boyer, L.; Fukofuka, S., & Smith, N. (2018). *Summary of longline bycatch at a regional scale, 2003–2017*. WCPFC-SC14-2018/ST-WP-03 Rev 3 (15 April 2019). Report to the Western and Central Pacific Fisheries Commission Scientific Committee. Fourteenth Regular Session, 8–16 August 2018, Busan, Korea.

Pilling, G. & Brouwer, S. (2019). *Report from the SPC Pre-Assessment Workshop, Nouméa, April 2019*. WCPFC-SC15/SA-IP-01. Report to the Western and Central Pacific Fisheries Commission Scientific Committee. Fifthteen Regular Session, 12–0 August 2019, Pohnpei, Federated States of Micronesia.

Rice, J. (2012a). *Alternate catch estimates for silky and oceanic whitetip sharks in Western and Central Pacific Ocean*, WCPFC-SC8/SA-IP-12. Report to the Western and Central Pacific Fisheries Commission Scientific Committee. Eighth Regular Session, 7–15 August 2012, Busan, Korea.

Rice, J. (2018). *Report for Project 78: Analysis of observer and logbook data pertaining to key shark species in the Western and Central Pacific Ocean*. WCPFC-SC14/EB-WP-02. Report to the Western and Central Pacific Fisheries Commission Scientific Committee. Fourteenth Regular Session, 8–16 August 2018, Busan, Korea.

Rice, J. (2012b). *Catch per unit effort of oceanic whitetip sharks in the Western and Central Pacific Ocean*. WCPFC-SC8/SA-IP-10. Report to the Western and Central Pacific Fisheries Commission Scientific Committee. Eighth Regular Session, 7–15 August 2012, Busan, Korea.

Rice, J. & Harley, S. (2012). *Stock assessment of oceanic whitetip sharks in the western and central Pacific Ocean*. WCPFC-SC8-2012/SA-WP-06 Rev 1. Report to the Western and Central Pacific Fisheries Commission Scientific Committee. Eighth Regular Session, 7–15 August 2012, Busan, Korea.

Ruck, C. L. (2016). *Global genetic connectivity and diversity in a shark of high conservation concern, the oceanic whitetip*, Carcharhinus longimanus. Unpublished M.Sc. thesis, Nova Southeastern University, Fort Lauderdale, United States.

Seki, T.; Taniuchi, T.; Nakano, H., & Shimizu, M. (1998). Age, growth and reproduction of the oceanic whitetip shark from the Pacific Ocean. *Fisheries Science*, *64*(1), 14–20.

Tolotti, M. T.; Bach, P.; Hazin, F.; Travassos, P., & Dagorn, L. (2015). Vulnerability of the oceanic whitetip shark to pelagic longline fisheries. *PloS one*, *10*(10), e0141396.

Tremblay-Boyer, L. & Neubauer, P. (2019). *Data inputs to the stock assessment for oceanic whitetip shark in the Western and Central Pacific Ocean*. WCPFC-SC15/SA-IP-XX. Report to the Western and Central Pacific Fisheries Commission Scientific Committee. Fifteenth Regular Session, 12–20 August 2018, Pohnpei, Federated States of Micronesia.

Vehtari, A.; Gelman, A., & Gabry, J. (2016). *loo: Efficient leave-one-out cross-validation and WAIC for Bayesian models*. R package version 0.1.6. Retrieved from https://github.com/jgabry/loo

White, W.; Gisawa, L.; Baje, L.; Usu, T.; Yaman, L.; Sabub, B.; Appleyard, S.; Green, M.; Vieira, S.; Chin, A.; Smart, J.; Grant, M., & Simpfendorfer, C. (2018). *Sustainable management of the shark resources of Papua New Guinea: socioeconomic and biological characteristics of the fishery*. FR2018/20, Australia.

Young, C.; Carlson, J.; Hutchinson, M.; Hutt, C.; Kobayashi, D.; McCandless, C., & Wraith, J. (2018). *Status review report: Oceanic whitetip shark* Carcharhinus longimanus. Final Report to the National Marine Fisheries Service, Office of Protected Resources. National Marine Fisheries Service, National Oceanic and Atmospheric Administration.

Zhou, S.; Deng, R.; Hoyle, S., & Dunn, M. (2018). *Identifying appropriate reference points for elasmobranchs within the WCPFC*. WCPFC-SC14-2018/MI-WP-07. Report to the Western and Central Pacific Fisheries Commission Scientific Committee. Fourteenth Regular Session, 8–16 August 2018, Busan, Korea.

Zhou, S.; Smith, A. D., & Fuller, M. (2011). Quantitative ecological risk assessment for fishing effects on diverse data-poor non-target species in a multi-sector and multi-gear fishery. *Fisheries Research*, *112*(3), 168–178.

6. TABLES

Table 1: Key fecundity and maturity parameters from recent studies of oceanic whitetip shark in the Pacific Ocean (TL, total length).

Parameter	Value	Source
Growth (VB)	$k = 0.103cm, L_0 = 82.9cm, L_\infty = 341.7cm$	Seki et al. (1998)
	$k = 0.085, L_0 = 64, L_\infty = 309.4$	Joung et al. (2016)
	$k = 0.045, L_0 = 99cm, L_\infty = 342.5cm$	D'Alberto et al. (2017)
Litter size	1–14 (mean: 6.2, $n = 97$)	Seki et al. (1998)
	10–11 ($n = 2$)	Joung et al. (2016)
	–	D'Alberto et al. (2017)
Birth size	55–77 cm (TL)	Seki et al. (1998)
	64 cm	Joung et al. (2016)
	Unobserved (99 cm TL modelled)	D'Alberto et al. (2017)
Maturity (TL)	Males: 167–195 cm; females: 175–189 cm	Seki et al. (1998)
	Males: 194.4 cm; females: 193.4 cm	Joung et al. (2016)
	Males: 193 cm; females: 224 cm	D'Alberto et al. (2017)

Oceanic whitetip shark assessment

Table 2: Model covariates of operational fishing features likely to influence catch rates of oceanic whitetip shark and environmental variables that may represent habitat of this species (LBEST and SBEST are databases of the SPC for longline and purse-seine fisheries, respectively).

Covariate	Description
Year	Year when the fishing set occurred, treated as categorical .
Flag	Country-assignation for the vessel performing the fishing set.
Programme	Country observer programme for fisheries observer observing the fishing sets.
HBF	Hooks-between-floats for the longline fishing set.
SetType	Set category for the purse-seine fishing set: anchored FADs (fishing aggregation devices), drifting FADS, whales, logs or floating objects, baited and unbaited free schools.
HBF.cat	Hooks-between-floats of the fishing set assigned to a categorical variable: shallow for ≤10 HBF, deep for >10 HBF.
Cluster	Predicted targeting strategy for longline fishing set based on k-means clustering of the proportion in the total catch in number of albacore, bigeye, yellowfin and bluefin tuna, swordfish and other billfish. Cluster composition was predicted based on LBEST records and assuming 5 centres, resulting in a categorical variable with values from 1 to 5. Longline observed set targeting strategy was predicted according to the LBEST classification.
SST	Sea surface temperature aggregated at 5-degree scale for LBEST and 1-degree scale for SBEST, obtained from NOAA (https://www.esrl.noaa.gov/psd/data/gridded/data.noaa.oisst.v2.html).
Chl-*a*	Sea surface chlorophyll-*a* concentration aggregated at 5-degree scale for LBEST and 1-degree scale for SBEST (https://coastwatch.pfeg.noaa.gov/erddap/griddap/erdMH1chlamday).
Bathymetry	Depth of the sea floor at the location where the fishing set occurred, aggregated at 5-degree scale for LBEST and 1-degree scale for SBEST (https://coastwatch.pfeg.noaa.gov/erddap/griddap/srtm15plus).
Dist2Coast	Distance of the set to the nearest coastline, aggregated at 5-degree scale for LBEST and 1-degree scale for SBEST.

Table 3: Description of the 6 catch scenarios used in the stock assessment. The scenario used for the diagnostic case is highlighted with a ⋆. The total mortality is the cumulative mortality assumed for individuals from the time they are hooked to after they are released back to the water.

Catch scenario	Catch levels	Discard and post-release-mortality	Total mortality
MedianDM100	Median	100% mortality on all catches, independently of discard status	100%
MedianDM44	Median	25% mortality on discards and 25% mortality on individuals released alive	43.75%
MedianDM25 (⋆)	Median	25% mortality on discards (assuming 0% mortality of individuals released alive)	25%
HighDM100	90th quantile	100% mortality on all catches, independently of discard status	100%
HighDM44	90th quantile	25% mortality on discards and 25% mortality on individuals released alive	43.75%
HighDM25	90th quantile	25% mortality on discards (assuming 0% mortality of individuals released alive)	25%

Table 4: Description of the axes for the structural uncertainty grid, and assigned weight by level in the final resampling of stock status metrics. Settings used under the diagnostic case are highlighted with a star.

Axis	Description	Weight
Growth and fecundity	Joung et al. (2016)(⋆), Seki et al. (1998) (Figure 18)	0.5, 0.5
Catch	MedianDM100, MedianDM44, MedianDM25 (⋆), HighDM100, HighDM44, HighDM25	0.1, 0.25, 0.15, 0.1, 0.25, 0.15
Initial F	0.1, 0.15 (⋆), 0.2	0.25, 0.5, 0.25
Steepness	0.34, 0.41 (⋆), 0.49	0.25, 0.5, 0.25
Natural mortality	0.1, 0.18 (⋆), 0.26	0.35, 0.5, 0.15
Recruitment deviation (σ_R)	0.1 (⋆), 0.2	0.5, 0.5

Table 5: Description of the symbols used in the yield and stock status analyses. In this assessment, 'recent' is the average of the metric over the period 2013–2015, and 'latest' is 2016.

Symbol	Description
C_{latest}	Catch in the last year of the assessment (2016)
C_{recent}	Catch in a recent period of the assessment (2013–2015)
MSY	Equilibrium yield at F_{MSY}
SB_0	Equilibrium unfished spawning biomass
SB_{MSY}	Spawning biomass that will produce MSY
SB_{latest}	Spawning biomass in the last year of the assessment (2016)
SB_{recent}	Spawning biomass in a recent period of the assessment (2013–2015)
$SB_{latest}/SB_{F=0}$	Spawning biomass in the latest time period (2016) relative to the equilibrium unfished spawning biomass
SB_{recent}/SB_0	Spawning biomass in the recent time period (2013–2015) relative to the equilibrium unfished spawning biomass
$SB_{latest}/SB_{\mathrm{MSY}}$	Spawning biomass in the latest time period (2016) relative to that which will produce the maximum sustainable yield (MSY)
$SB_{recent}/SB_{\mathrm{MSY}}$	Spawning biomass in the recent time period (2013–2015) relative to that which will produce the maximum sustainable yield (MSY)
F_{MSY}	Fishing mortality producing the maximum sustainable yield (MSY)
$F_{lim,\mathrm{AS}}$	Fishing mortality resulting in 0.5 of SB_{MSY}
$F_{crash,\mathrm{AS}}$	Fishing mortality resulting in population extinction when sustained on the long-term
F_{latest}	Average fishing mortality-at-age for the last year of the assessment (2016)
F_{recent}	Average fishing mortality-at-age for a recent period (2013–2015)
$F_{recent}/F_{\mathrm{MSY}}$	Average fishing mortality-at-age for a recent period (2013–2015) relative to F_{MSY}
$F_{latest}/F_{\mathrm{MSY}}$	Latest fishing mortality (2016) compared to that producing maximum sustainable yield (MSY)
$F_{recent}/F_{\mathrm{MSY}}$	Recent fishing mortality (2013–2015) compared to that producing maximum sustainable yield (MSY)
$F_{latest}/F_{lim,\mathrm{AS}}$	Latest fishing mortality (2016) compared to that resulting in 0.5 of SB_{MSY}
$F_{recent}/F_{lim,\mathrm{AS}}$	Recent fishing mortality (2013–2015) compared to that resulting in 0.5 of SB_{MSY}
$F_{latest}/F_{crash,\mathrm{AS}}$	Latest fishing mortality (2016) compared to that resulting in population extinction
$F_{recent}/F_{crash,\mathrm{AS}}$	Recent fishing mortality (2013–2015) compared to that resulting in population extinction

Table 6: Summary of reference points over the 648 models in the structural uncertainty grid

	Mean	Median	Min	10%	90%	Max
C_{latest}	2585	2156	681	956	5058	9233
C_{recent}	3087	2627	893	1216	5639	10348
MSY	6755	5790	1774	2808	11668	19122
SB_0	9641	7880	1510	3228	19842	34572
SB_{MSY}	4038	3245	523	1157	8398	15593
SB_{latest}	367	298	43	86	779	1217
SB_{recent}	387	310	36	93	789	1616
SB_{latest}/SB_0	0.04	0.04	0.02	0.03	0.05	0.07
SB_{recent}/SB_0	0.04	0.04	0.02	0.03	0.05	0.08
SB_{latest}/SB_{MSY}	0.09	0.09	0.05	0.06	0.13	0.16
SB_{recent}/SB_{MSY}	0.10	0.09	0.05	0.07	0.13	0.17
F_{MSY}	0.060	0.057	0.026	0.031	0.091	0.116
$F_{lim,AS}$	0.094	0.096	0.041	0.050	0.144	0.183
$F_{crash,AS}$	0.145	0.140	0.060	0.076	0.238	0.290
F_{latest}	0.216	0.177	0.096	0.115	0.362	0.473
F_{recent}	0.229	0.215	0.136	0.164	0.316	0.395
F_{latest}/F_{MSY}	4.03	3.35	1.09	1.82	7.18	12.07
F_{recent}/F_{MSY}	4.24	3.92	1.81	2.57	6.27	9.88
$F_{latest}/F_{lim,AS}$	2.57	2.14	0.69	1.16	4.58	7.73
$F_{recent}/F_{lim,AS}$	2.70	2.51	1.15	1.62	4.07	6.33
$F_{latest}/F_{crash,AS}$	1.69	1.41	0.44	0.73	2.95	5.26
$F_{recent}/F_{crash,AS}$	1.78	1.66	0.72	1.04	2.87	4.31

Table 7: Summary of reference points over the 108 models in the structural uncertainty grid using the median catch scenario and assuming 100% total discard mortality.

	Mean	Median	Min	10%	90%	Max
C_{latest}	2497	2323	1736	1838	3416	4092
C_{recent}	2645	2502	1760	1883	3639	4412
MSY	4459	4299	1903	2545	6901	8922
SB_0	6373	5378	1609	2086	11888	16128
SB_{MSY}	2670	2289	558	831	5038	7274
SB_{latest}	232	219	43	64	449	575
SB_{recent}	277	253	51	76	519	722
SB_{latest}/SB_0	0.04	0.03	0.02	0.02	0.05	0.06
SB_{recent}/SB_0	0.04	0.04	0.02	0.03	0.06	0.07
$SB_{latest}/SB_{\text{MSY}}$	0.09	0.08	0.05	0.06	0.12	0.14
$SB_{recent}/SB_{\text{MSY}}$	0.10	0.10	0.06	0.08	0.14	0.16
F_{MSY}	0.060	0.054	0.026	0.031	0.091	0.116
$F_{lim,\text{AS}}$	0.094	0.083	0.041	0.050	0.144	0.183
$F_{crash,\text{AS}}$	0.145	0.126	0.060	0.076	0.238	0.290
F_{latest}	0.332	0.326	0.258	0.282	0.393	0.447
F_{recent}	0.287	0.285	0.219	0.242	0.337	0.371
$F_{latest}/F_{\text{MSY}}$	6.22	5.87	2.97	3.91	8.56	11.21
$F_{recent}/F_{\text{MSY}}$	5.32	5.10	2.94	3.59	7.20	9.30
$F_{latest}/F_{lim,\text{AS}}$	3.96	3.86	1.88	2.40	5.44	7.18
$F_{recent}/F_{lim,\text{AS}}$	3.39	3.21	1.86	2.23	4.56	5.96
$F_{latest}/F_{crash,\text{AS}}$	2.61	2.48	1.19	1.52	3.68	4.89
$F_{recent}/F_{crash,\text{AS}}$	2.23	2.15	1.17	1.39	3.13	4.06

Table 8: Summary of reference points over the 108 models in the structural uncertainty grid using the median catch scenario and assuming 43.75% total discard mortality.

	Mean	Median	Min	10%	90%	Max
C_{latest}	1341	1253	955	1003	1823	2149
C_{recent}	1637	1551	1105	1173	2245	2706
MSY	4238	4068	1803	2422	6572	8505
SB_0	6039	5088	1532	1976	11253	15279
SB_{MSY}	2529	2154	531	793	4813	6891
SB_{latest}	234	223	45	67	447	561
SB_{recent}	227	208	39	61	430	596
SB_{latest}/SB_0	0.04	0.04	0.02	0.03	0.06	0.07
SB_{recent}/SB_0	0.04	0.04	0.02	0.02	0.05	0.06
SB_{latest}/SB_{MSY}	0.10	0.09	0.05	0.07	0.13	0.15
SB_{recent}/SB_{MSY}	0.09	0.09	0.05	0.07	0.12	0.14
F_{MSY}	0.060	0.056	0.026	0.031	0.091	0.116
$F_{lim,AS}$	0.094	0.089	0.041	0.050	0.145	0.183
$F_{crash,AS}$	0.145	0.133	0.060	0.076	0.238	0.290
F_{latest}	0.175	0.172	0.138	0.150	0.207	0.235
F_{recent}	0.208	0.206	0.160	0.175	0.244	0.271
F_{latest}/F_{MSY}	3.26	3.08	1.58	2.07	4.49	5.85
F_{recent}/F_{MSY}	3.83	3.69	2.14	2.61	5.21	6.70
$F_{latest}/F_{lim,AS}$	2.08	2.02	1.00	1.27	2.84	3.75
$F_{recent}/F_{lim,AS}$	2.44	2.31	1.36	1.62	3.29	4.29
$F_{latest}/F_{crash,AS}$	1.37	1.33	0.63	0.80	1.95	2.55
$F_{recent}/F_{crash,AS}$	1.61	1.56	0.85	1.02	2.24	2.92

Table 9: Summary of reference points over the 108 models in the structural uncertainty grid using the median catch scenario and assuming 25% total discard mortality.

	Mean	Median	Min	10%	90%	Max
C_{latest}	942	878	681	713	1270	1487
C_{recent}	1310	1236	893	945	1783	2146
MSY	4171	4005	1774	2385	6466	8370
SB_0	5942	5004	1510	1942	11054	15006
SB_{MSY}	2489	2119	523	781	4743	6768
SB_{latest}	238	227	47	68	451	562
SB_{recent}	212	195	36	57	404	558
SB_{latest}/SB_0	0.04	0.04	0.02	0.03	0.06	0.07
SB_{recent}/SB_0	0.04	0.03	0.02	0.02	0.05	0.06
SB_{latest}/SB_{MSY}	0.10	0.09	0.05	0.07	0.14	0.16
SB_{recent}/SB_{MSY}	0.09	0.08	0.05	0.06	0.11	0.14
F_{MSY}	0.060	0.056	0.026	0.031	0.091	0.116
$F_{lim,AS}$	0.094	0.089	0.041	0.050	0.145	0.183
$F_{crash,AS}$	0.145	0.133	0.060	0.076	0.238	0.290
F_{latest}	0.121	0.119	0.096	0.104	0.143	0.162
F_{recent}	0.176	0.174	0.136	0.148	0.207	0.229
F_{latest}/F_{MSY}	2.26	2.14	1.09	1.42	3.11	4.06
F_{recent}/F_{MSY}	3.25	3.13	1.81	2.21	4.42	5.69
$F_{latest}/F_{lim,AS}$	1.44	1.40	0.69	0.88	1.97	2.60
$F_{recent}/F_{lim,AS}$	2.07	1.95	1.15	1.37	2.79	3.64
$F_{latest}/F_{crash,AS}$	0.95	0.92	0.44	0.56	1.36	1.77
$F_{recent}/F_{crash,AS}$	1.36	1.32	0.72	0.86	1.90	2.48

Oceanic whitetip shark assessment

Table 10: Summary of reference points over the 108 models in the structural uncertainty grid using the high catch scenario and assuming 100% total discard mortality.

	Mean	Median	Min	10%	90%	Max
C_{latest}	5633	5209	3860	4107	7680	9233
C_{recent}	6229	5855	4122	4420	8545	10348
MSY	9658	9312	4090	5690	14796	19122
SB_0	13789	11686	3454	4476	25469	34572
SB_{MSY}	5776	4950	1197	1784	10802	15593
SB_{latest}	494	462	93	138	946	1217
SB_{recent}	632	572	120	176	1168	1616
SB_{latest}/SB_0	0.04	0.03	0.02	0.02	0.05	0.06
SB_{recent}/SB_0	0.05	0.05	0.02	0.03	0.06	0.08
$SB_{latest}/SB_{\text{MSY}}$	0.09	0.08	0.05	0.06	0.12	0.13
$SB_{recent}/SB_{\text{MSY}}$	0.11	0.11	0.06	0.08	0.14	0.17
F_{MSY}	0.060	0.057	0.026	0.031	0.091	0.116
$F_{lim,\text{AS}}$	0.095	0.096	0.041	0.050	0.144	0.182
$F_{crash,\text{AS}}$	0.146	0.140	0.060	0.076	0.238	0.290
F_{latest}	0.354	0.346	0.275	0.300	0.417	0.473
F_{recent}	0.305	0.302	0.232	0.257	0.360	0.395
$F_{latest}/F_{\text{MSY}}$	6.60	6.22	3.16	4.15	9.17	12.07
$F_{recent}/F_{\text{MSY}}$	5.63	5.34	3.14	3.83	7.65	9.88
$F_{latest}/F_{lim,\text{AS}}$	4.20	3.96	2.00	2.55	5.85	7.73
$F_{recent}/F_{lim,\text{AS}}$	3.58	3.41	1.99	2.38	4.84	6.33
$F_{latest}/F_{crash,\text{AS}}$	2.76	2.63	1.26	1.62	3.92	5.26
$F_{recent}/F_{crash,\text{AS}}$	2.36	2.26	1.25	1.48	3.33	4.31

Table 11: Summary of reference points over the 108 models in the structural uncertainty grid using the high catch scenario and assuming 43.75% total discard mortality.

	Mean	Median	Min	10%	90%	Max
C_{latest}	3037	2821	2136	2252	4112	4843
C_{recent}	3788	3571	2549	2705	5184	6224
MSY	9131	8744	3872	5315	14080	18225
SB_0	13072	11070	3289	4231	24102	32715
SB_{MSY}	5478	4725	1140	1699	10325	14756
SB_{latest}	501	478	100	147	944	1188
SB_{recent}	510	469	92	140	956	1310
SB_{latest}/SB_0	0.04	0.04	0.02	0.03	0.05	0.06
SB_{recent}/SB_0	0.04	0.04	0.02	0.03	0.05	0.06
SB_{latest}/SB_{MSY}	0.09	0.09	0.05	0.07	0.13	0.14
SB_{recent}/SB_{MSY}	0.09	0.09	0.05	0.07	0.12	0.15
F_{MSY}	0.060	0.056	0.026	0.031	0.090	0.116
$F_{lim,AS}$	0.094	0.089	0.041	0.050	0.140	0.182
$F_{crash,AS}$	0.144	0.133	0.060	0.076	0.223	0.290
F_{latest}	0.186	0.183	0.148	0.161	0.219	0.248
F_{recent}	0.217	0.215	0.167	0.183	0.255	0.284
F_{latest}/F_{MSY}	3.50	3.29	1.68	2.23	4.85	6.27
F_{recent}/F_{MSY}	4.04	3.88	2.25	2.77	5.47	7.03
$F_{latest}/F_{lim,AS}$	2.23	2.15	1.07	1.36	3.07	4.02
$F_{recent}/F_{lim,AS}$	2.57	2.43	1.43	1.72	3.45	4.50
$F_{latest}/F_{crash,AS}$	1.47	1.41	0.67	0.87	2.09	2.73
$F_{recent}/F_{crash,AS}$	1.69	1.64	0.90	1.08	2.36	3.07

Oceanic whitetip shark assessment

Table 12: Summary of reference points over the 108 models in the structural uncertainty grid using the high catch scenario and assuming 25% total discard mortality.

	Mean	Median	Min	10%	90%	Max
C_{latest}	2125	1971	1532	1609	2850	3336
C_{recent}	2983	2796	2046	2166	4053	4862
MSY	8947	8603	3811	5128	13846	17932
SB_0	12738	10723	3242	4175	23636	32112
SB_{MSY}	5335	4540	1124	1679	10153	14484
SB_{latest}	507	487	104	152	955	1192
SB_{recent}	471	430	85	131	889	1220
SB_{latest}/SB_0	0.04	0.04	0.02	0.03	0.06	0.07
SB_{recent}/SB_0	0.04	0.04	0.02	0.02	0.05	0.06
$SB_{latest}/SB_{\text{MSY}}$	0.10	0.09	0.05	0.07	0.14	0.15
$SB_{recent}/SB_{\text{MSY}}$	0.09	0.09	0.05	0.07	0.12	0.14
F_{MSY}	0.060	0.056	0.026	0.031	0.091	0.116
$F_{lim,\text{AS}}$	0.094	0.089	0.041	0.050	0.144	0.182
$F_{crash,\text{AS}}$	0.145	0.133	0.060	0.076	0.238	0.290
F_{latest}	0.129	0.127	0.103	0.112	0.152	0.172
F_{recent}	0.183	0.181	0.139	0.154	0.215	0.237
$F_{latest}/F_{\text{MSY}}$	2.42	2.28	1.16	1.51	3.36	4.40
$F_{recent}/F_{\text{MSY}}$	3.37	3.24	1.88	2.29	4.59	5.92
$F_{latest}/F_{lim,\text{AS}}$	1.54	1.49	0.73	0.93	2.13	2.82
$F_{recent}/F_{lim,\text{AS}}$	2.15	2.03	1.19	1.43	2.91	3.79
$F_{latest}/F_{crash,\text{AS}}$	1.02	0.98	0.46	0.59	1.46	1.92
$F_{recent}/F_{crash,\text{AS}}$	1.42	1.37	0.75	0.89	1.98	2.58

Oceanic whitetip shark assessment
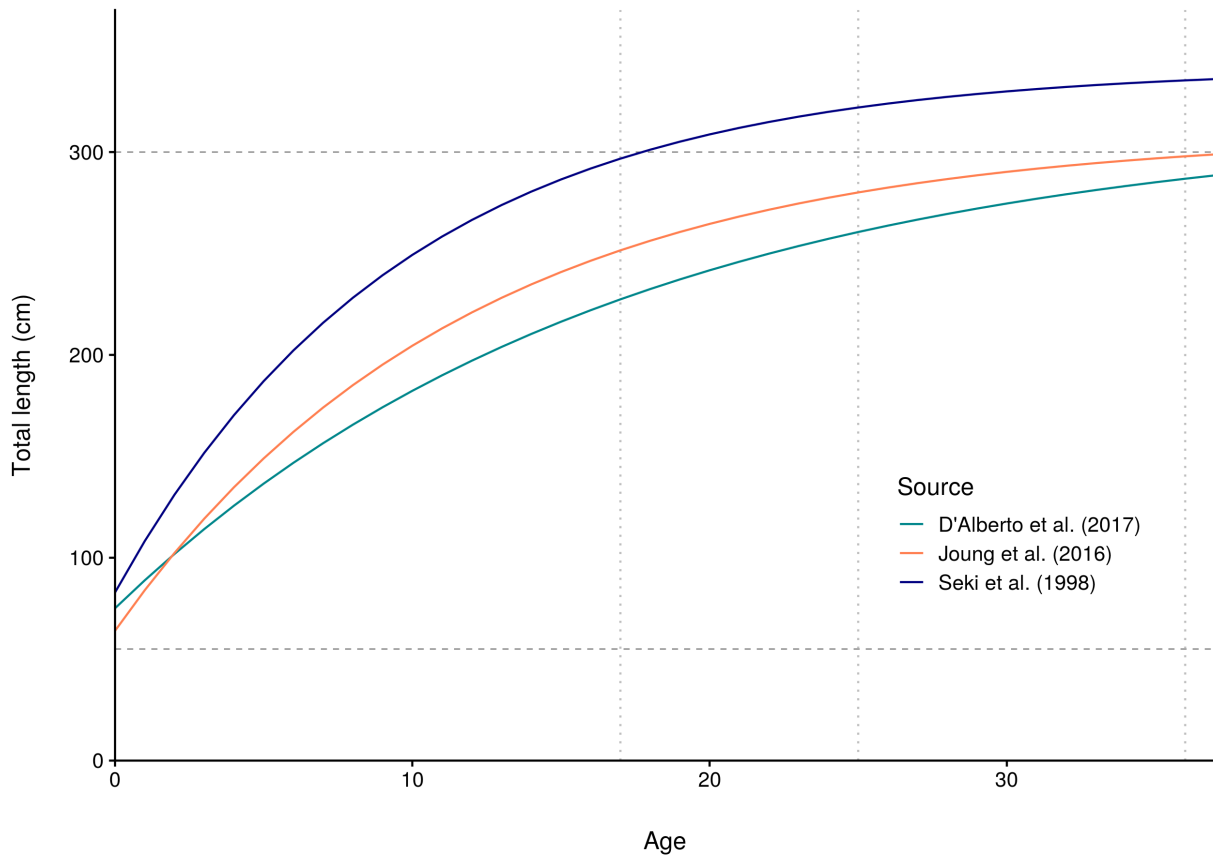
7. FIGURES

Figure 1: Comparison of growth curves of oceanic whitetip shark from the three most recent studies in the Pacific Ocean. Dashed lines at ages 17, 25 and 36 indicate the maximum observed age (Clarke et al. 2015), the maximum age specified in the current assessment, and the maximum age specified in the previous assessment (Rice & Harley 2012), respectively.

.
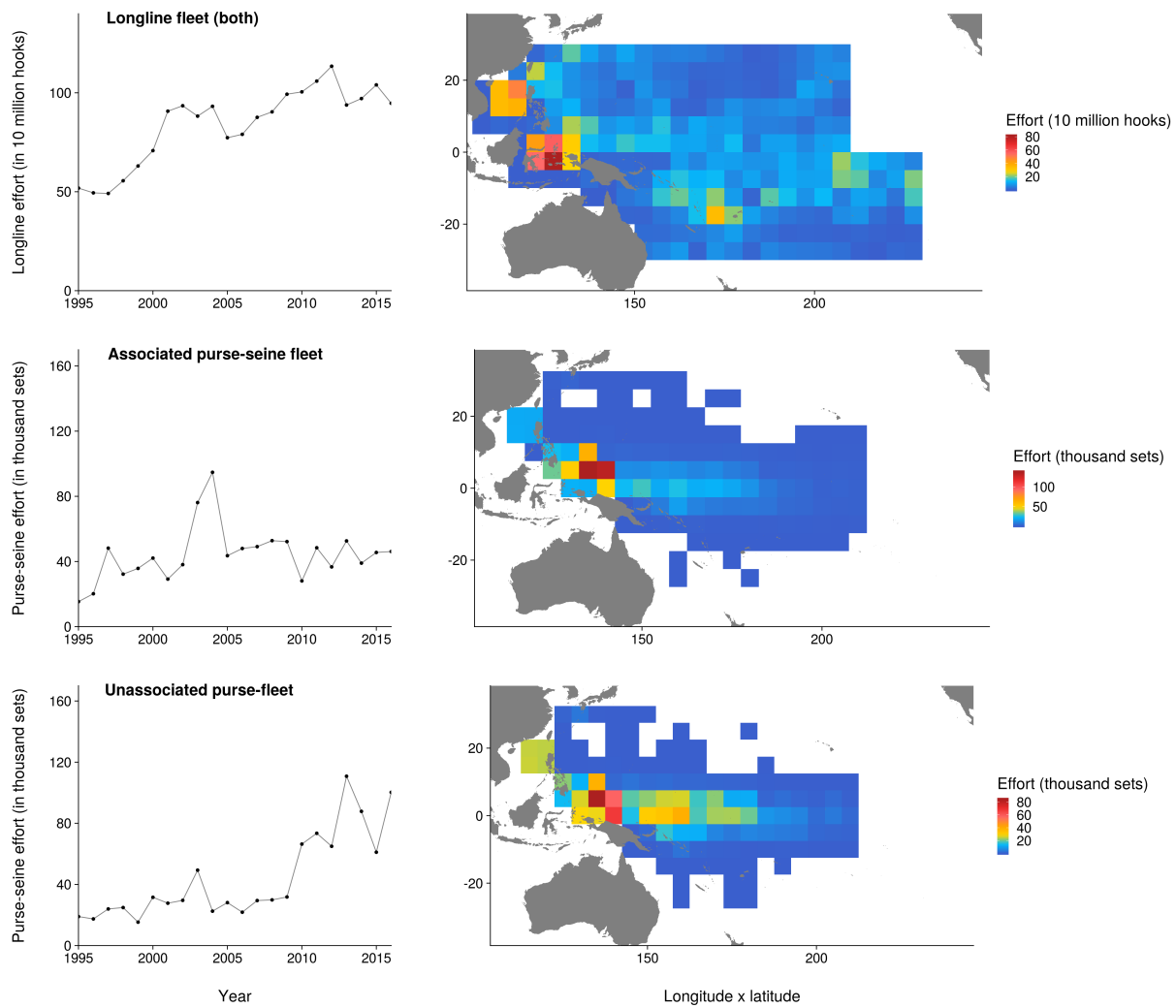
Figure 2: Summary of effort for the key fleets catching oceanic whitetip shark in the Western and Central Pacific Ocean assessment region. Time‑series (left) and spatial distribution (right; aggregated 5‑°cell). Key fleets were longline shark bycatch or target fleets and purse seine fleets using fishing aggregating devices (associated) or free schools (unassociated).

Oceanic whitetip shark assessment
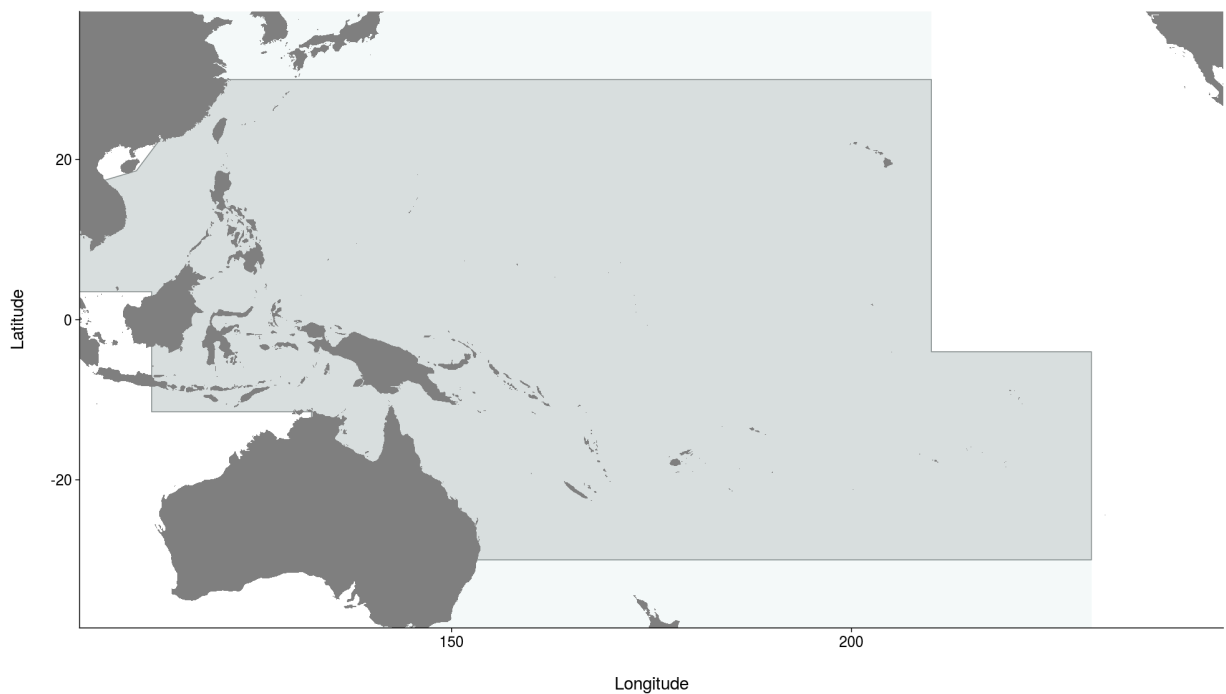
Figure 3: Western and Central Pacific Fisheries Commission convention area (light grey), including the stock assessment area for oceanic whitetip shark (dark grey), bounded by the 30°N and 30°S parallels

Oceanic whitetip shark assessment
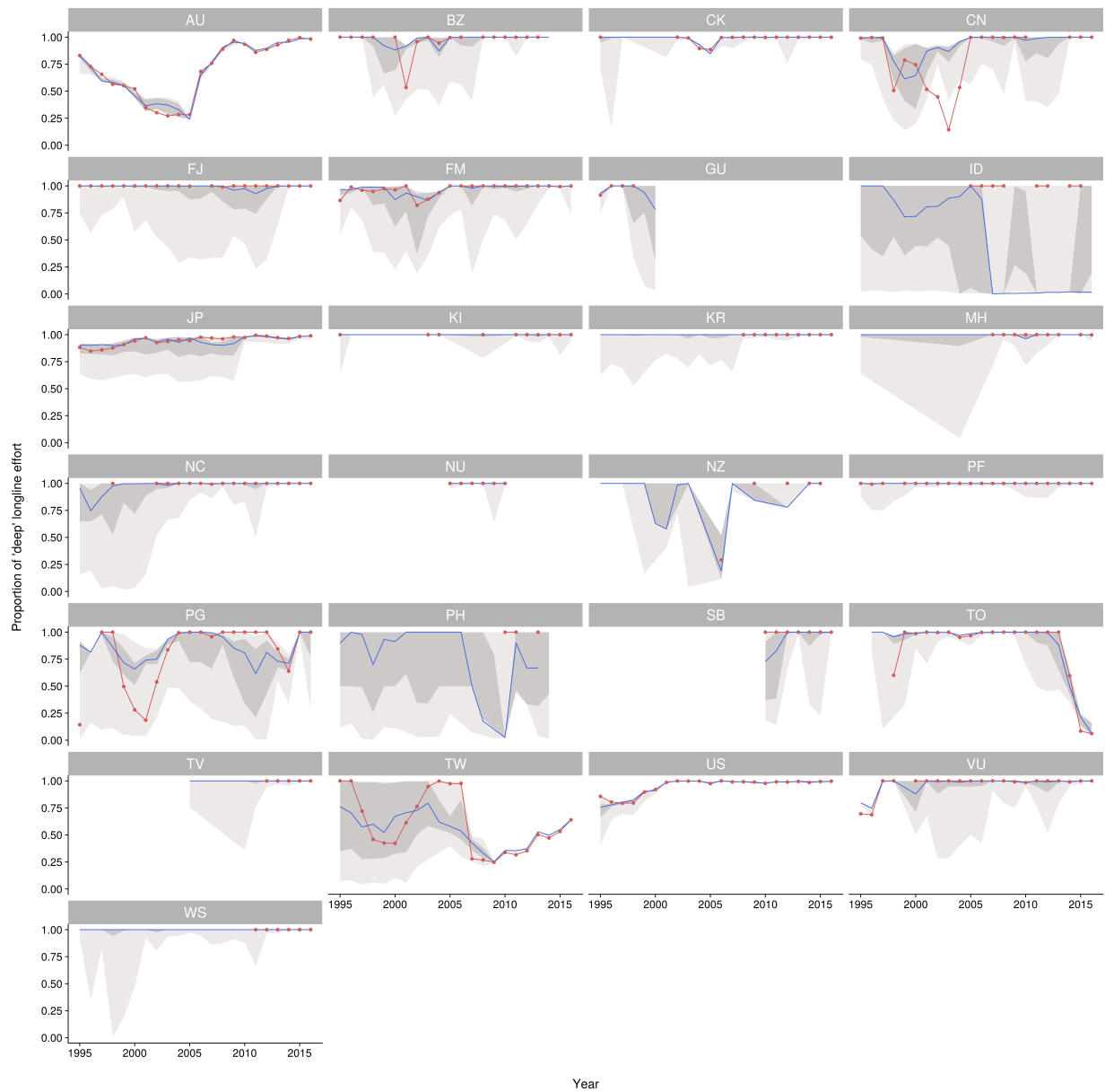
Figure 4: Prediction of the proportion of 'deep' LBEST effort over time for key longline countries in LBEST active over the assessment's region. The red line shows the observed proportion of 'deep' effort when provided and the blue line shows the prediction accounting for both observations and the random forest prediction for unobserved strata. The light and dark grey bounds show the 0.025^{th} - 0.975^{th} and 0.25^{th} - 0.75^{th} uncertainty bounds for the effort classification, also accounting for effort already provided with HBF resolution.
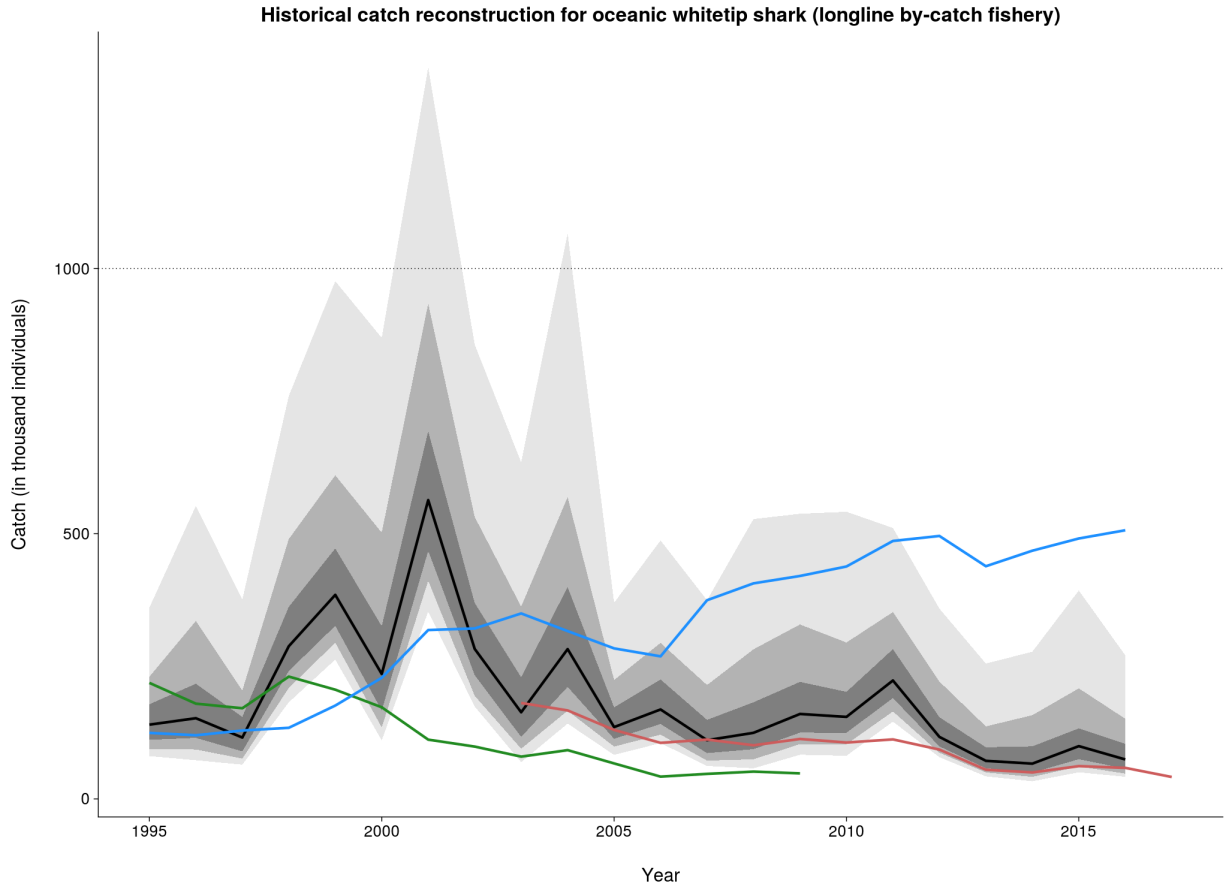
Figure 5: Median predictions of oceanic whitetip shark catch in the WCPO for the longline by‑catch fleet based on a model of longline observed catch rates applied to LBEST effort. The light, dark and darker grey bounds show the 0.025^{th} ‑ 0.975^{th}, 0.10^{th} ‑ 0.90^{th} and 0.25^{th} ‑ 0.75^{th} uncertainty bounds. For comparison with our estimates, the blue line shows the median prediction of historical catch based on global fin trade statistics, the red line shows the prediction of historical catch published in（Peatman et al. 2018）, and the green line shows the historical catches used for this fleet in the reference case for the 2012 assessment.

Oceanic whitetip shark assessment
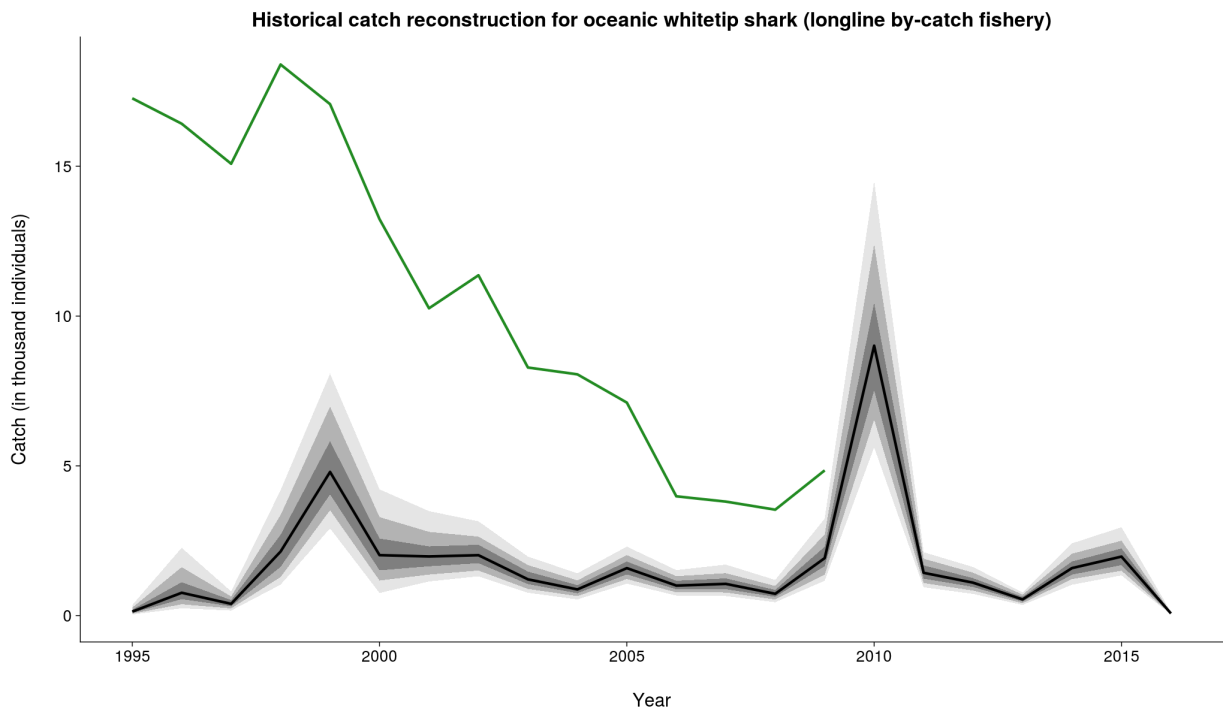
Figure 6: Median predictions of oceanic whitetip shark catch in the WCPO for the longline target fleet based on a model of longline observed catch rates applied to LBEST effort. The light, dark and darker grey bounds show the 0.025^{th}-0.975^{th}, 0.10^{th}-0.90^{th} and 0.25^{th}-0.75^{th} uncertainty bounds. For comparison with our estimates, the green line shows the historical catches used for this fleet in the reference case for the 2012 assessment.
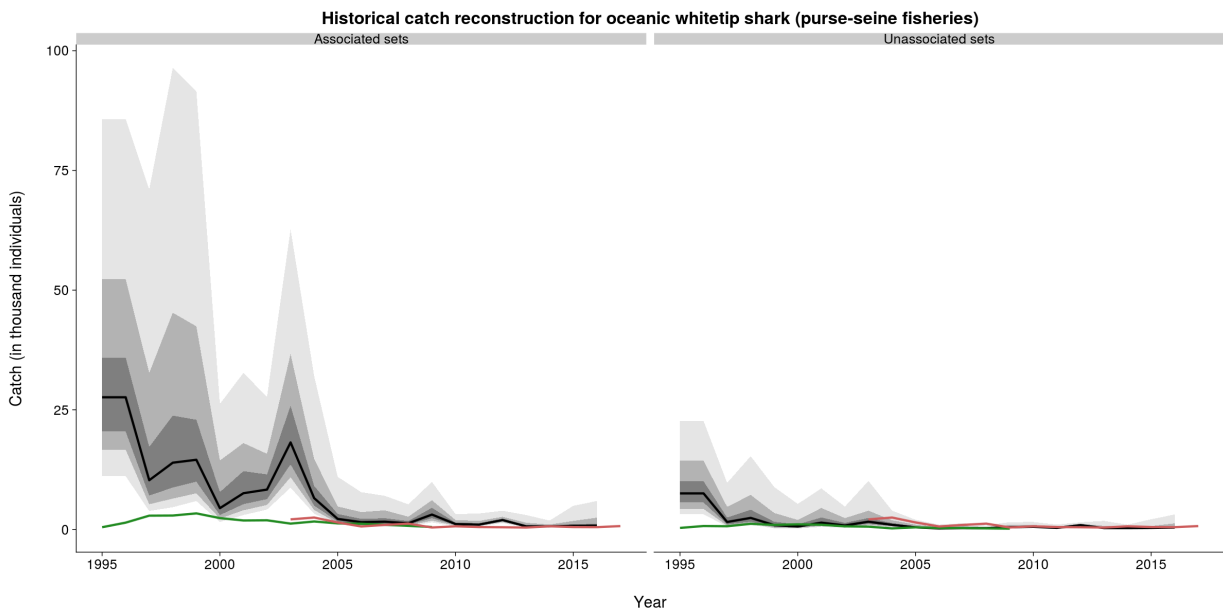
Figure 7: Median predictions of oceanic whitetip shark catch in the WCPO for the associated and unassociated purse-seine fleets based on a model of purse-seine observed catch rates applied to SBEST effort. The light, dark and darker grey bounds show the 0.025^{th}-0.975^{th}, 0.10^{th}-0.90^{th} and 0.25^{th}-0.75^{th} uncertainty bounds. For comparison with our estimates, the red line shows the prediction of historical catch published in (Peatman et al. 2018) for these fleets and the green line shows the corresponding historical catches used in the reference case for the 2012 assessment.

Oceanic whitetip shark assessment

Figure 8: Median predictions of oceanic whitetip shark catch in the WCPO based on global fin trade statistics. Predictions are shown in numbers with 95% credible bounds, using three approaches to scale the global catch to the WCPO area.
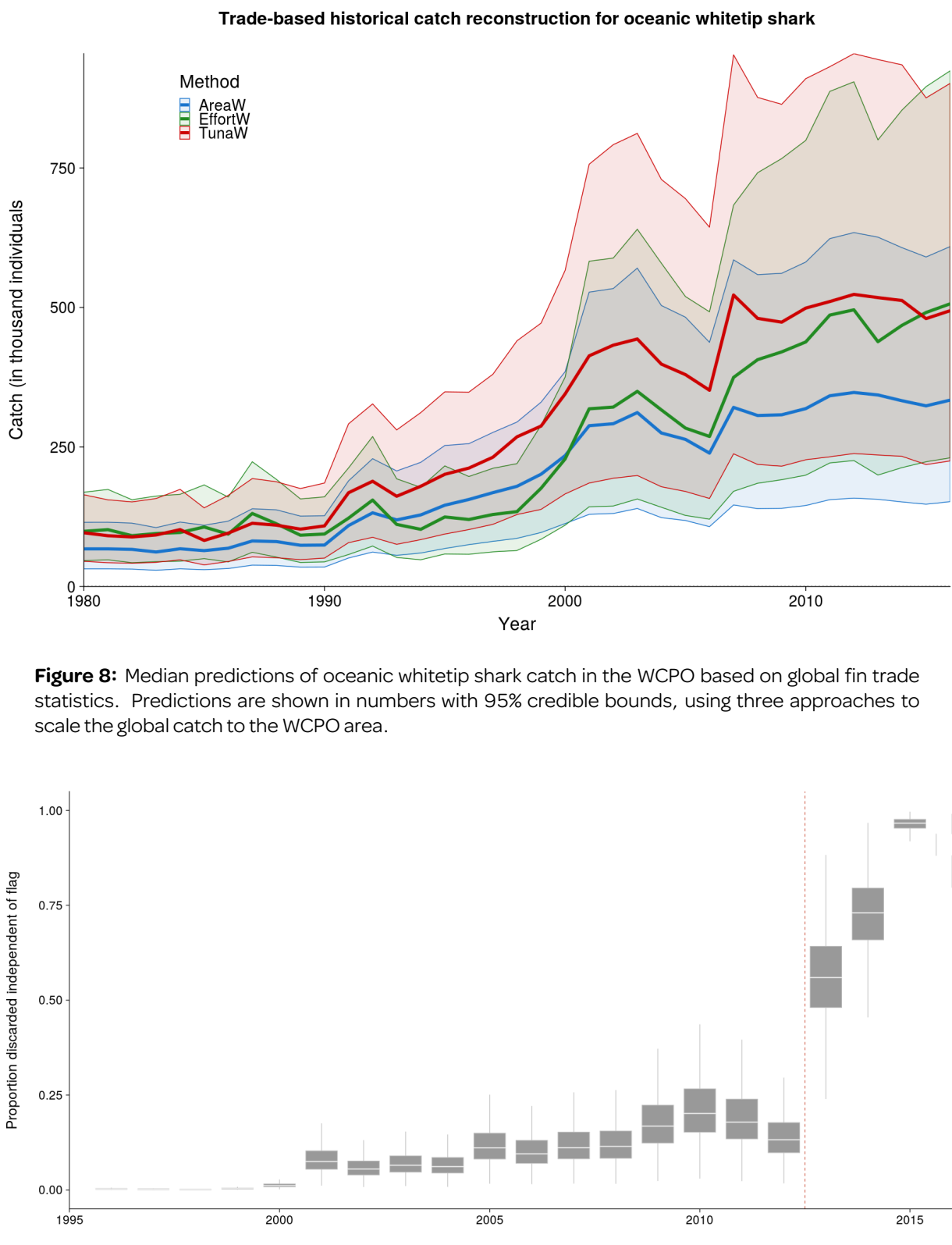
Figure 9: Year effects, independent of flag, estimated for the proportion of individuals discarded by year in the binomial model predicting discard rates over time. The white line shows the median and the box outlines the inter-quartile range.

Oceanic whitetip shark assessment
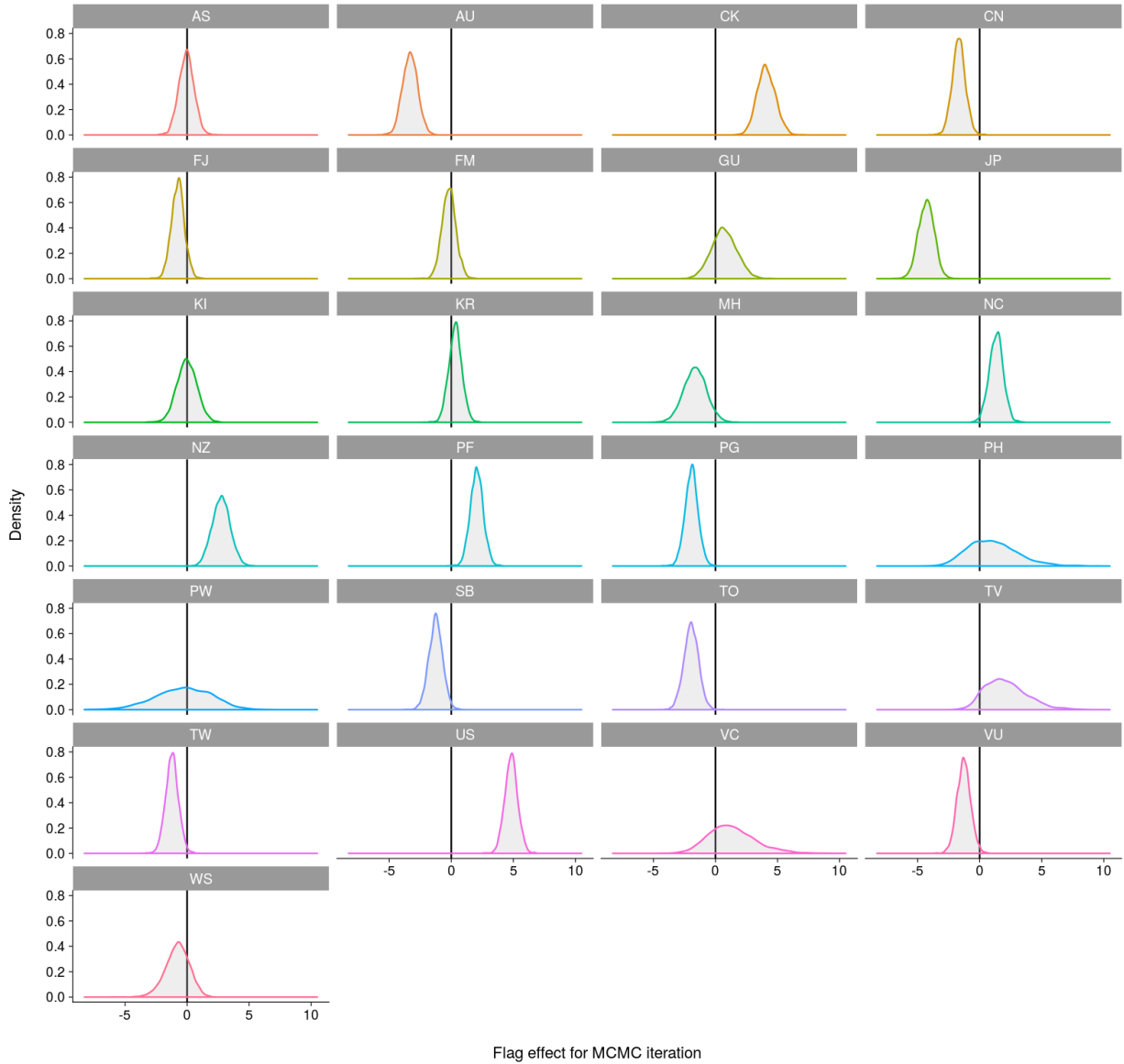
Figure 10: Random effects estimated for key longline observed flags in the binomial model predicting discard rates over time. The vertical line at 0 shows the mean. Effect distributions below the mean indicate lower discard rates (i.e. higher retention rates) compared to other flags, and conversely distributions above the mean indicate higher discard rates compared to other flags.
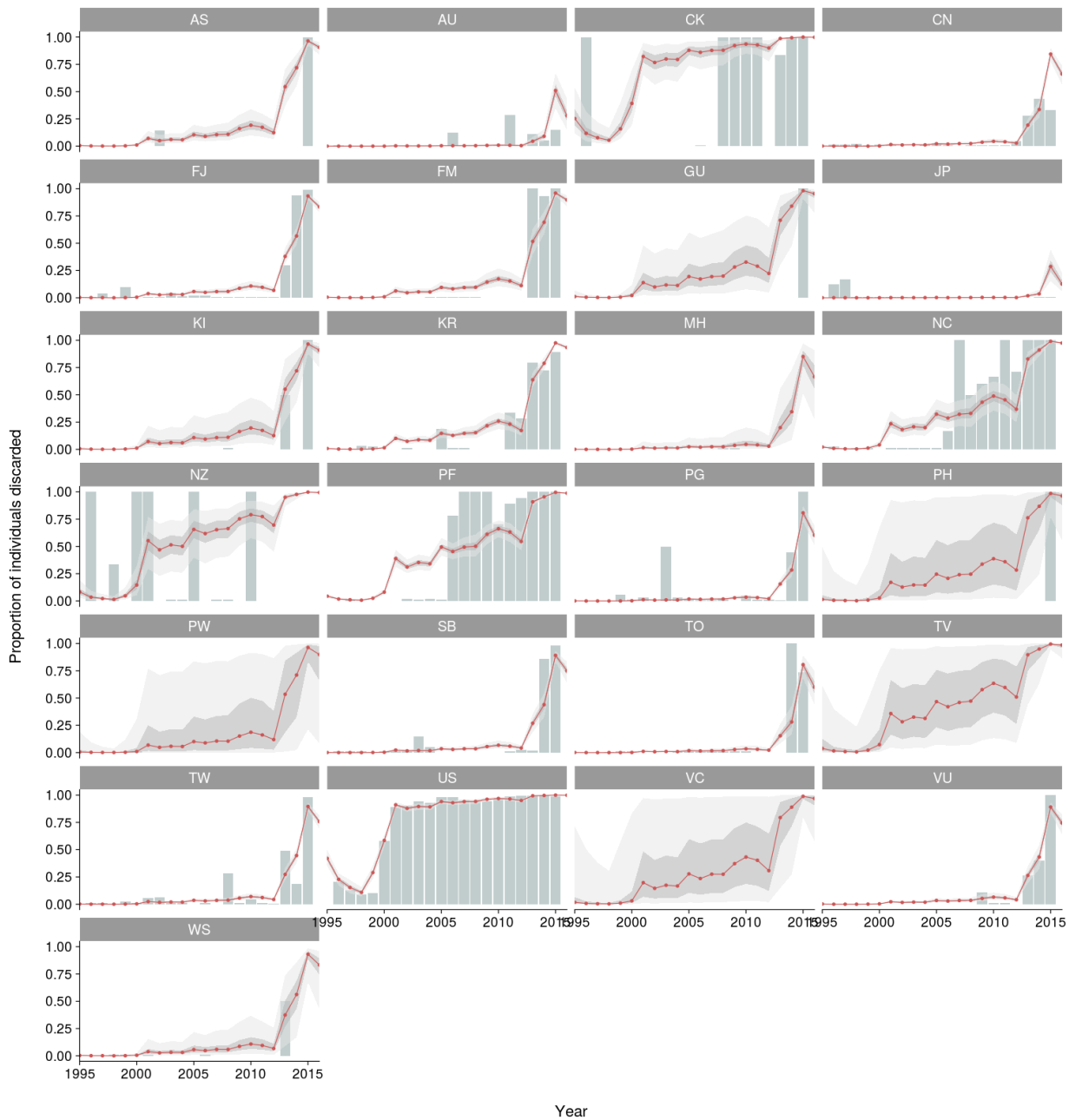
Figure 11: Observed (light blue) vs. predicted (red; median) proportion of discarded individuals by key longline LBEST flags operating in the assessment region. The light and dark grey bounds show the 0.025^{th} - 0.975^{th} and 0.25^{th} - 0.75^{th} uncertainty bounds.

Oceanic whitetip shark assessment
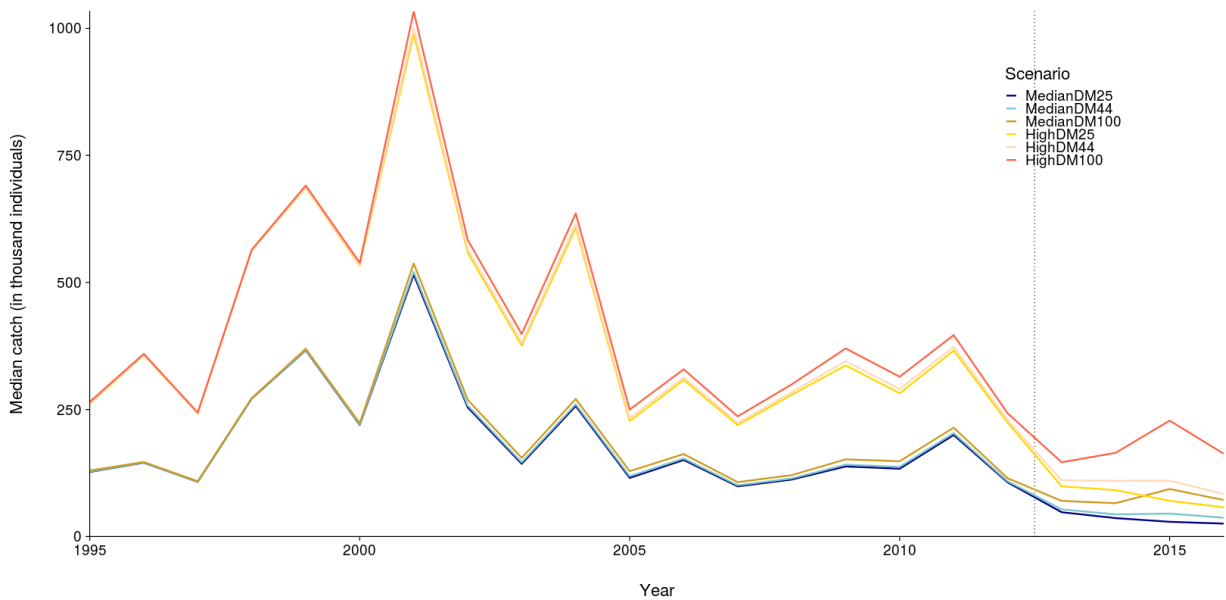
Figure 12: Median historical catch for the longline by‑catch fleet for the three discard and post‑release mortality catch scenarios assuming 100% (darker), 43.75% and 25% (lighter) total mortality for discarded individuals in turquoise and blue for the 'high' and 'median' catch scenarios, respectively. The dotted line at 2013 highlights the start of CMM‑2011‑04 prohibiting the retention of oceanic whitetip sharks for vessels fishing in the WCPFC Convention Area.
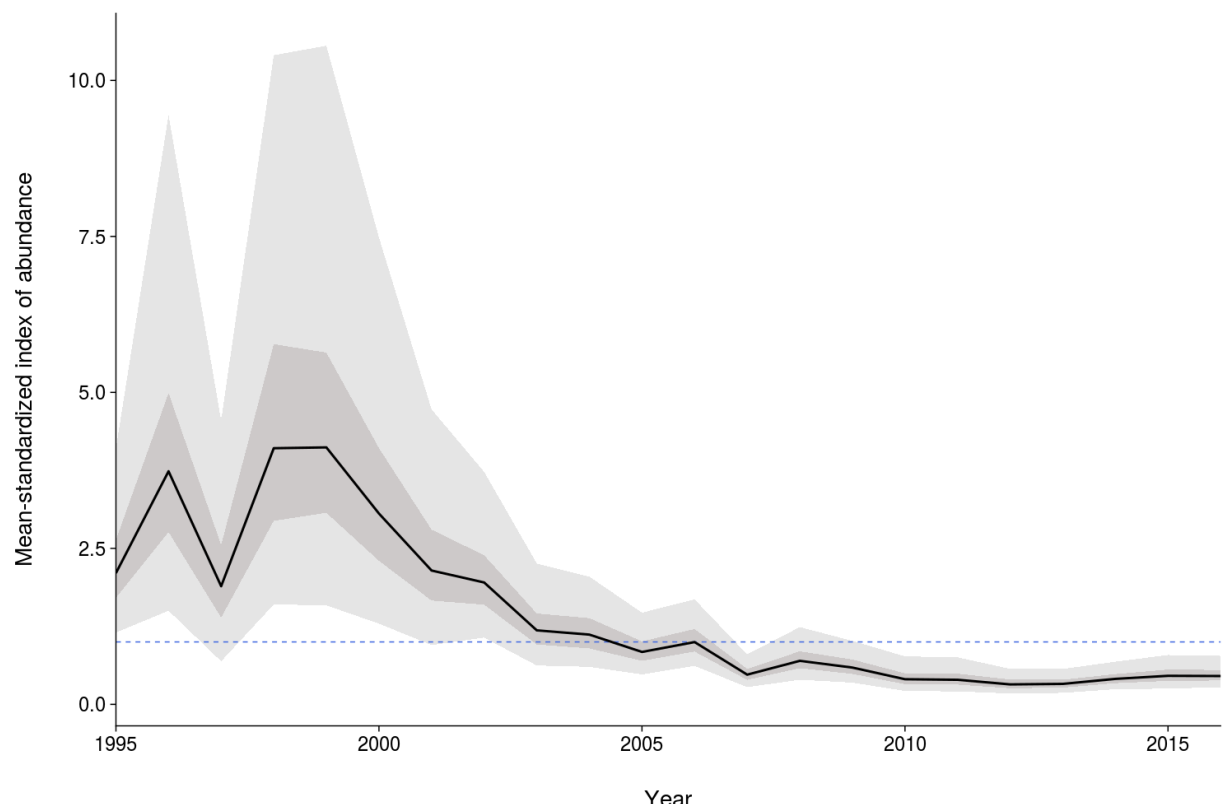
Figure 13: Mean‑standardized CPUE index used in this assessment of oceanic whitetip shark. The light and dark grey bounds show the 0.025^{th}‑0.975^{th} and 0.25^{th}‑0.75^{th} uncertainty bounds around the year effects. The dashed line at 1 shows the reference mean value.
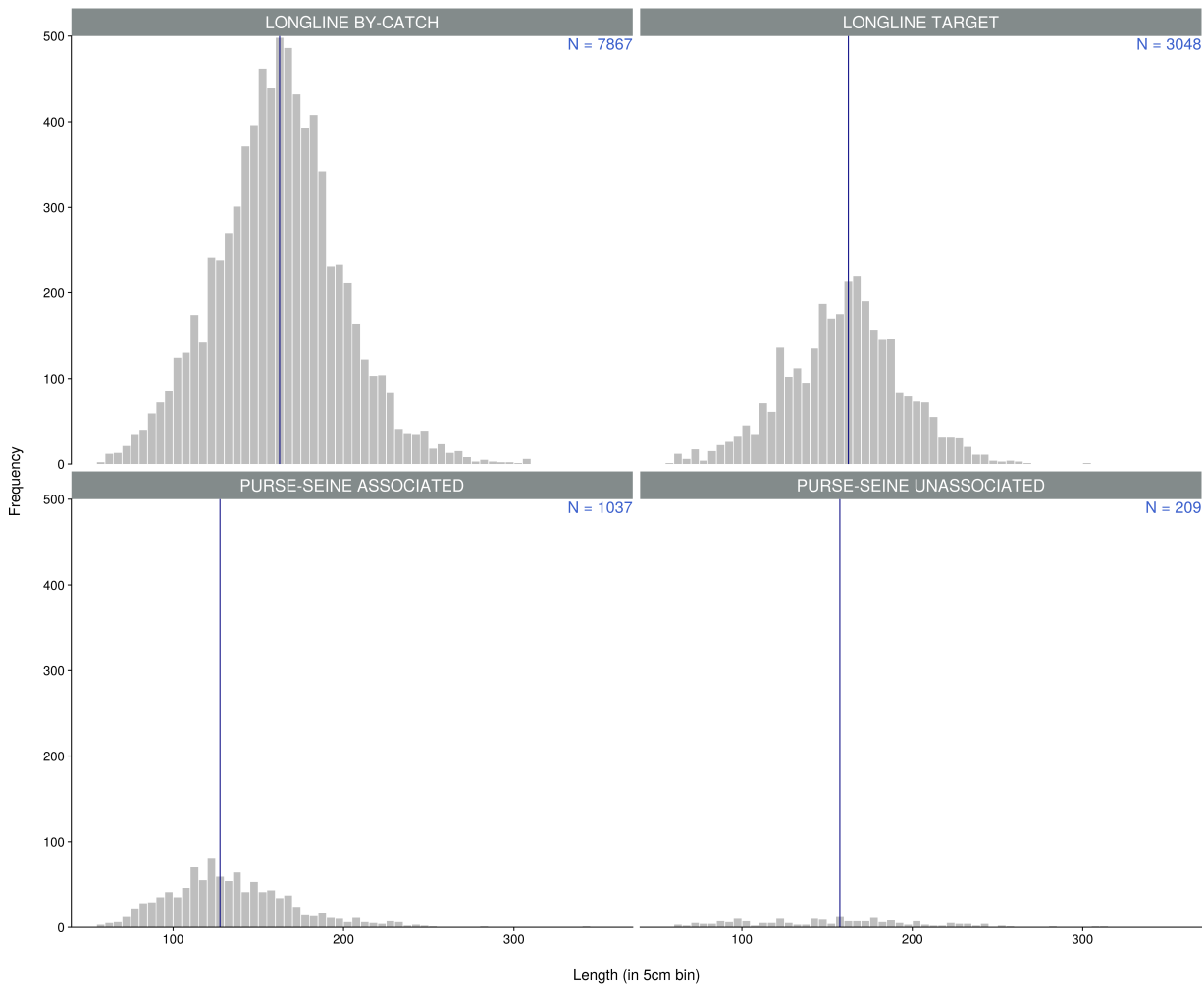
Figure 14: Length-compositions for oceanic whitetip shark in the four fleets used in the assessment, aggregated in 5cm bins. The sample size for each fleet is shown in the upper right. The vertical line shows the median length (in cm) for each fleet across all years.
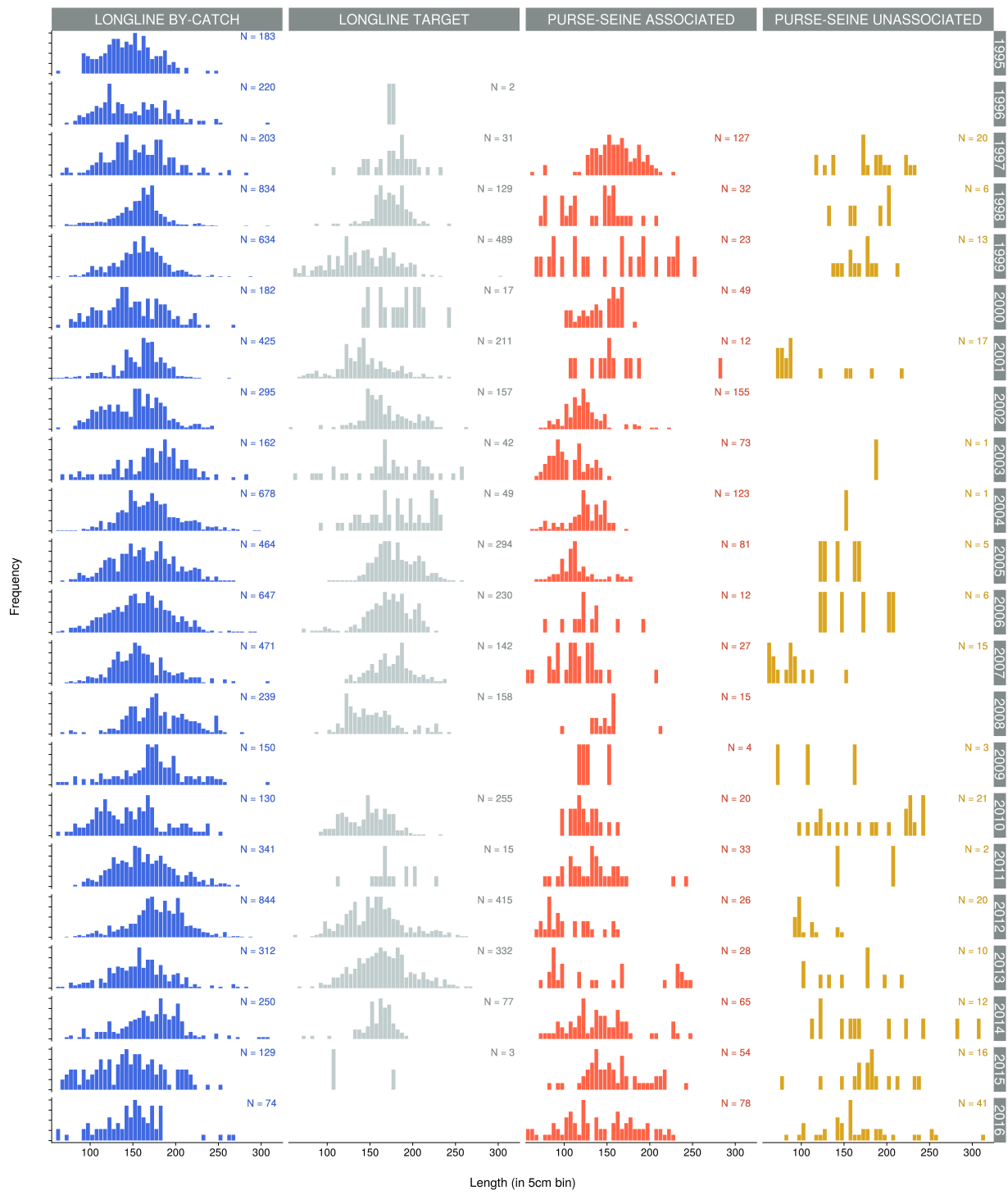
Figure 15: Annual length-compositions for oceanic whitetip shark for the four fleets used in the assessment, aggregated in 5cm bins. Fleets are in columns and years are in rows. The sample size for each fleet is shown in the upper right of each year-fleet panel.

Oceanic whitetip shark assessment
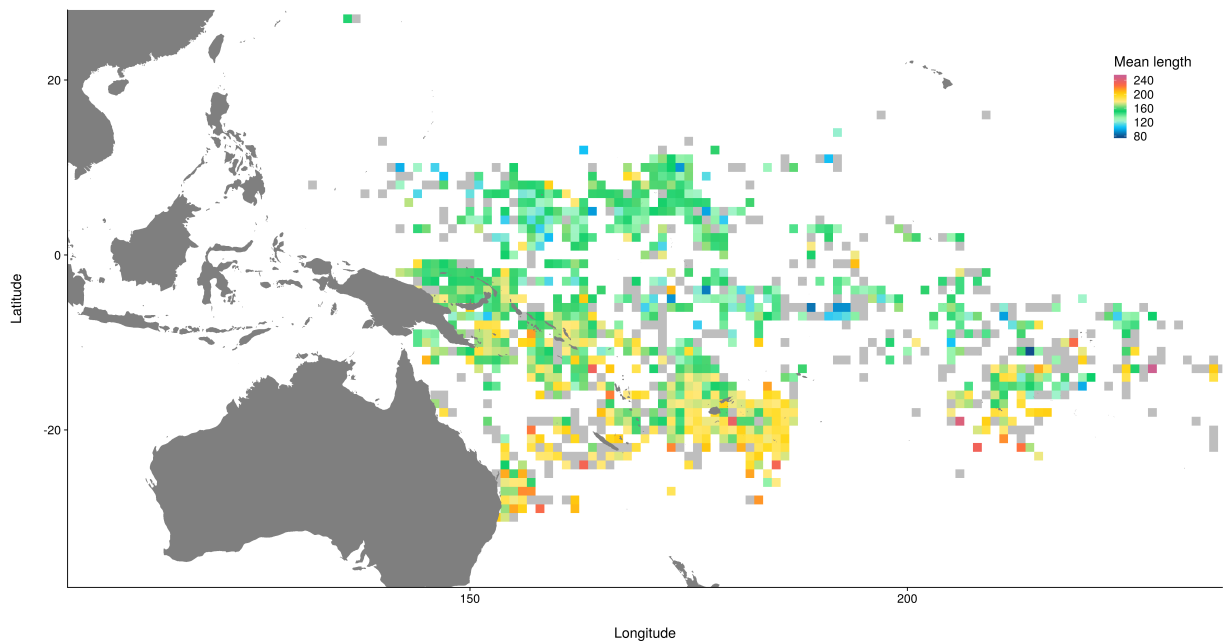
Figure 16: Mean length (total length in cm) from 1995 to 2016 for observed longline individuals (bycatch and target fleets) over the assessment region. Only cells with at least 2 individuals measured are shown (cells with a single measured individual are in grey).
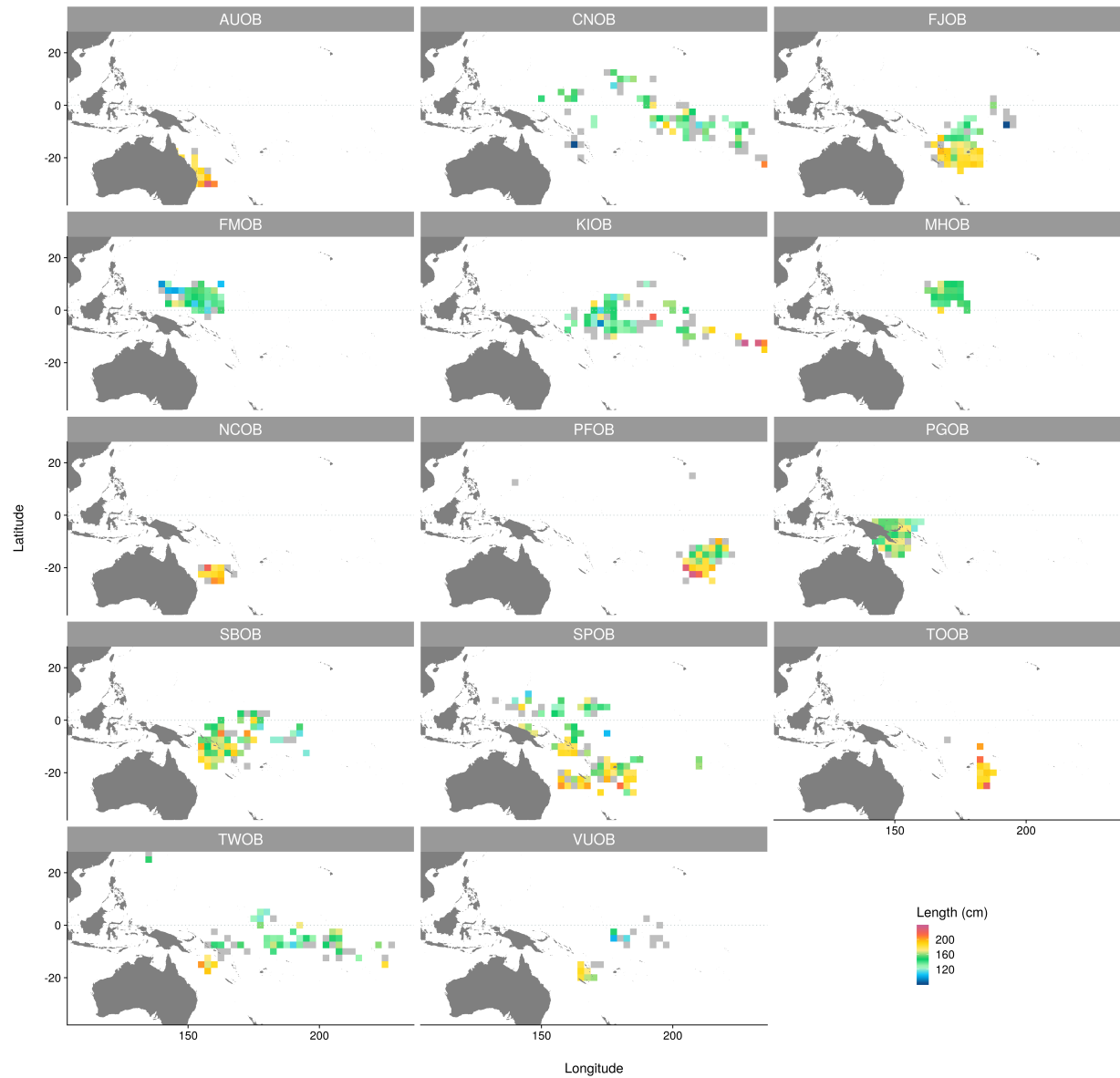
Figure 17: Mean length (total length in cm) from 1995 to 2016 for observed longline individuals (bycatch and target fleets) over the assessment region, split between observer program. Only cells with at least 2 individuals measured are shown (cells with a single measured individual are in grey)
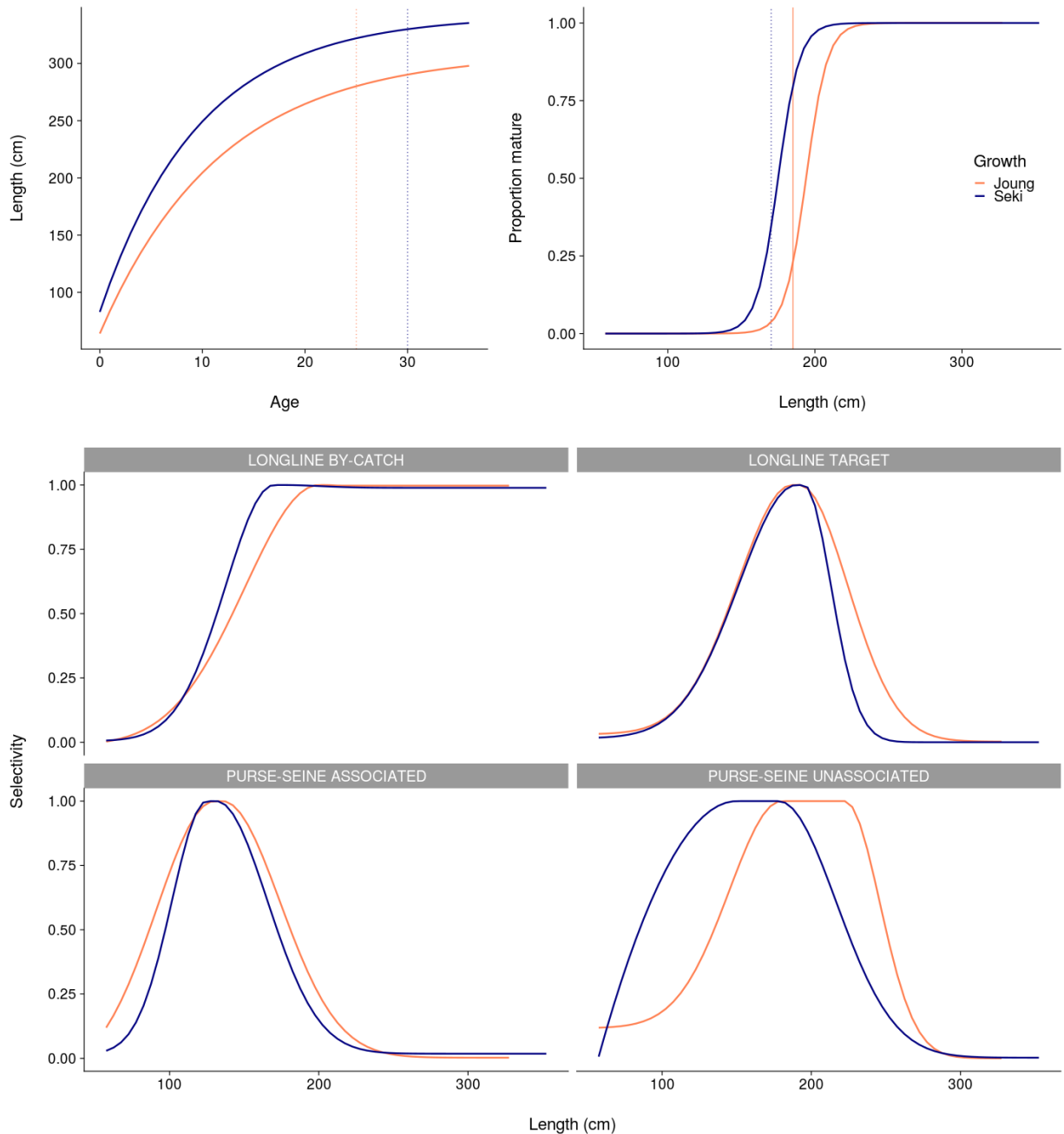
Figure 18: Comparison between the biological and fleet model parameters used for the two growth profiles based on the Seki et al. 1998 and Joung et al. 2016 studies: length‑at‑age (top left), maturity‑at‑length (top right) and selectivity by fleet (bottom). The dotted lines on the maturity‑at‑length plots indicate the average length at first maturity based on the first age‑at‑maturity specified for each model.

Oceanic whitetip shark assessment
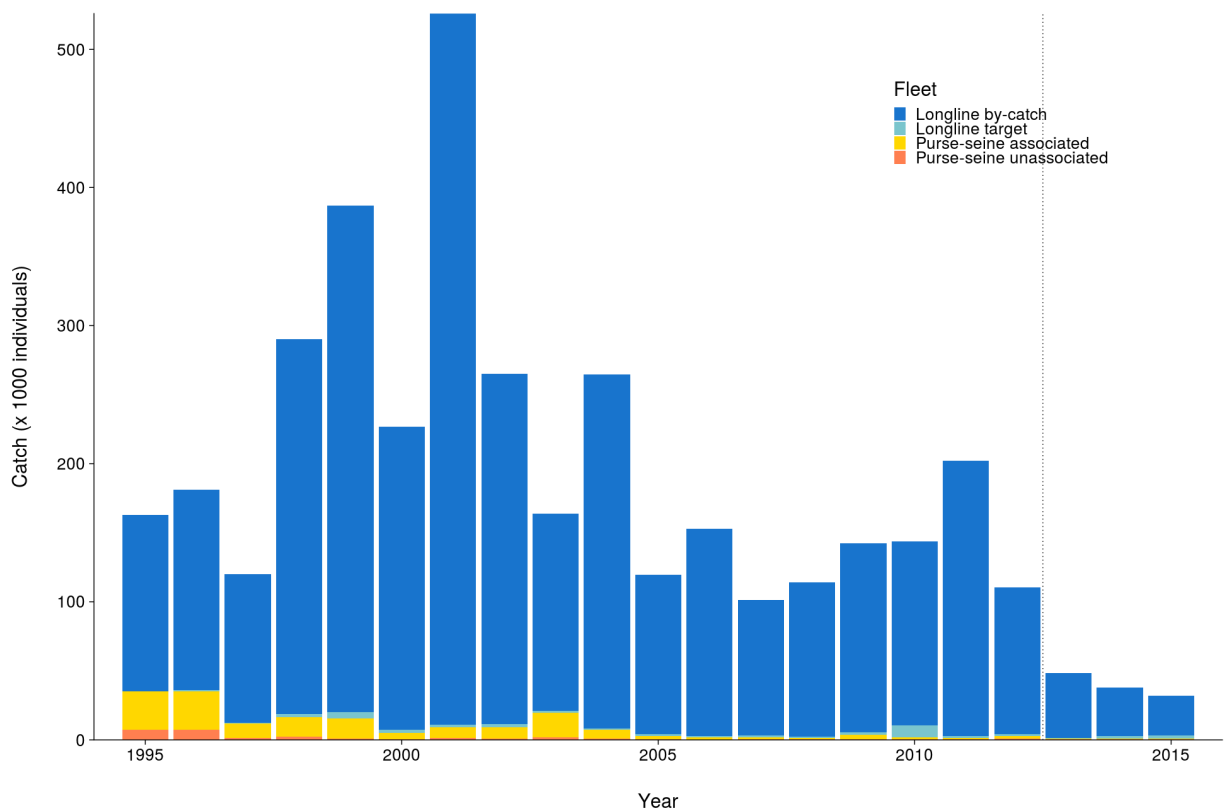
Figure 19: Total catches by fleet over time used for the diagnostic case. These catches were obtained from the median catch scenario assuming 25% discard mortality.

Oceanic whitetip shark assessment
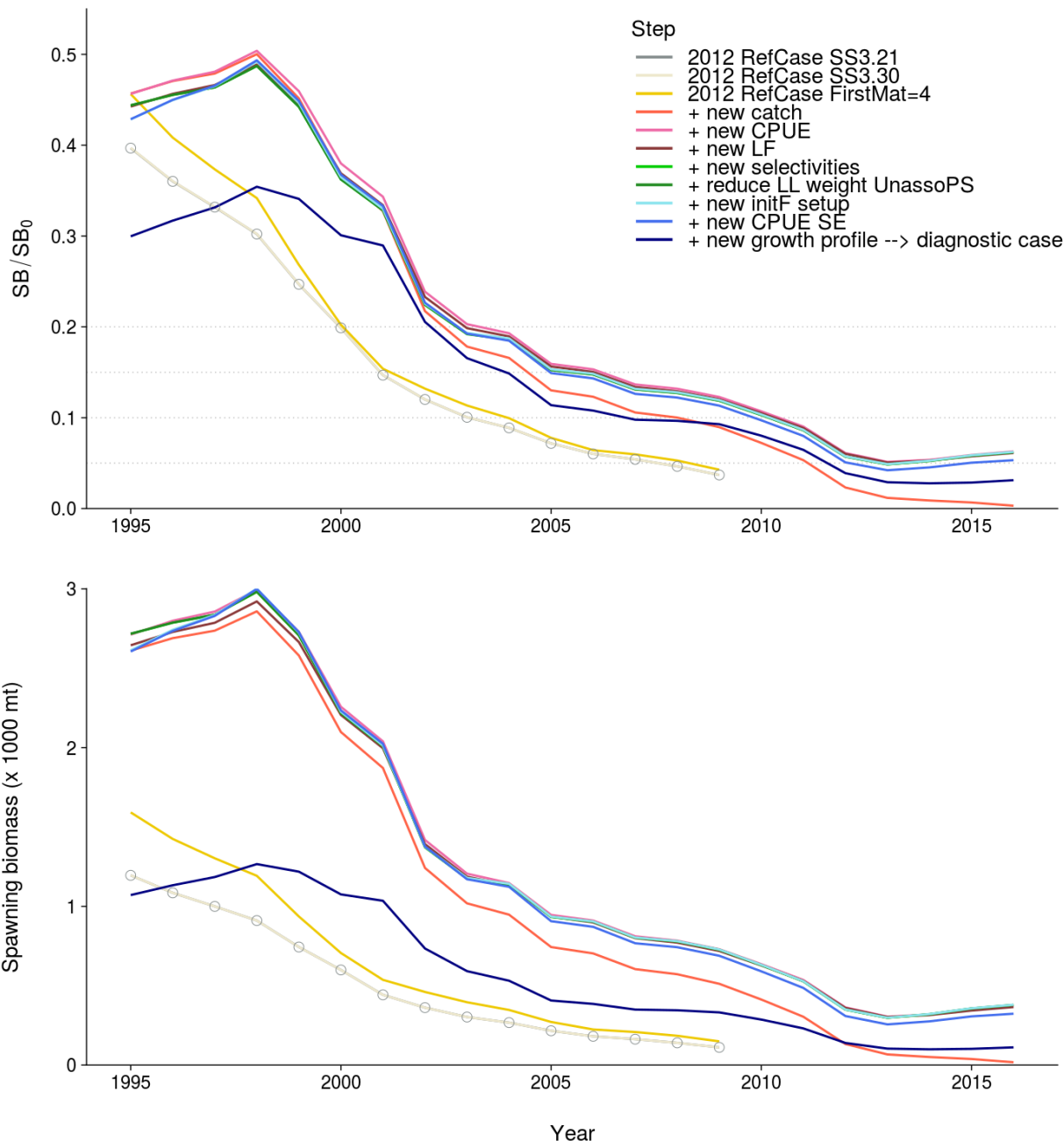
Figure 20: Impact on spawning biomass depletion of stepwise changes from the previous assessment model to the current diagnostic case.

Oceanic whitetip shark assessment
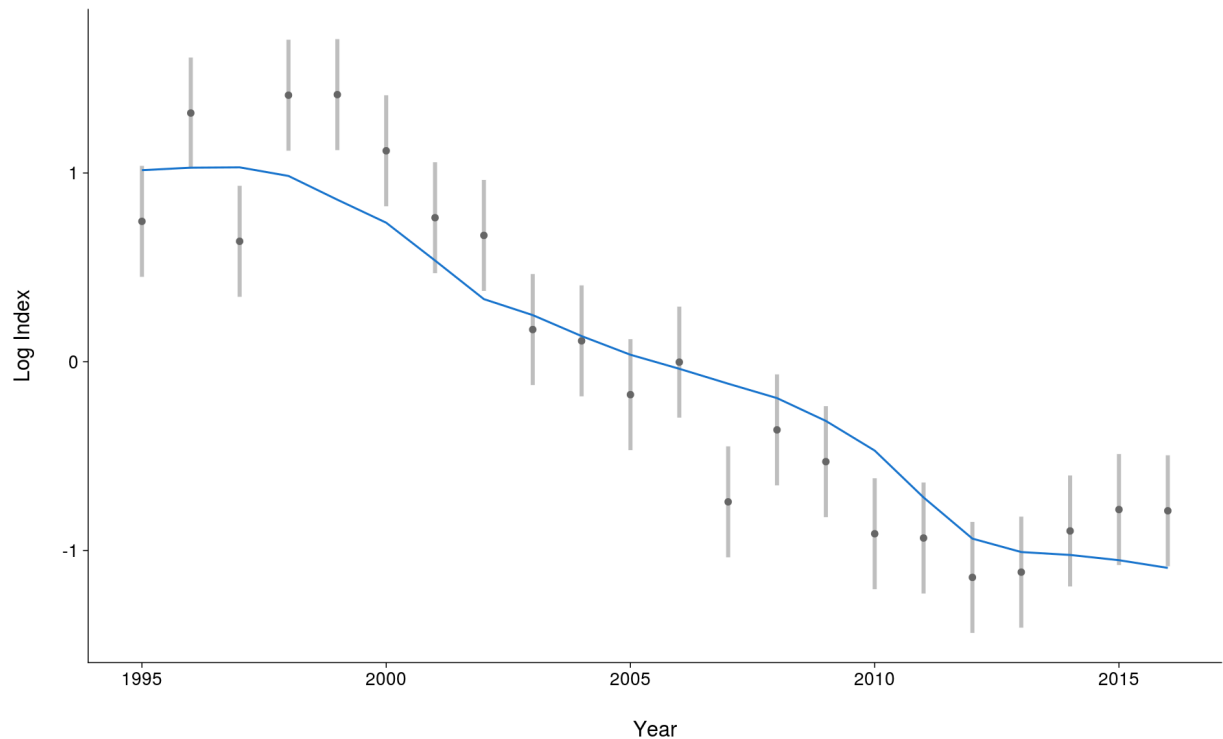
Figure 21: Observed (black) vs. predicted (blue) CPUE on the log‑scale for the by‑catch longline fleet under the diagnostic case, with the 95% confidence interval assumed for each year in grey.
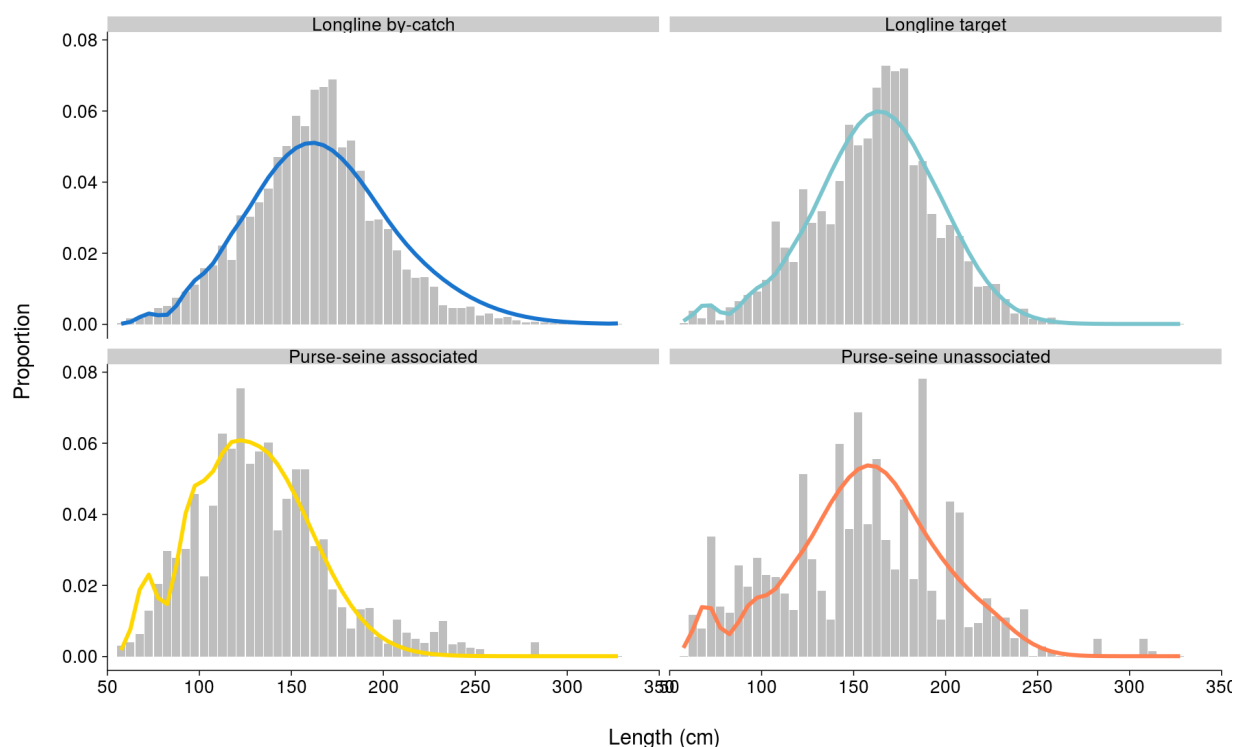
Figure 22: Observed vs. predicted catch‑at‑length for each fleet aggregated over all years for the diagnostic case.

Oceanic whitetip shark assessment
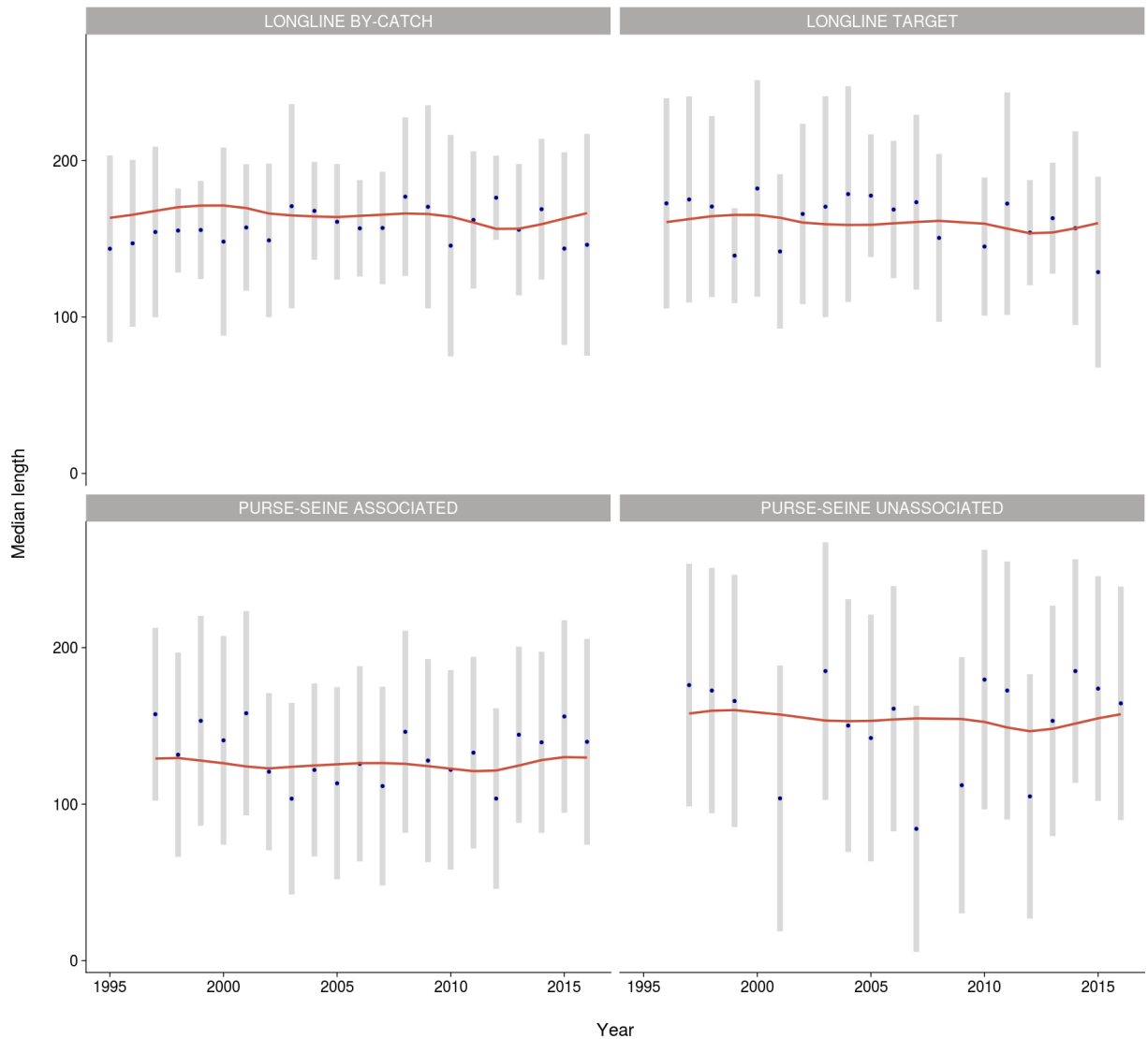
Figure 23: Temporal trend in the observed (blue points) vs. predicted (red line) catch‑at‑length for each fleet for the diagnostic case. The grey bands cover the 95% confidence interval for the observations.

Oceanic whitetip shark assessment
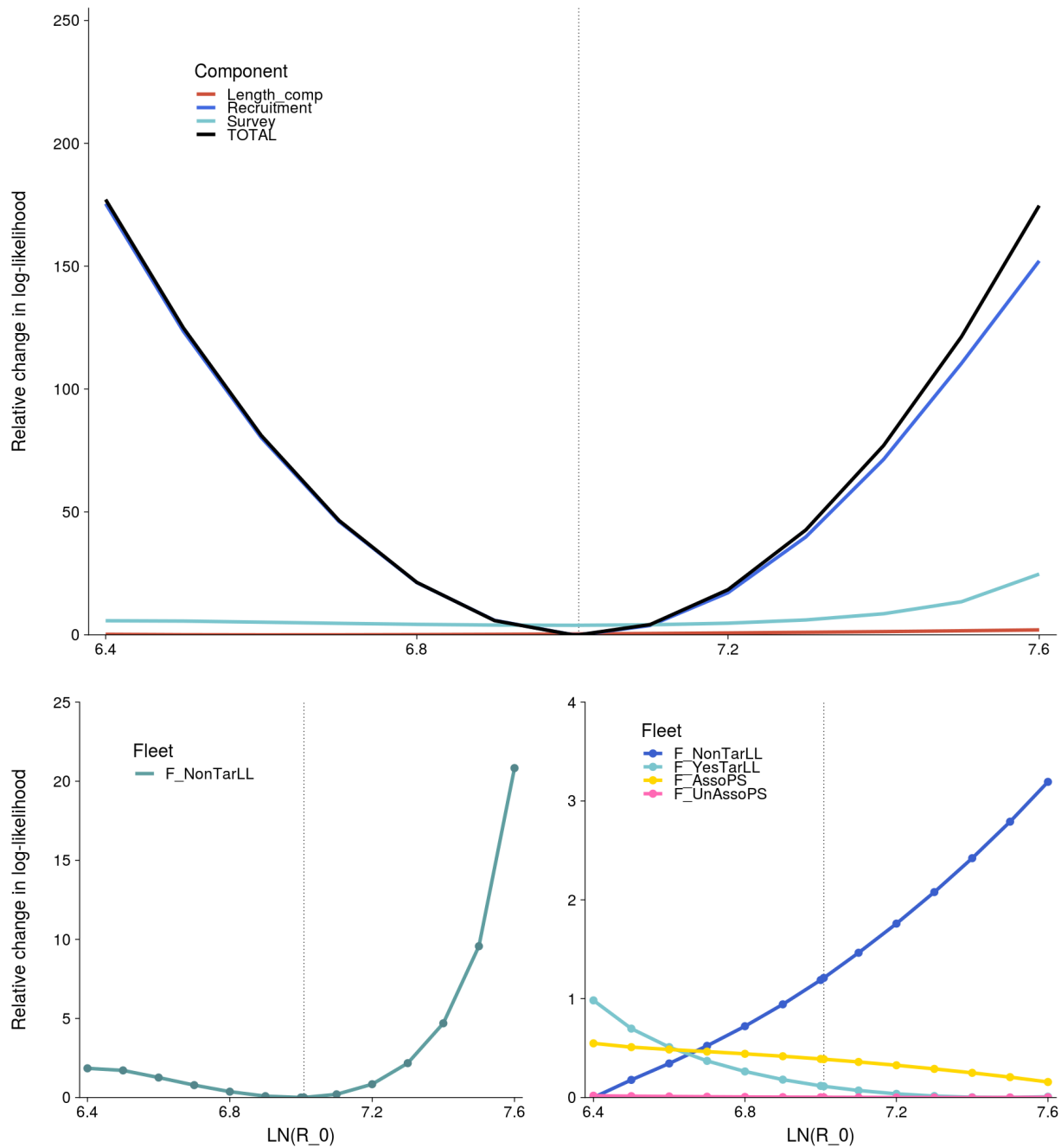
Figure 24: Relative change in log-likelihood for different values of $LN(R_0)$. The top panel shows the total likelihood and contribution by each component. The bottom panels show individual components by fleet for the CPUE and catch-at-length data. The dotted line shows the value for $LN(R_0)$ estimated under the diagnostic case.
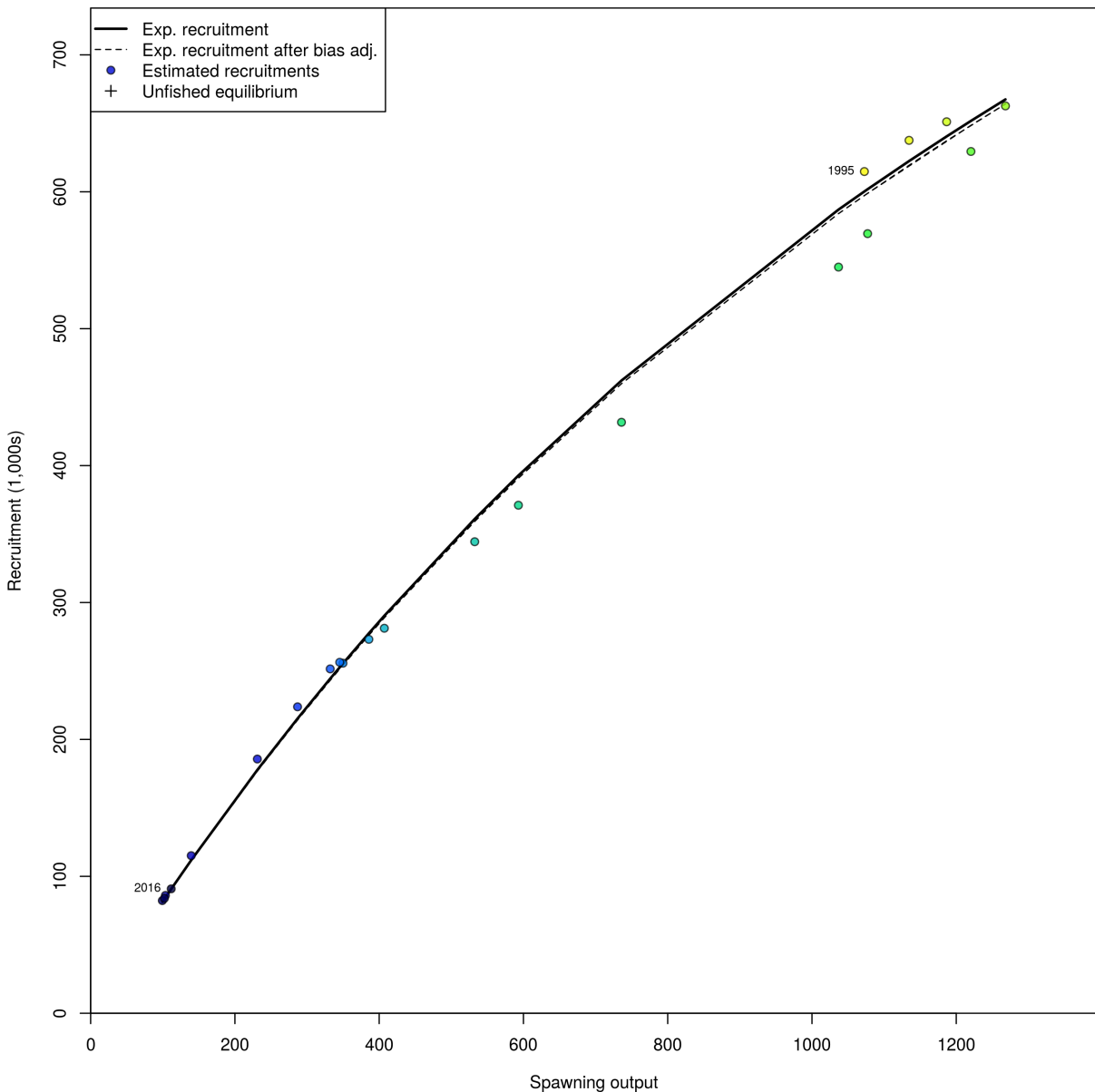
Figure 25: Estimated relationship between recruitment and spawner biomass for the diagnostic case model.

Oceanic whitetip shark assessment
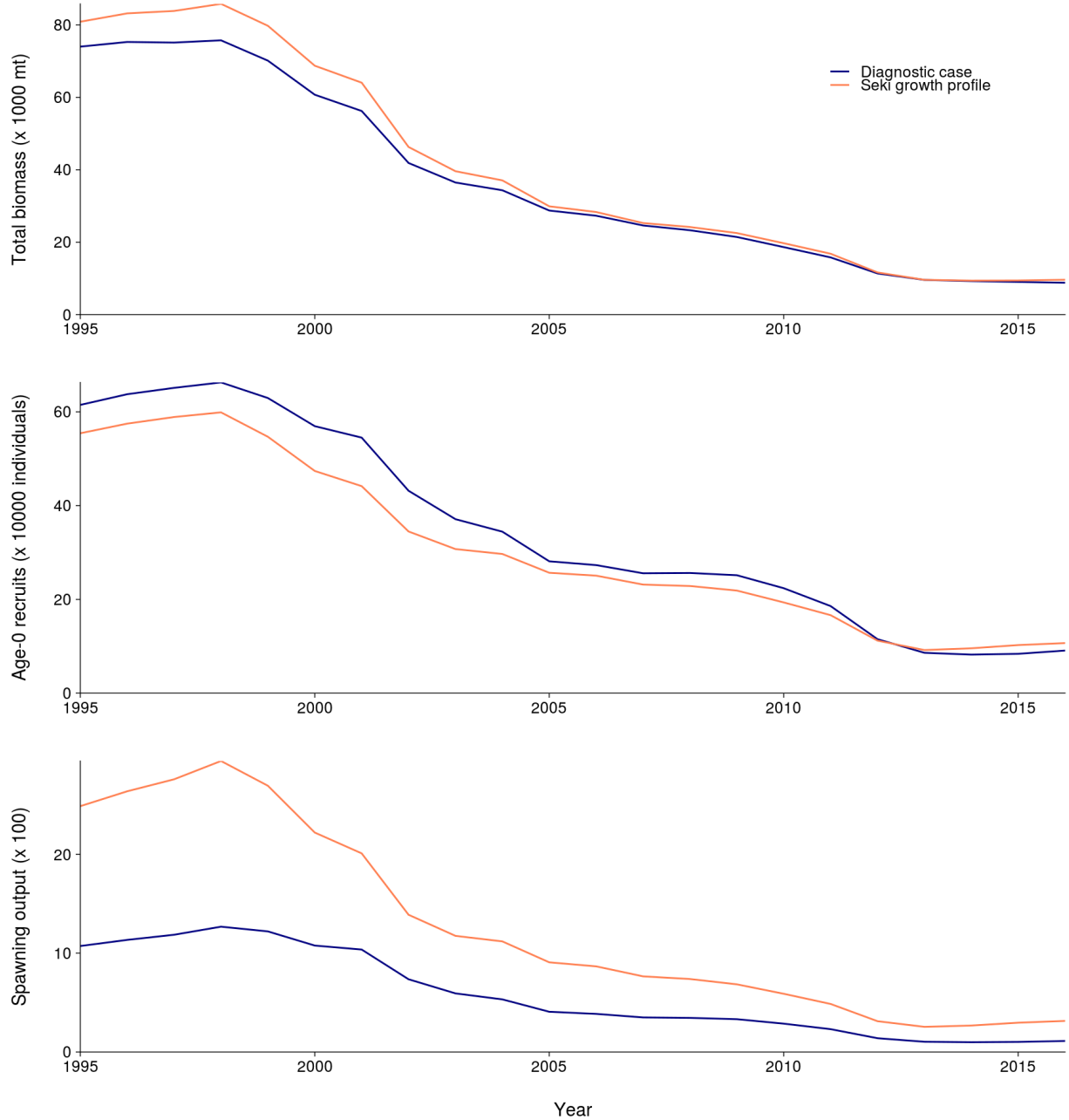
Figure 26: Total biomass, recruitment and spawning biomass for the diagnostic case and the alternative growth and fecundity profile predicted over 1995 - 2016.

Oceanic whitetip shark assessment
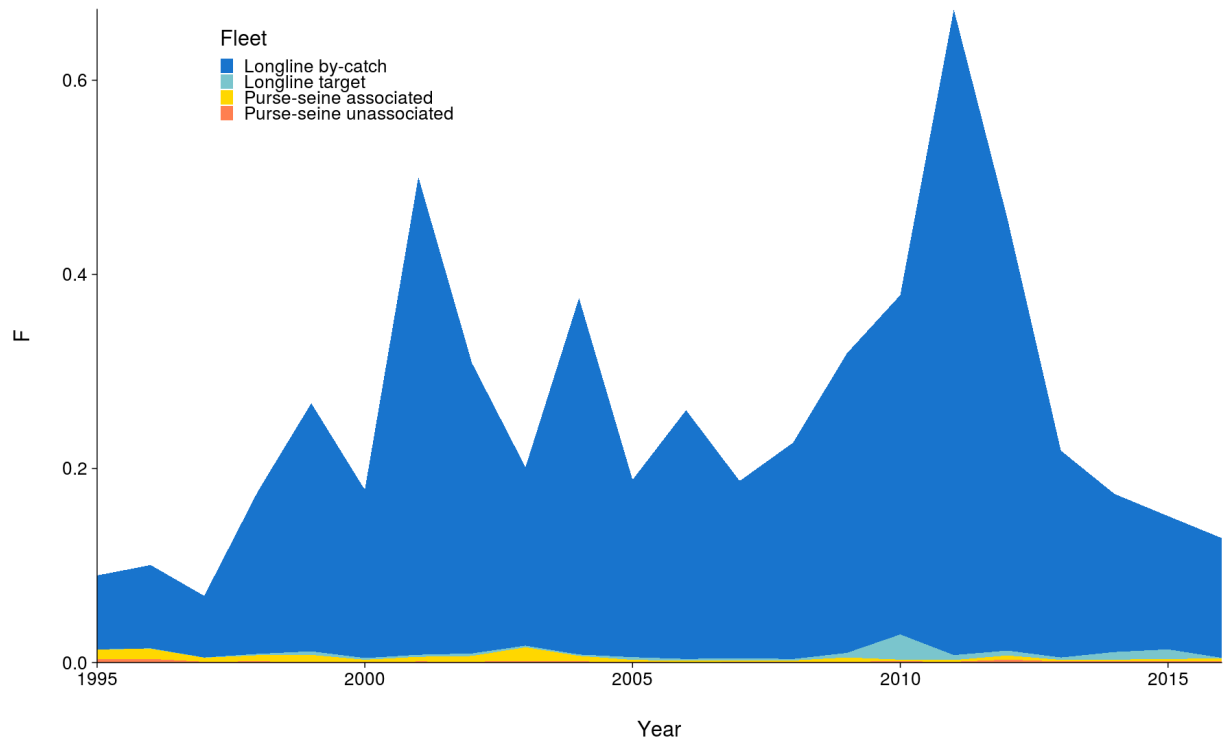
Figure 27: Fishing mortality by fleet estimated for the reference case over the time‑span of the assessment.
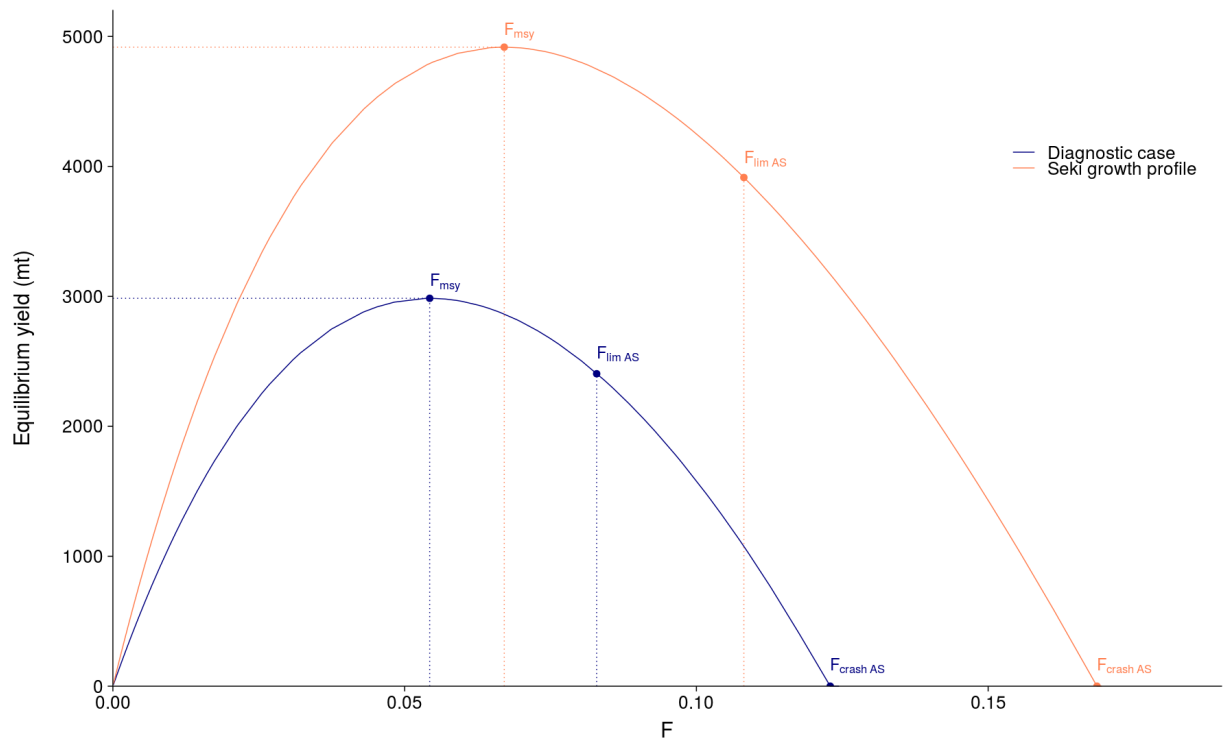
Figure 28: Yield as a function of fishing mortality for the diagnostic case and the alternative growth and fecundity scenario. The horizontal and vertical dotted lines indicate Maximum Sustainable Yield and F_{MSY}, respectively. The location of the three types of F‑based reference points presented in this assessment is indicated with the dots.
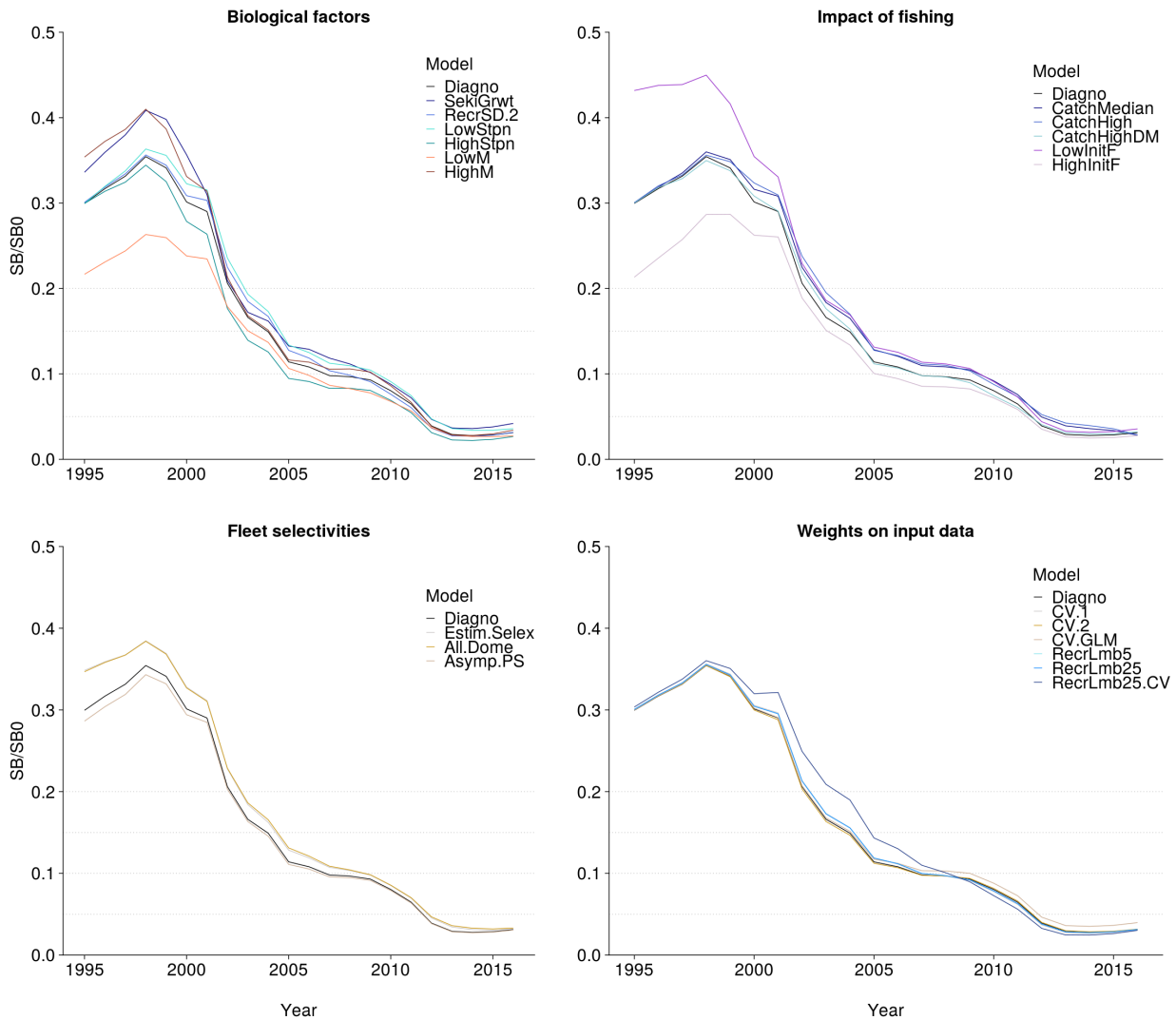
Figure 29: Impact of one‑off sensitivities from the diagnostic case on spawning biomass depletion trajectories, by parameter category.
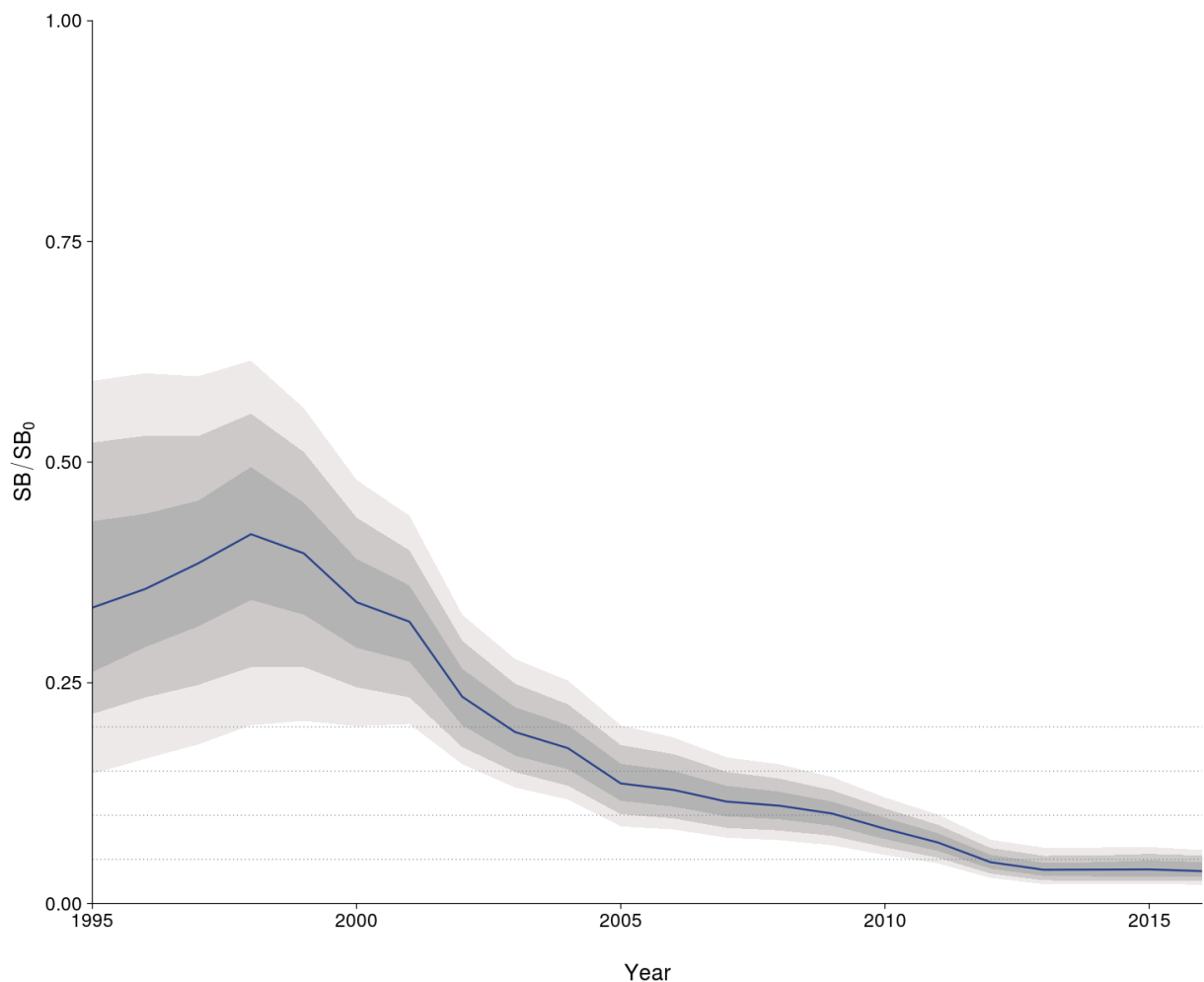
Figure 30: Median prediction of depletion in spawning biomass over all (unweighted) grid runs, with 0.025^{th} - 0.975^{th}, 0.10^{th} - 0.90^{th} and 0.25^{th} - 0.75^{th} quantile intervals. The horizontal grey lines are placed at intervals of 5% in the lower part of the graph to aid visualization.

Oceanic whitetip shark assessment
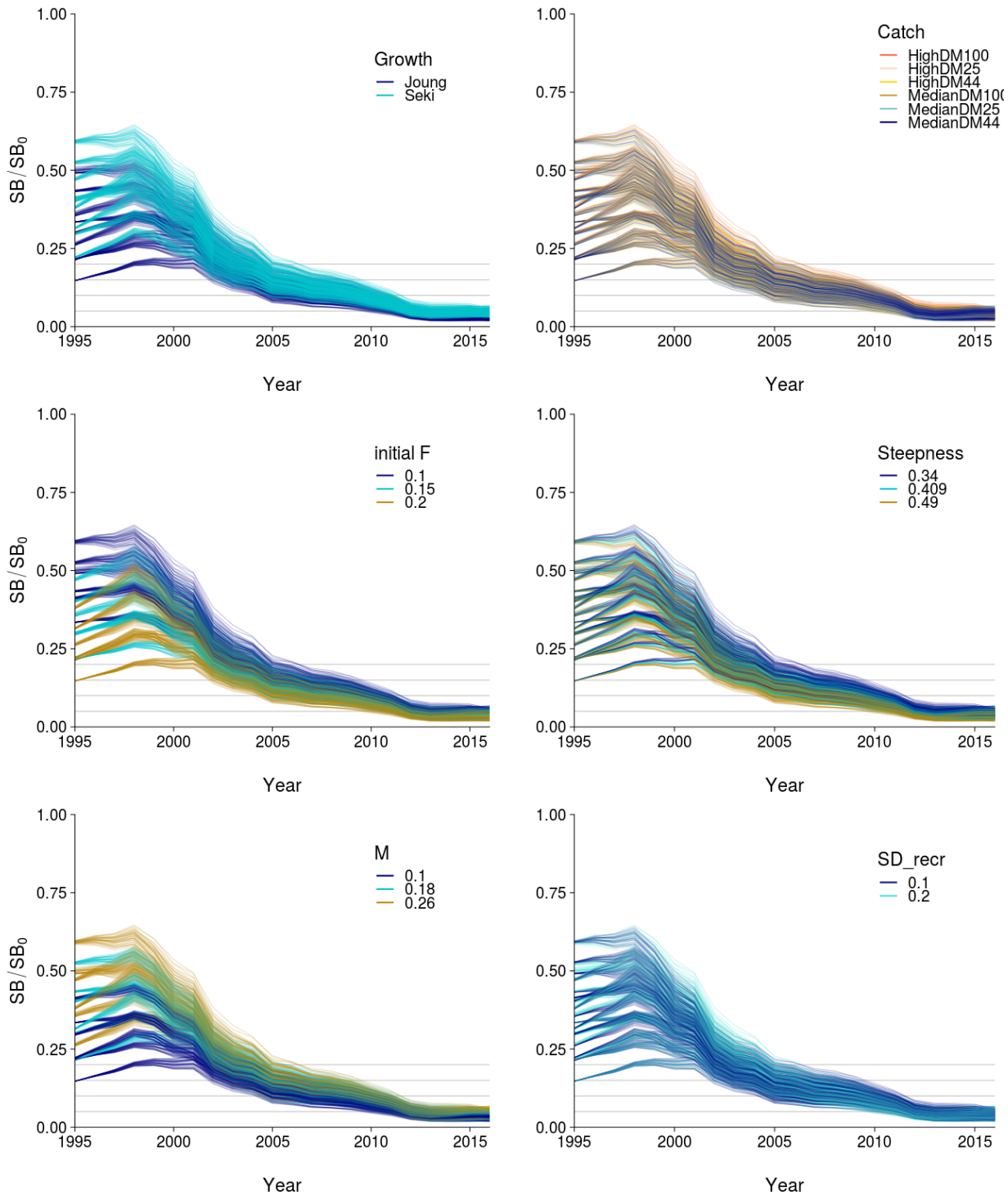
Figure 31: Prediction of depletion in spawning biomass for each structural uncertainty grid run, with each panel for each grid axis highlighting the different levels within. The horizontal grey lines are placed at intervals of 5% in the lower part of the graph to aid visualization.

Oceanic whitetip shark assessment
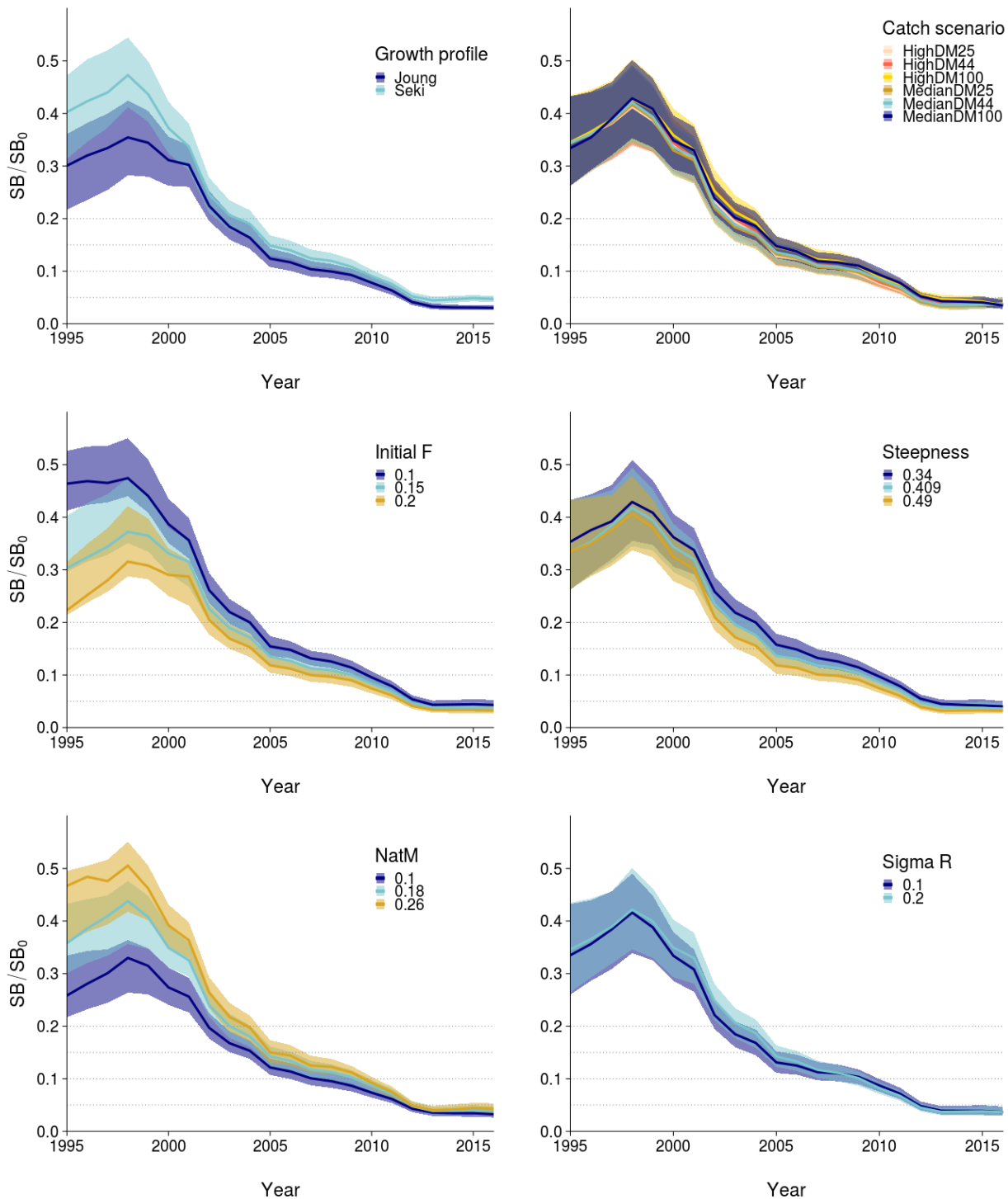
Figure 32: Median and inter‑quartile bounds for depletion in spawning biomass for each structural uncertainty axis, colour‑code by the level used for each axis. The horizontal grey lines are placed at intervals of 5% in the lower part of the graph to aid visualization.

Oceanic whitetip shark assessment
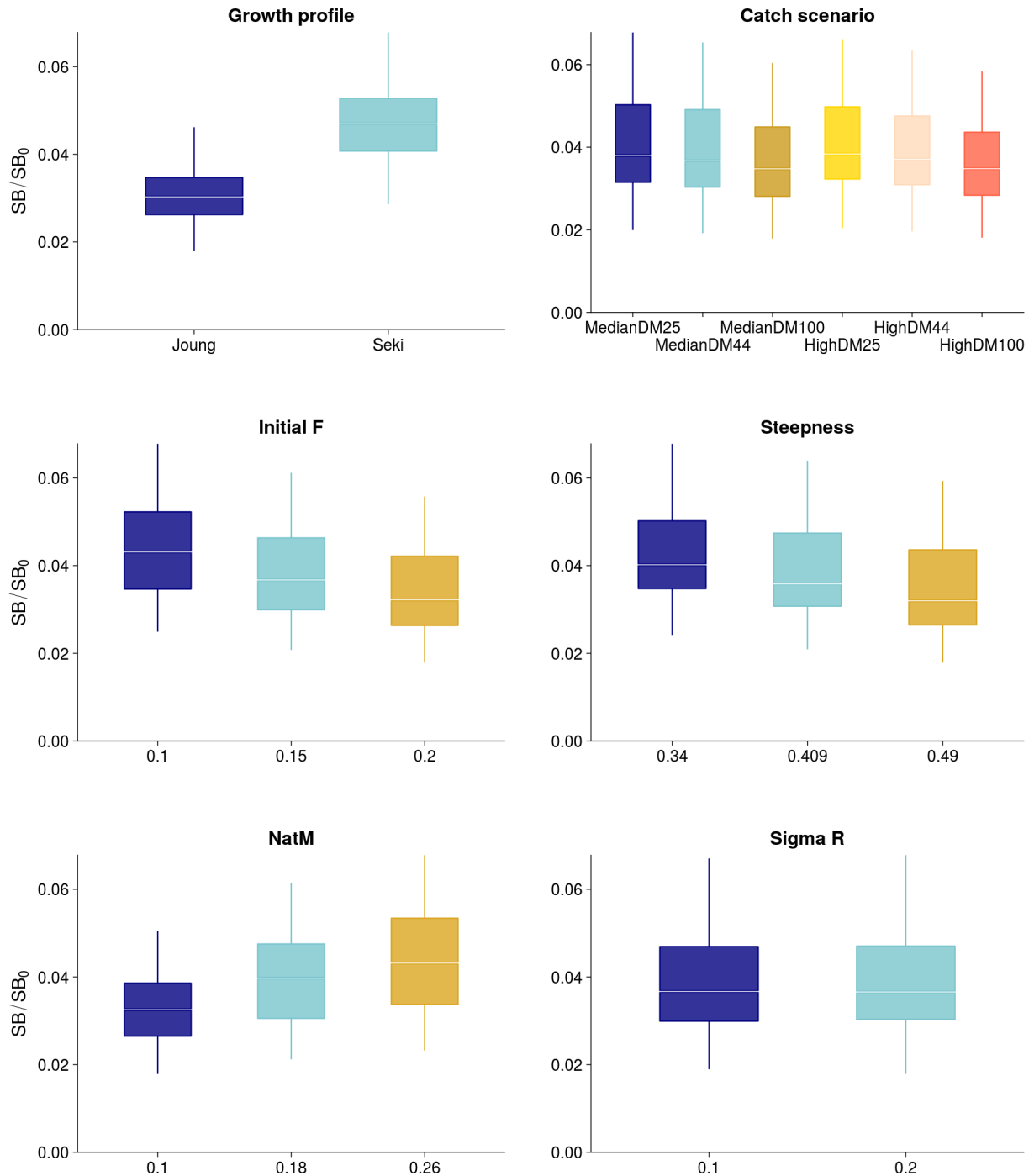
Figure 33: Median (white bar) and inter-quartile bounds (box) for SB/SB_0 in the final year of the assessment for each structural uncertainty axis. The whiskers extend to $1.5\times$ the interquartile range.

Oceanic whitetip shark assessment
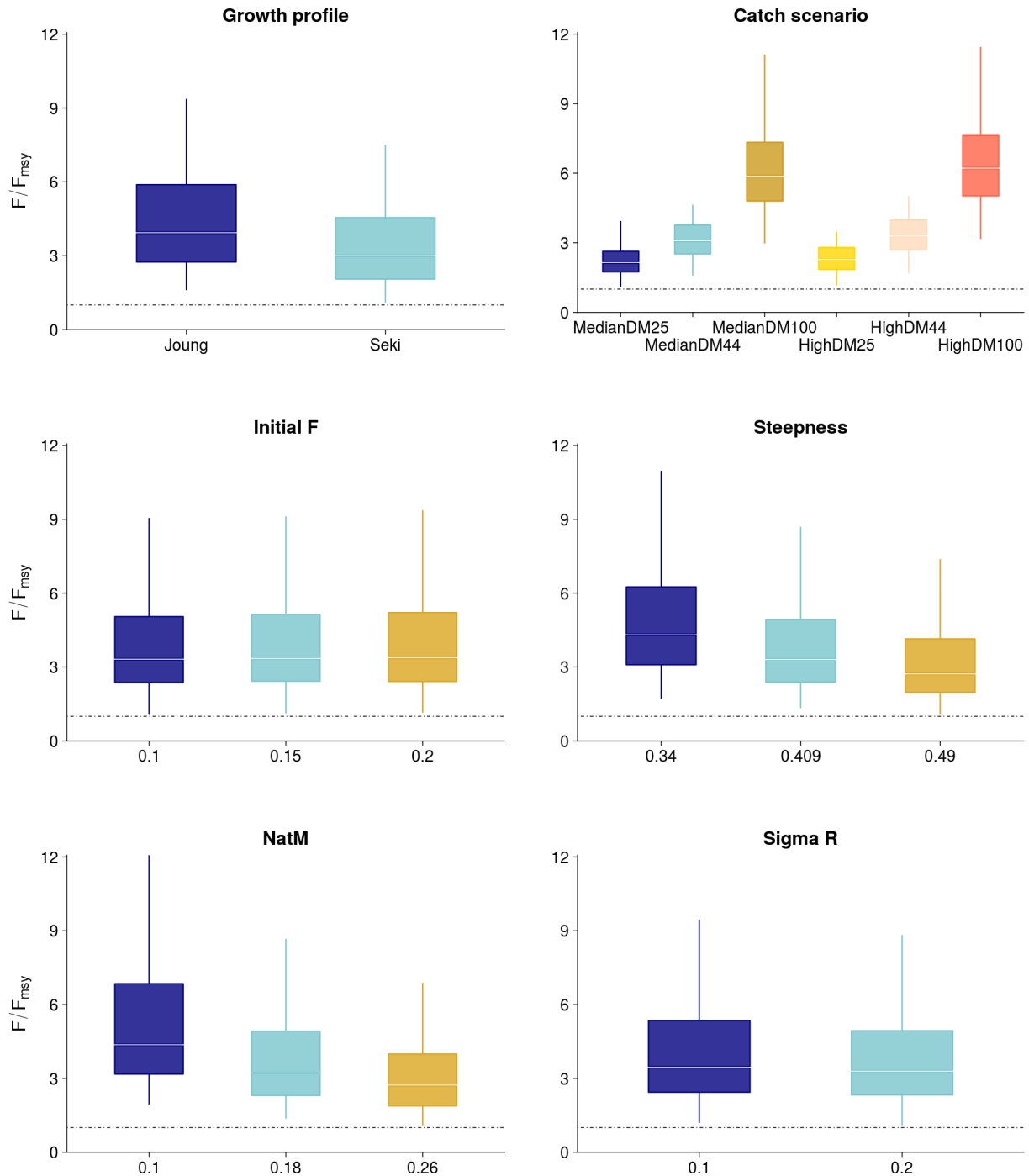
Figure 34: Median（white bar）and inter‑quartile bounds（box）for F/F_{MSY} in the final year of the assessment for each structural uncertainty axis. The whiskers extend to $1.5\times$ the interquartile range.
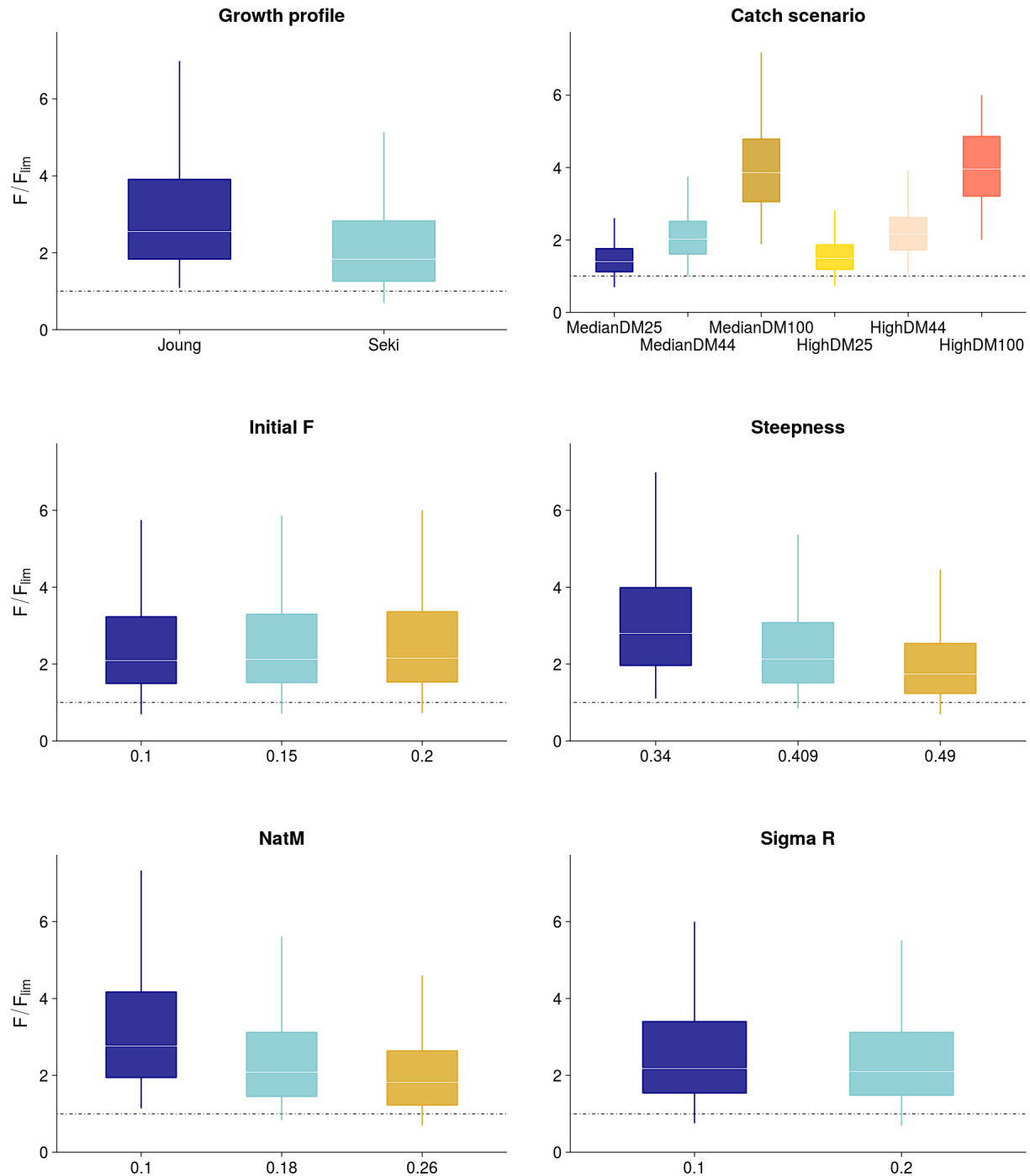
Figure 35: Median (white bar) and inter-quartile bounds (box) for F/F_{lim} in the final year of the assessment for each structural uncertainty axis. The whiskers extend to $1.5\times$ the interquartile range.

Oceanic whitetip shark assessment
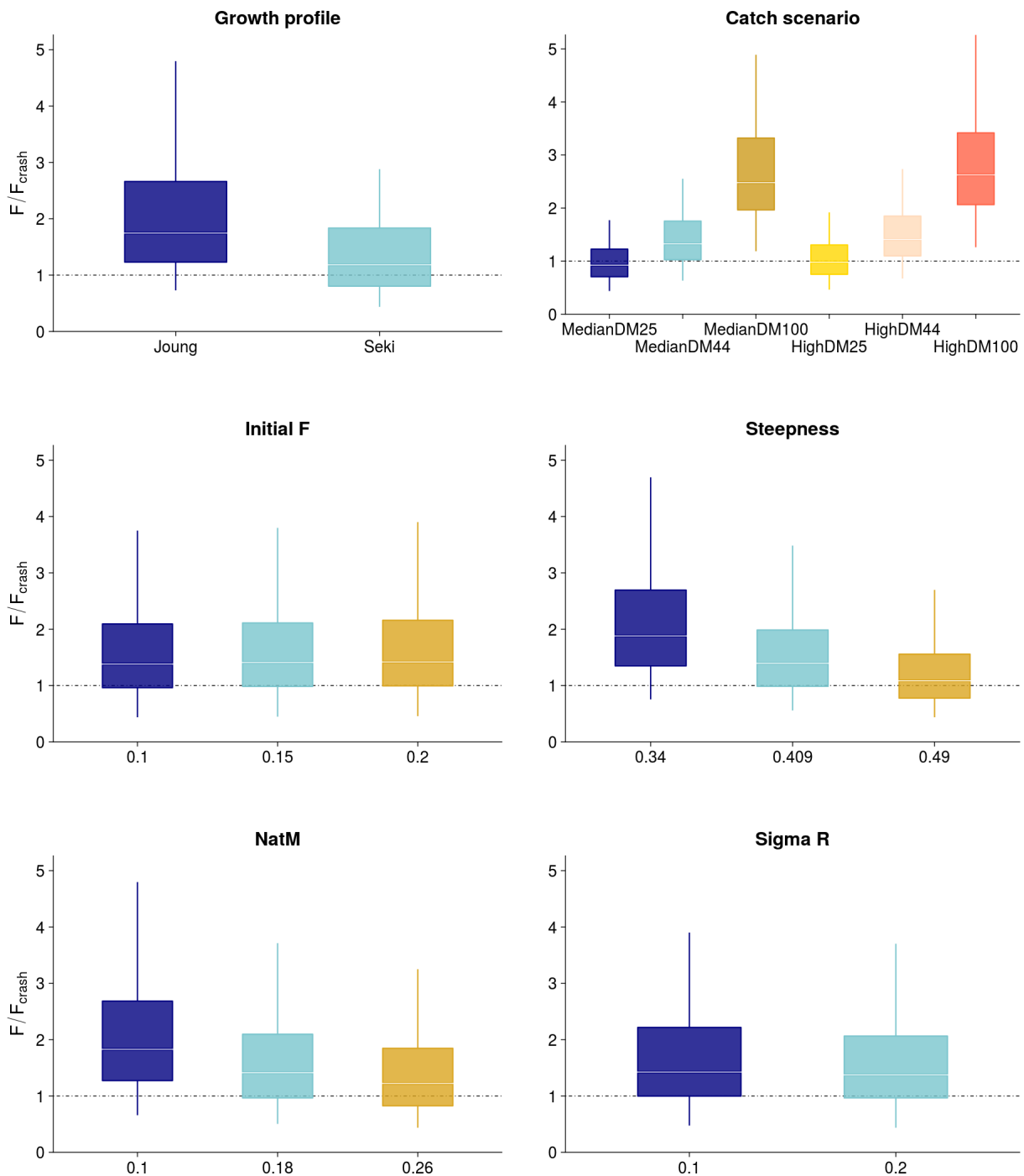
Figure 36: Median (white bar) and inter-quartile bounds (box) for F/F_{crash} in the final year of the assessment for each structural uncertainty axis. The whiskers extend to $1.5\times$ the interquartile range.
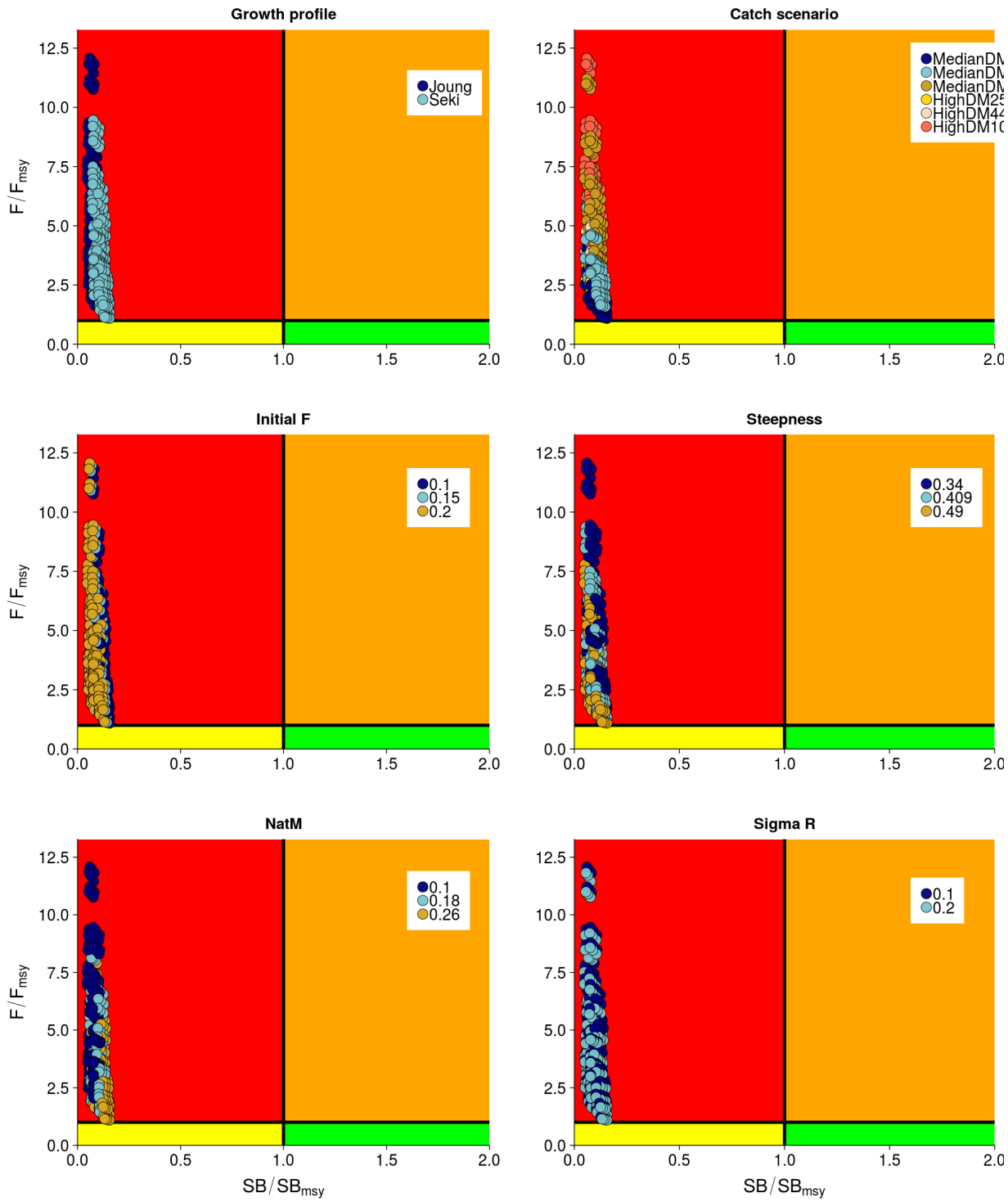
Figure 37: Kobe plots summarising status in the final year for each of the models in the structural uncertainty grid, based on SB/SB_{MSY} and F/F_{MSY}. The stock is considered to be overfished when $SB/SB_{MSY} > 1$ and undergoing overfishing when $F/F_{MSY} > 1$.
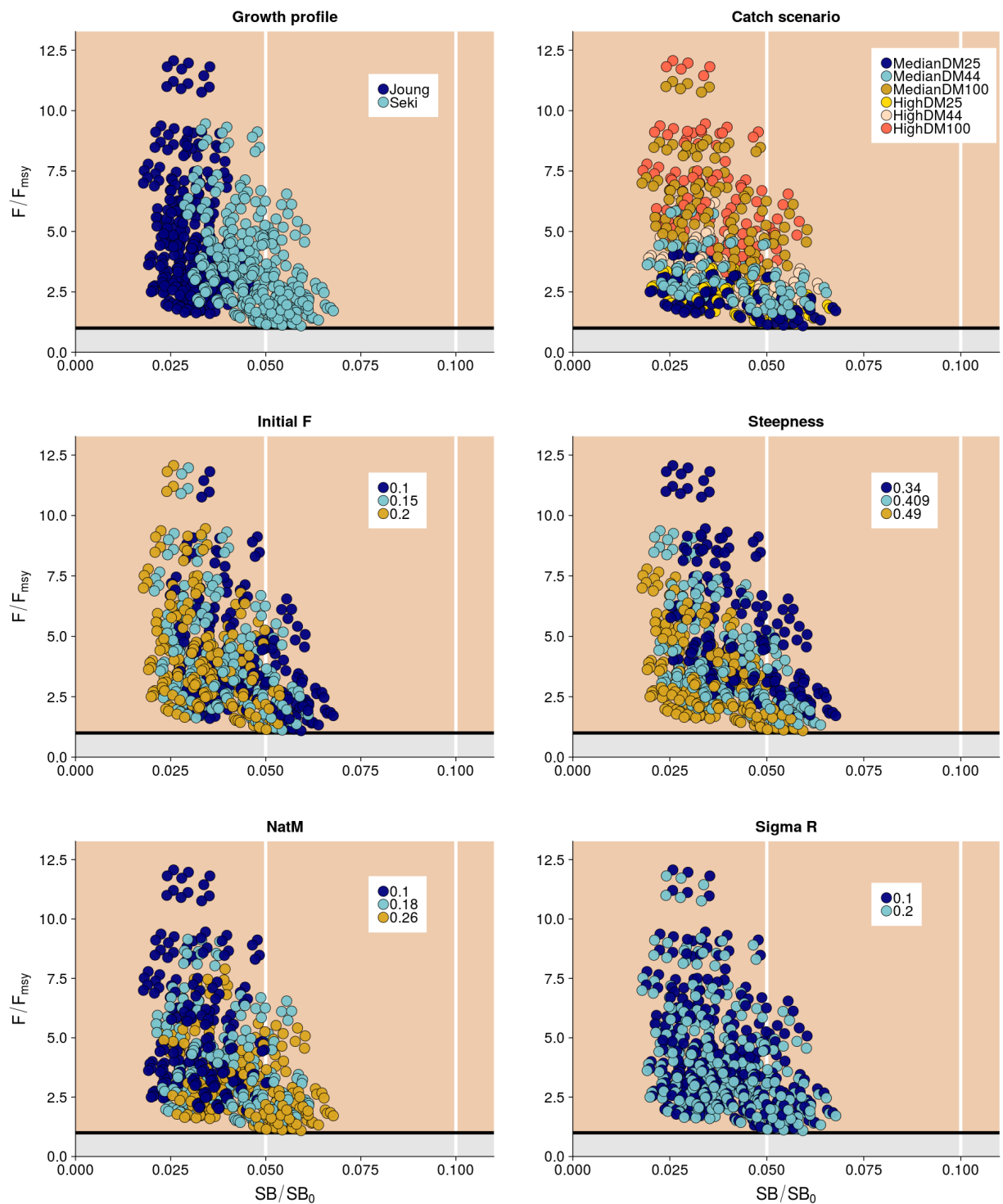
Figure 38: Panel plot summarising stock status in the final year for each of the models in the structural uncertainty grid for SB/SB_0 and F/F_{MSY}. The stock is considered to be undergoing overfishing when $F/F_{MSY} > 1$ (beige zone). The SB/SB_0 axis was scaled to span the range of depletion values. Guidelines were added in white at $0.5SB/SB_0$ and $0.1SB/SB_0$.

Oceanic whitetip shark assessment
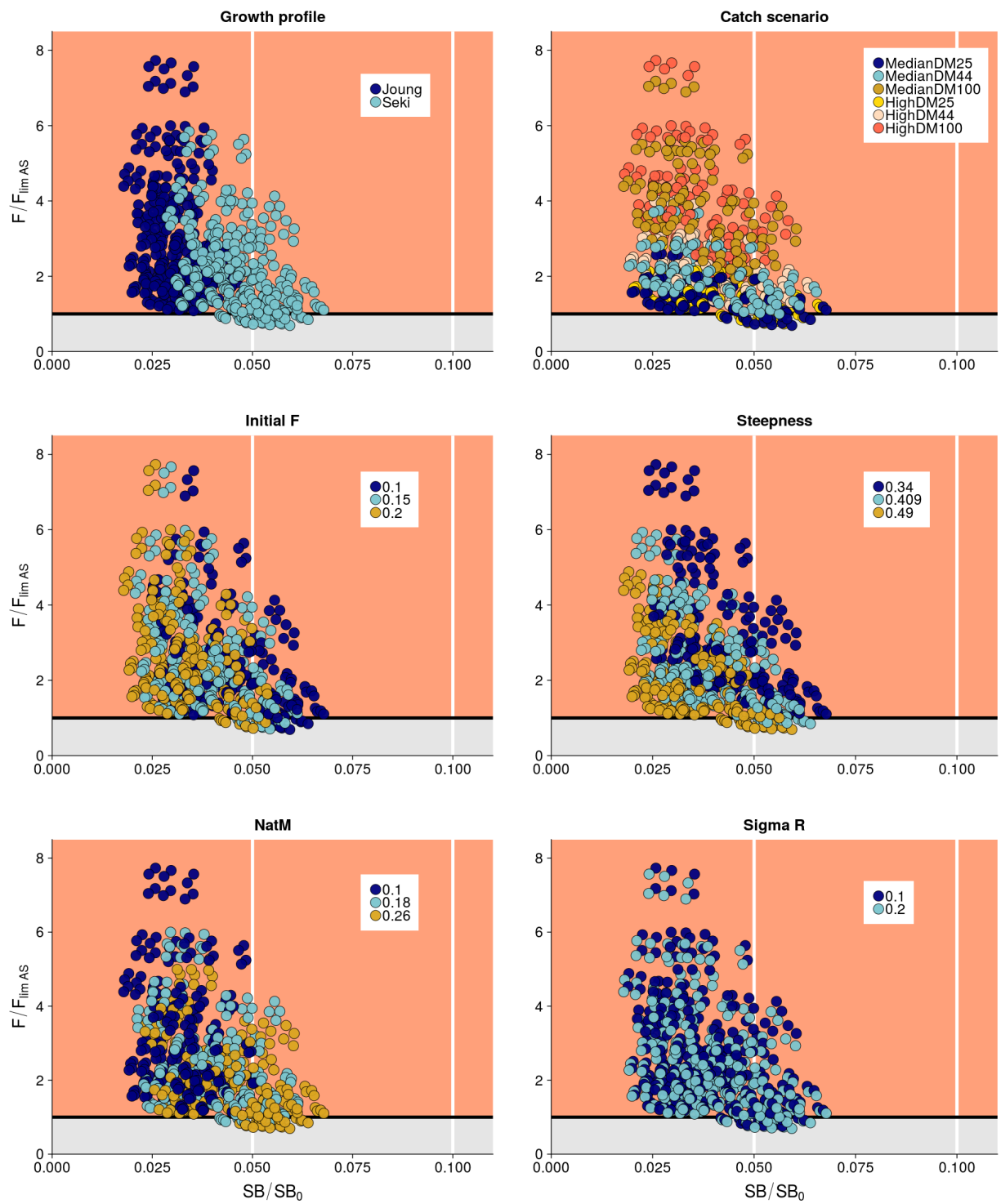
Figure 39: Panel plot summarising stock status in the final year for each of the models in the structural uncertainty grid for SB/SB_0 and $F/F_{lim,\text{AS}}$. When $F/F_{lim,\text{AS}} > 1$ (orange zone), the spawning biomass has declined below $0.5SB_{MSY}$. The SB/SB_0 axis was scaled to span the range of depletion values. Guidelines were added in white at $0.5SB/SB_0$ and $0.1SB/SB_0$.

Oceanic whitetip shark assessment
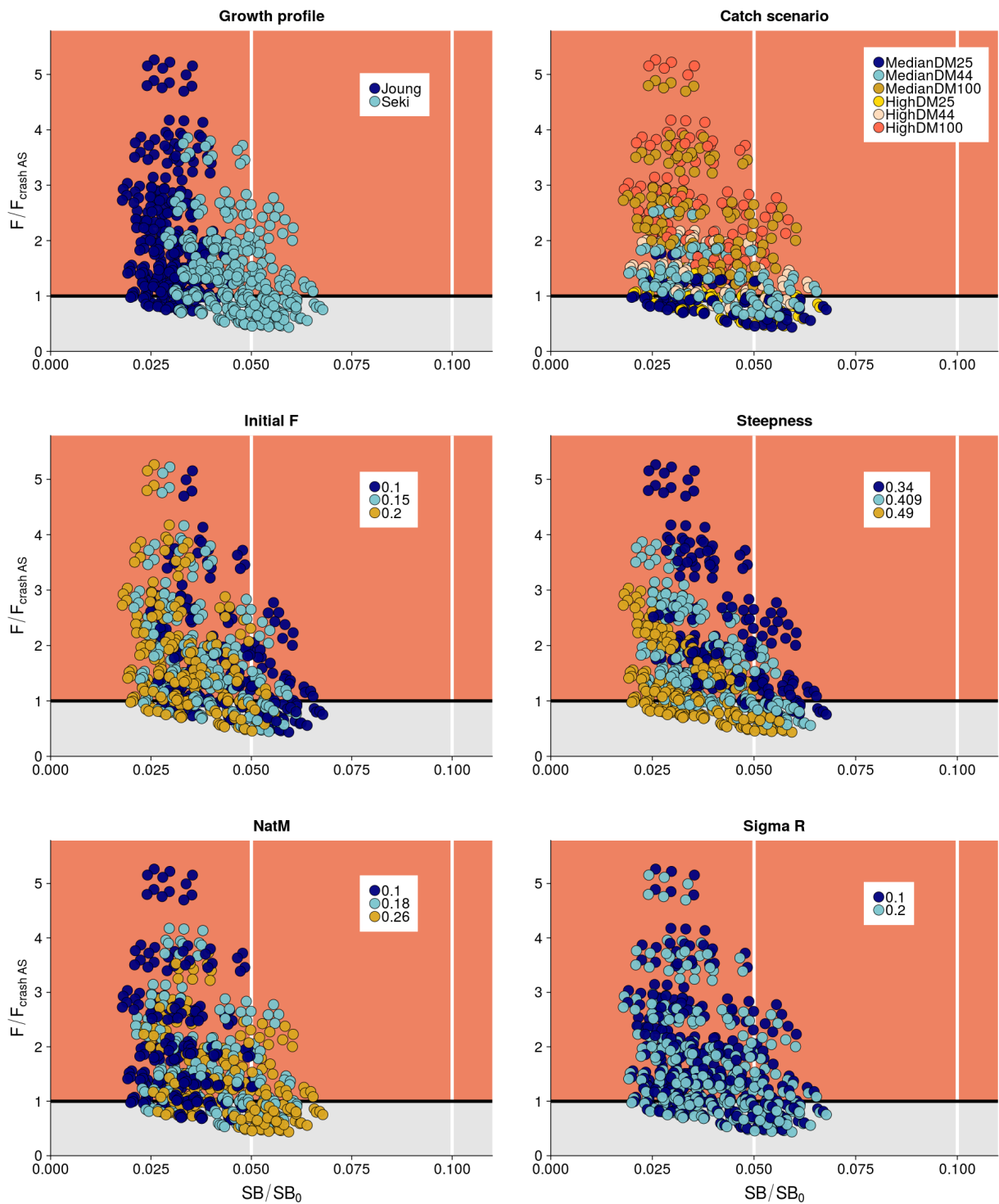
Figure 40: Panel plot summarising stock status in the final year for each of the models in the structural uncertainty grid for SB/SB_0 and $F/F_{crash,\mathrm{AS}}$. The population is expected to become extinct when levels of F in excess of $F_{crash,\mathrm{AS}}$ (i.e. $F/F_{crash,\mathrm{AS}} > 1$; pink zone) are maintained on the long-term. The SB/SB_0 axis was scaled to span the range of depletion values. Guidelines were added in white at $0.5 SB/SB_0$ and $0.1 SB/SB_0$.

Oceanic whitetip shark assessment

APPENDIX A: Retrospective analyses

Retrospective analyses allow to assess model bias by rerunning a key model (here, the diagnostic case) and consecutively removing successive years of data (Cadrin & Vaughan 1997, Cadigan & Farrell 2005). A series of five additional models were thus fitted starting with the full data-set (i.e. the diagnostic case through 2016), followed by models with the retrospective removal of all input data from the years 2016 to 2012, sequentially. A comparison of the depletion, spawning potential and recruitment trajectories are shown in Figure A-41. There is a small temporal bias in the presented stock metrics that results from the removal of successive years. This could be due to the fact that there was a high period of catches up to 2012 and a sudden drop thereafter. The sustained period of high catches could inform the model that the stock is more productive for the models spanning longer time periods up to 2016. The difference in estimated SB/SB_0 was the greatest for the model stopping in 2011 (-0.03 compared to 2016), and the smallest for the model stopping in 2015 (-0.004).
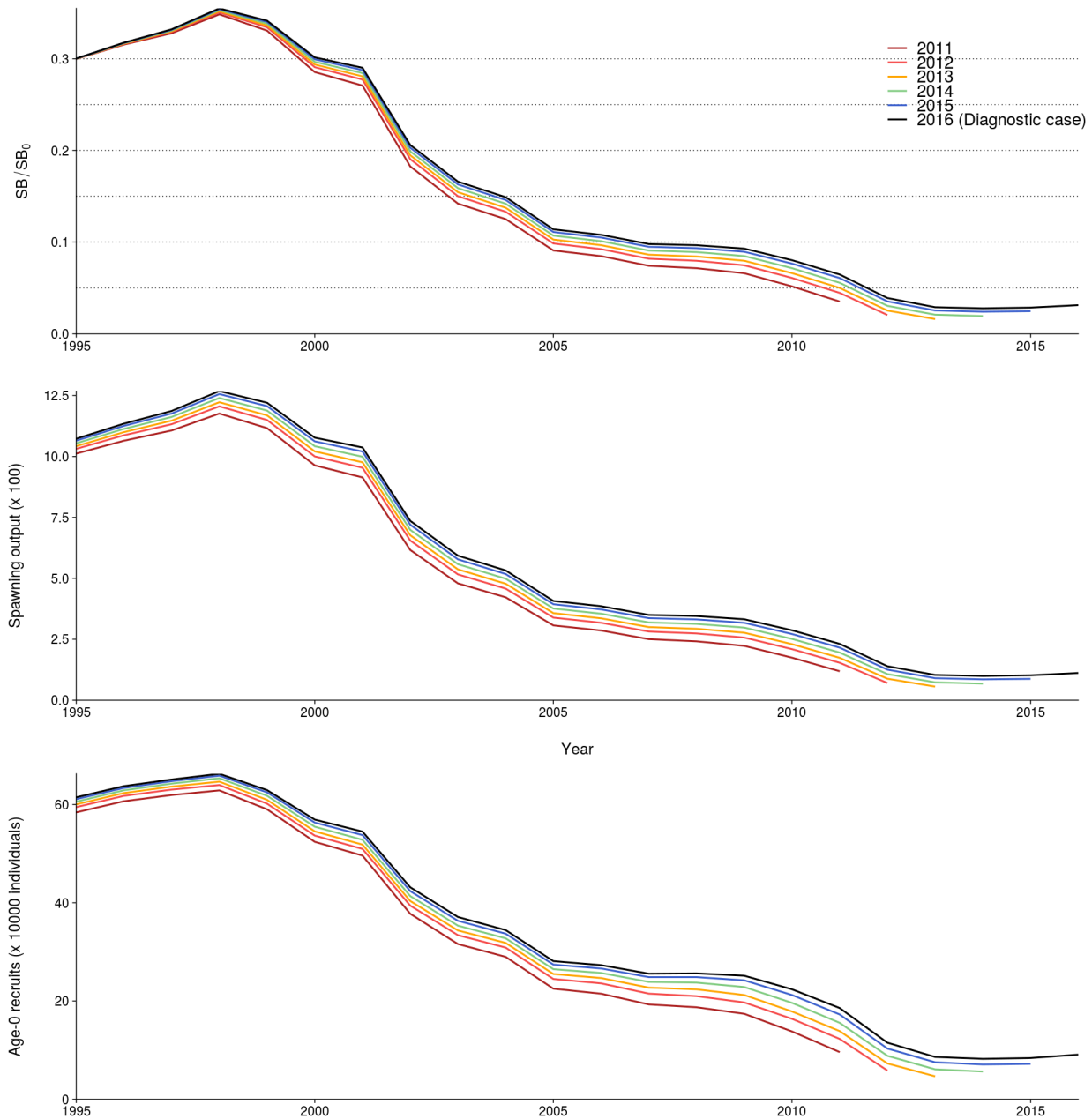
Figure A-41: Estimated depletion (SB/SB_0), spawning potential and recruitment for each of the retrospective models sequentially removing one year of the data for the tail end of the time-series. Model labels refer to the final year of data included in the retrospective run.

Oceanic whitetip shark assessment

Table B-13: Likelihood components for the diagnostic case model and the one-off models exploring sensitivity to biological factors.

	Diagno	SekiGrwt	RecrSD.2	LowStpn	HighStpn	LowM	HighM
Recruitment	-53.72	-53.50	-34.61	-53.78	-53.63	-54.09	-53.50
Survey	5.21	7.63	-1.08	6.11	4.21	4.85	6.57
Length comps	53.14	68.54	53.27	53.63	53.43	63.65	55.11
Catch	0.00	0.00	0.00	0.00	0.00	0.00	0.00
Total	4.63	22.66	17.58	5.95	4.01	14.41	8.19

Table B-14: Likelihood components for the diagnostic case model and the one-off models exploring sensitivity to weights on input data.

	Diagno	CV.1	CV.2	CV.GLM	RecrLmb5	RecrLmb25	RecrLmb25.CV1
Recruitment	-53.72	-48.67	-54.70	-54.49	-25.00	-25.00	-0.33
Survey	5.21	47.33	-8.31	-7.07	2.60	2.60	25.45
Length comps	53.14	53.36	53.08	52.92	53.13	53.13	54.31
Catch	0.00	0.00	0.00	0.00	0.00	0.00	0.00
Total	4.63	52.02	-9.93	-8.63	30.73	30.73	79.42

Table B-15: Likelihood components for the diagnostic case model and the one-off models exploring sensitivity to impact of fishing.

	Diagno	CatchMedian	CatchHigh	CatchHighDM	LowInitF	HighInitF
Recruitment	-53.72	-53.17	-53.12	-53.77	-53.75	-53.67
Survey	5.21	15.24	16.02	4.22	5.31	5.15
Length comps	53.14	53.00	52.82	52.89	53.74	52.93
Catch	0.00	0.00	0.00	0.00	0.00	0.00
Total	4.63	15.06	15.72	3.33	5.30	4.41

Table B-16: Likelihood components for the diagnostic case model and the one-off models exploring sensitivity to fleet selectivities.

	Diagno	Estim.Selex	All.Dome	Asymp.PS
Recruitment	-53.72	-52.67	-52.94	-53.75
Survey	5.21	1.31	2.97	4.99
Length comps	53.14	51.34	52.98	52.40
Catch	0.00	0.00	0.00	0.00
Total	4.63	-0.01	3.02	3.64